Synthesis of 13-Group Metal Oxides via Solvothermal Reaction and Control of the Pore Structure of Al$_2$O$_3$

Sung-Wook Kim

2010

Contents

General introduction

1. Background

1-1. Introduction

As for heterogeneous catalyst systems, the surface structure is a very important factor affecting catalyst activity, selectivity, and life time. Control of surface structure during the synthesis of metal oxide catalysts is, therefore, crucial. Generally, catalyst supports having large pore sizes are desired for use in industrial processes because of easy diffusion of reactants and products inside catalysts. For example, in hydrotreating of heavy oil, shell oil, and coal liquefaction oil, catalysts with large pore sizes show high activities as compared with catalysts of small pore sizes even with large surface areas [1,2]. This indicates that large pores are favorable for reactant diffusion. In addition, it is known that when catalysts having small pore sizes are used, deactivation of hydrotreating catalysts easily takes place even if active sites still exist inside the catalysts, because the entrances of pores are plugged by particles of V and Ni compounds generated by the hydrogenolysis of the related organo-metallic compounds present in raw materials [3]. The pore structure of catalyst supports is, therefore, very important to design high-performance catalysts, and its control is still an interesting research field. Many researches have accomplished excellent pore structure control of catalyst supports [4–10].

Among the materials for catalyst supports, aluminum oxides (alumina, Al_2O_3) are most widely used in industrial processes because of their chemical stabilities and low prices [11]. Al_2O_3 exist in various metastable polymorphs and these crystal structures can offer suitable surface conditions (surface area, pore size, pore volume,

1

and active site, etc) for many reactions [11]. Recently, gallium oxide-based compounds attract attention as catalysts/catalyst supports for various reactions [12–16]. Gallium belongs to 13th group in the periodic table as aluminum, and gallia (gallium oxide, Ga_2O_3) is known to have various crystal structures like Al_2O_3 and is highly expected for application as catalysts [17].

Various synthesis methods to obtain metal oxides have been investigated for a long time. The solvothermal reaction is one of the methods to prepare metal oxides. Recently, this method attracts much attention because the products obtained have novel physical/chemical properties as compared with the products obtained by conventional methods [18–21].

The past research trends for the synthesis of Al_2O_3 and Ga_2O_3 by the solvothermal reaction and researches aiming at controlling the pore structures of Al_2O_3 are described below.

1-2. *Preparation of alumina/gallia by the solvothermal method*

1-2-1. *Solvothermal method*

Generally, metal oxides are obtained by a thermal decomposition of precursors such as hydroxides, nitrates, carbonates, carboxylates, etc. However, a large amount of energy (high temperature) is required to prepare metal oxides by this method. As a result, sintering between particles easily takes place and aggregated particles are formed. Therefore, this method is not suitable to control the morphology and surface structure of the products. To overcome this problem, liquid phase methods such as sol-gel, precipitation, and co-precipitation methods are useful. Since the reactions are carried out at low temperature regions, the obtained products have small particle sizes

(nano/micro) and narrow particle size distributions [20,22]. However, by the liquid-phase methods, calcination at high temperatures is necessary to obtain well-crystallized products, because amorphous products are usually formed by these methods [23,24]. The hydrothermal reaction is carried out in water at temperatures higher than the boiling point of water in a liquid state or even under supercritical state. Basically, solvothermal reactions include hydrothermal reaction. In this thesis, the term, "solvothermal reaction" refers to a reaction using organic solvents instead of water. When glycols are used, the reaction is termed 'glycothermal reaction', and in the case of alcohol solvents the reaction is called 'alcohothermal reaction'.

Various products, such as metal oxides, nitrides, phosphides, organic-inorganic hybrid complexes, and carbon nanotubes can be obtained by the solvothermal reaction using organic solvents [25]. Particles having various shapes such as nano-rod, wire, tube, sheet, etc. are obtained depending upon the kind of starting materials, solvents, and additives which promotes crystallization [26–28].

Operation variables in the solvothermal reaction are temperature, pressure, and the kinds of precursors, solvents, mineralizers and seed crystals. Various organic solvents can be used in the solvothermal reaction (Table 1). Besides the organic solvents shown in Table 1, inorganic media have been applied for the synthesis of inorganic materials [25]. Liquid ammonia (boiling point, bp, 78 ^{o}C; critical point, T_c, 132 ^{o}C; critical pressure, P_c, 113 atm) and hydrofluoric acid (bp, 19.5 ^{o}C; T_c, 188 ^{o}C; P_c, 100 atm) are also used for the solvothermal synthesis of inorganic materials such as metal nitrides [31–34]. However, the reactions in these media usually have to be carried out under quite high pressures because the boiling points of these solvents are generally low.

Table 1. Solvents used as reaction media in the solvothermal reaction [25].

Alcohols	Methanol, Ethanol, 1-Propanol, 1-Butanol, 1-Pentanol,…
Glycols	Ethyl glycol, 1,4-Butanediol, 1,6-Hexanediol,…
Paraffins	n-Hexane, Hexadecane,…
Aromatics	Benzene, Toluene, Xylenes,…
Ethers	Dibutyl Ether, THF, 1,4-Dioxane,…
Nitriles	Acetonitrile, Nitromethane,…
Amines	Ethanolamine, Diethanolamine, Ethylenediamine,…
Aprotic Polar Solvents	Dimethylsulfoxide, N,N-dimethylformamide, Hexamethylphosphamide,…

Fyfe et al. reported that the equilibrium temperature of diaspore and α-Al_2O_3 is 360 ^{o}C under water pressure (bp, 100 ^{o}C; T_c, 374 ^{o}C; P_c, 218 atm) [29]. Moreover, synthesis of α-Al_2O_3 under the hydrothermal condition needs 10 h at 445 ^{o}C under 1000 atm in a NaOH solution [30]. In this way, since quite long reaction times must be applied to attain the equilibrium conversion of minerals under the hydrothermal condition, researchers recently have made studies to prepare inorganic materials more easily and rapidly.

On the other hand, organic solvents are composed of various substances (Table 1), and, by selecting appropriate substances, reaction can proceed under low temperatures in easily attained supercritical states. In recent years, solvothermal syntheses of inorganic materials in various organic solvents have been investigated by many researchers, and various results reported. Among them, the results of the recent researches for the preparation of aluminum and gallium oxides by the solvothermal reaction with organic solvents are described in the following paragraphs.

1-2-2. Synthesis of aluminum oxide by the solvothermal reaction in organic solvents

Crystallographically, Al_2O_3 has many metastable structures besides the thermodynamically stable phase, α-Al_2O_3 (corundum structure). These metastable phases of Al_2O_3 can be divided into two groups depending on the stacking patterns of oxygen sublattice: γ-, η-, θ- and δ-Al_2O_3 have oxygen sublattices formed by face-centered cubic packing (fcc), while α-Al_2O_3 has a hexagonal close-packed (hcc) arrangement of oxygen anions. Some researchers believe that κ- and χ-Al_2O_3 also have a hcc oxygen sublattice; however, this is a controversial issue. Aluminum cations are distributed within the oxygen sublattice [35]. Generally, transformation sequences of

Table 2. Common processing routes resulting in the formation of different metastable Al_2O_3 structures and the sequence of phase transformations toward the stable α-Al_2O_3 phase [38].

Approximate packing modes of oxygen for the metastable Al_2O_3 structures

---

hcp groups

α-AlOOH (diaspore) $\xrightarrow{700-800\,^{\circ}C}$ α-Al_2O_3

γ-Al(OH)$_3$ (gibbsite) $\xrightarrow{150-300\,^{\circ}C}$ χ $\xrightarrow{650-700\,^{\circ}C}$ κ $\xrightarrow{1000\,^{\circ}C}$ α-Al_2O_3

$5Al_2O_3\cdot H_2O$ (tohdite) $\xrightarrow{700-800\,^{\circ}C}$ κ' $\xrightarrow{750\,^{\circ}C}$ κ $\xrightarrow{900\,^{\circ}C}$ α-Al_2O_3

Vapor (CVD) $\longrightarrow$ κ $\longrightarrow$ α-Al_2O_3

fcc groups

γ-AlOOH (boehmite) $\xrightarrow{300-500\,^{\circ}C}$ γ $\xrightarrow{700-800\,^{\circ}C}$ δ $\xrightarrow{900-1000\,^{\circ}C}$ θ $\xrightarrow{1000-1100\,^{\circ}C}$ α-Al_2O_3

α-Al(OH)$_3$ (bayerite) $\xrightarrow{200-300\,^{\circ}C}$ η $\xrightarrow{600-800\,^{\circ}C}$ θ $\xrightarrow{1000-1100\,^{\circ}C}$ α-Al_2O_3

Amorphous (anodic film) $\longrightarrow$ γ $\longrightarrow$ δ $\longrightarrow$ θ $\longrightarrow$ α-Al_2O_3

Melt $\longrightarrow$ γ $\longrightarrow$ δ, θ $\longrightarrow$ α-Al_2O_3

Al$_2$O$_3$ show different patterns depending on the kind of precursors [36,37] during calcination process, and the generally observed transformation routes are summarized in Table 2 [38]. Such metastable Al$_2$O$_3$ phases contribute to form Al$_2$O$_3$ with various surface structures. They can be applied to many reaction processes as catalysts and/or catalyst supports depending on their morphologies [11].

The direct synthesis of the thermodynamically stable α-Al$_2$O$_3$ by the solvothermal reaction has been reported by many researchers [29,30,40–44]. Aluminum compounds are easily transformed to boehmite (AlOOH) at approximately 200 ^{o}C under the hydrothermal conditions [39]. Formation of α-Al$_2$O$_3$ from boehmite requires quite high temperatures (> 450 ^{o}C). On the other hand, the temperature required for the formation of α-Al$_2$O$_3$ from aluminum hydroxide by the glycothermal reaction is much lower than that required by the hydrothermal reaction [29,30,40]. The overall reaction is dehydration as follows:
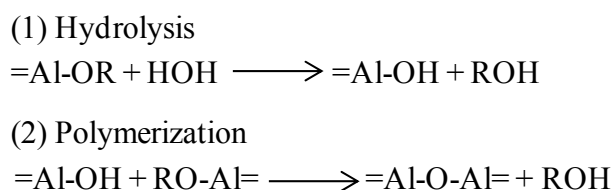
$$Al(OH)_3 \rightleftharpoons 1/2Al_2O_3 + 3/2\ H_2O.$$
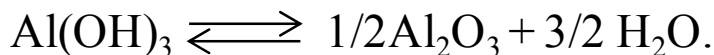
Therefore, water formed as a byproduct in this reaction has a very important role in the formation of α-Al$_2$O$_3$. However, in the hydrothermal reaction, a large excess of water is present in the system to affect the above equilibrium; therefore, the reaction to proceed to the right hand side is not favorable and much energy is required to complete the reaction. The glycothermal reaction contains only a small amount of water formed as a byproduct during the formation of the glycol derivative of boehmite. Therefore, crystallization proceeds rapidly due to increased dissolution rate of aluminum hydroxide by the water formed [41]. Besides the effect of water present in the reaction system, thermodynamic stability of the intermediates, particle size of precursor,

the presence of α-Al_2O_3 nuclei and alkali cations also affect the formation and morphology of α-Al_2O_3 in the solvothermal reaction [40,42–44].

In the case of the reaction of aluminum hydroxide (gibbsite) in simple alcohols, the reaction mechanism differs depending on the kind of alcohols used as reaction media [45]: The reaction of gibbsite in lower alcohols (below pentanol) proceeds through a dissolution-recrystallization mechanism, but, in higher alcohols, the reaction proceeds through thermal dehydration and intraparticle hydrothermal reaction. These results suggest that activity of water originated from gibbsite by dehydration increases with an increase in the carbon number of the alcohol, because lower solubility of water in higher alcohols increases the activity of water, thus facilitating the hydrothermal reaction. The intermediates formed by the reaction of gibbsite do not diffuse in the bulk of solvent because the reaction mainly takes place near the surface of solid and, therefore, the obtained products have particular shapes.

The solvothermal reaction starting from various aluminum precursors (gibbsite, aluminum metal, and aluminum alkoxide) in organic solvents has been also investigated by many researchers. Generally, aluminum alkoxide forms aluminum oxide via hydrolysis by water according to the following process:

(1) Hydrolysis
$$\equiv\text{Al-OR} + \text{HOH} \longrightarrow \equiv\text{Al-OH} + \text{ROH}$$

(2) Polymerization
$$\equiv\text{Al-OH} + \text{RO-Al}\equiv \longrightarrow \equiv\text{Al-O-Al}\equiv + \text{ROH}$$

In the reaction of aluminum alkoxide in alcohols, since water is spontaneously formed by dehydration of alcohols during the reaction, transitional Al_2O_3 can be obtained without adding water [46]. Various products such as transitional Al_2O_3 and boehmite can be obtained by changing reaction time and using additives as catalyst for
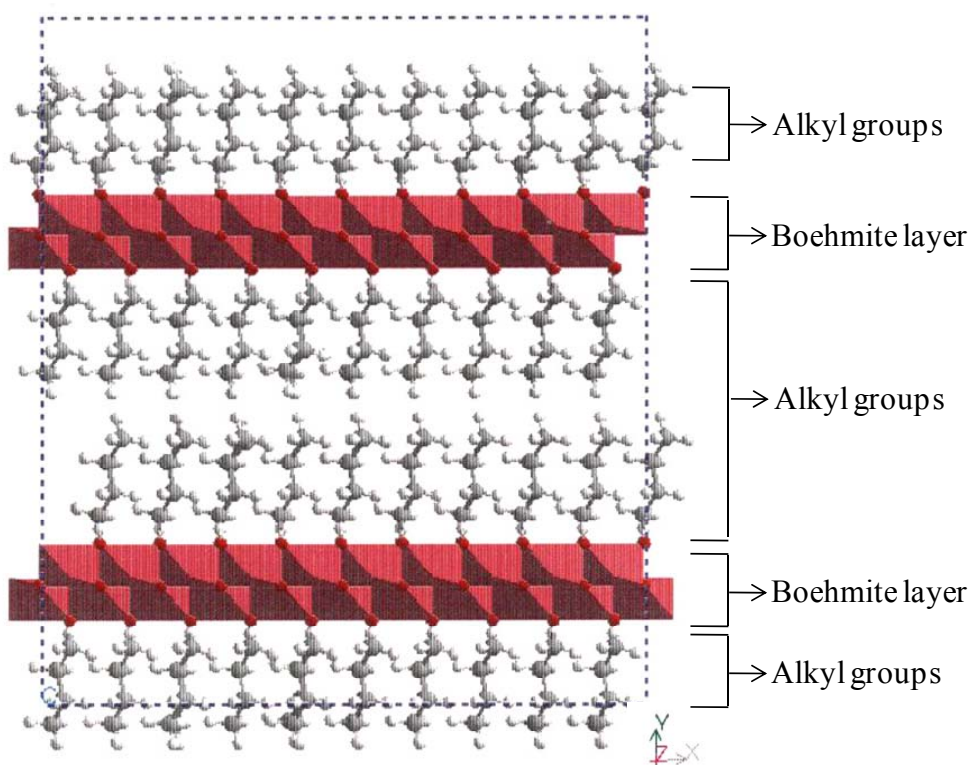
Fig. 1. Proposed structure of the products (alkoxyalumoxanes).

dehydration of alcohols such as sulphuric acid. Kubo et al. reported that, in the case of the solvothermal reaction of gibbsite in methanol, gibbsite does not dissolve into methanol, but methanol molecules diffuse into the bulk of gibbsite crystals. As a result, a methyl derivative of boehmite ($AlO(OH)_{0.5}(OCH)_3$) is obtained [47]. However, according to a report by Inoue et al., the reaction in higher alcohols (larger than ethanol) proceeds by a dissolution-recrystallization mechanism because diffusion of large molecules inside the lattice of crystals is difficult [48–54]. These reactions can proceed in the solvents having functional groups that can donate lone pair electrons such as amino and methoxy groups besides hydroxyl groups [25]. The product obtained by these reactions (alkyl derivatives of boehmite) has a molecular formular of $AlO(OH)_{(1-x)}(OR)_x$ and has a layered structure with a part of hydroxyl groups in the boehmite layers substituted by alkyl groups or ω-hydroxyalkyl groups (Fig.1) [54]. In the case of reactions in glycols, the crystallite size of the products increased with carbon number of the glycols in the following order: 2<3<6<4 [48]. This order corresponds to the order of hydrolysis rate of $BsO(CH_2)_nOCH_3$ (ω-methoxylalkyl bromobenzenesulphonate); the rate increases with carbon number n in the order of 2<3<6<4 [40]. These results suggest that heterolytic cleavage of O-C bond in the Al-O-C structure formed as the intermediate is a rate-controlling step. Peculiarity in the carbon number 4, namely 1,4-butandiol, can be explained by an assumption that the cleavage of the O-C bond is accelerated by the neighboring-group participation effect of OH group as follows [55]:
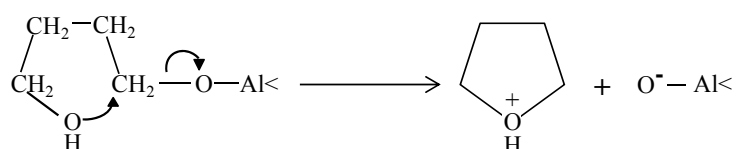
The physical properties of the Al_2O_3 derived from these products showed variation affected by carbon number n, and, especially, Al_2O_3 having a large pore size which can not be obtained by conventional methods is obtained from 4-hydroxybutyl derivative of boehmite formed by the reaction of aluminum alkoxide in 1,4-butandiol [53].

Solvothermal reactions of aluminum hydroxide are actually followed by hydrothermal reaction which is controlled by the water formed from the hydroxide by a dehydration process, whereas, in the case of alkoxide, the reactions proceed by heterolytic cleavage of the C-O bond of the intermediates. Formation of metastable phases is controlled by the thermodynamic unstability of the alkoxide formed as an intermediate in the reaction: The generation step of the crystal nuclei decides the kind of final products. Since crystal growth in the solvothermal reaction is very fast, defects are easily induced in the crystals, and, owing to these defects, the products obtained by the solvothermal reaction generally have large surface areas and high activities for catalytic reactions as compared with the products obtained by conventional methods.

1-2-3. *Synthesis of gallium oxide by the solvothermal reaction*

Gallium oxide-based catalysts are known to be active for dehydrogenation of light hydrocarbons, aromatization of light alkanes, and selective catalytic reduction of NO_x with hydrocarbons in the presence of oxygen [12–16]. Enhanced catalytic activities of zeolites containing gallium oxide as both framework and extra-framework components have been reported [14–16], and Ga_2O_3–Al_2O_3 mixed oxides are known as promising catalysts for selective catalytic reduction of nitrogen oxides in the exhaust gases from power stations [56–59]. Recently, researchers have also focused their

attention on the synthesis of Ga_2O_3 with various morphologies. Yada et al. reported the homogeneous-precipitation synthesis of mesostructured gallium oxide templated by a surfactant [60]. Cheng et al. prepared Ga_2O_3 nanotubes by immersing a porous Al_2O_3 membrane template in an amorphous $Ga_2O_3 \cdot nH_2O$ sol [61]. Synthesis of Ga_2O_3 nanowires by the evaporation of GaN in oxygen atmosphere [62,63] or by laser ablation of Ga_2O_3 [64] has been reported.

Gallium oxide has been reported to have five polymorphs: α, β, γ, δ and ε types [65]. The β-form is the thermodynamically stable phase and all of the other forms transform into the β-form at high temperatures [65]. Although Roy reported that γ-Ga_2O_3 has no obvious resemblance to γ-Al_2O_3, it is now generally believed that the γ-form has a defect spinel structure similar to that of γ-Al_2O_3 because Ga_2O_3–Al_2O_3 solid solutions were prepared [66,67]. In the solid solutions, Ga^{3+} ions preferentially occupy the tetrahedral sites of the defect spinel structure [66,67]. This polymorph is of particular interest because of its high surface area suitable for catalyst uses. Böhm first reported the synthesis of this phase by calcination of "gallium hydroxide gel" [68], but synthesis of this phase is not an easy task; the most important point is that the gel must be quickly dried [65,68,69]. Presumably, prolonged contact of the hydroxide gel particles with water causes the formation of GaOOH-like phase having a diaspore-type structure, which is a precursor of α-Ga_2O_3. This point is completely different from Al_2O_3 chemistry where prolonged contact of aluminum hydroxide gel particles with water would give a boehmite-like structure, which yields γ-Al_2O_3 on calcination.

The most reliable method for the synthesis of the gallium hydroxide gel as the precursor of γ-Ga_2O_3 is to add an ethanolic solution (50 vol%) of concentrated aqueous ammonia to a solution of gallium nitrate in ethanol at room temperature [69]; this

procedure have been used in most of the recent researchers [70–74] for the synthesis of γ-Ga$_2$O$_3$. Only few preparation methods other than that mentioned above have been reported; they are hydrothermal oxidation of gallium metal [18,75], glycothermal reaction of gallium acetylacetonate [20], and solvothermal reaction of GaCl$_3$ in DMF in the presence of amine bases [76]. However, physicals properties such as surface area, surface activity, and pore texture depend on the preparation method. Therefore, development of a variety of other synthetic procedures is highly desired.

1-3.   Control of Al$_2$O$_3$ pore structures

1-3-1.   Control of small pores (micro-, meso-pore; < 2 nm, 2~100 nm)

A series of Al$_2$O$_3$ for catalyst supports are prepared in the form of powder or pellet type from precursors such as aluminum hydroxide/oxyhydroxide (gibbsite, Al(OH)$_3$; boehmite, AlOOH). The pore structure of Al$_2$O$_3$ derived from aluminum hydroxide/oxyhydroxide is formed during drying/calcination processes. The aluminum hydroxide/oxyhydroxide obtained by precipitation are in the forms of various compounds, such as gibbsite, bayerite, boehmite and pseudoboehmite depending upon reaction conditions [77]. Characteristic pores are formed in the precipitates during the process of condensation. These pores are affected by the particle size and morphology of the precursors and precipitation conditions [77].

Among the various Al$_2$O$_3$ precursors, boehmite can be easily prepared by hydrothermal treatment of aluminum compounds, but thus-prepared boehmite is scarcely used for the precursor of Al$_2$O$_3$ catalyst, because the pore size of the Al$_2$O$_3$ derived from well-crystallized boehmite is too small for catalytic applications. For catalyst use, nanocrystalline boehmite, so called pseudoboehmite prepared by

precipitation methods [78], is preferred because aluminas with a wide range of pore-texture can be prepared by controlling the coagulation process for the primary particles of pseudoboehmite. Lippen et al. and Johnson et al. reported the formation behavior of pores in the Al_2O_3 derived from aluminum hydroxide/oxyhydroxide [77,79]. Gibbsite has a low surface area, and the pore size formed between crystals is large, while the pore volume is small. However, meso-pores are formed inside the Al_2O_3 particles retaining the morphology of starting aluminum hydroxide crystals (pseudomorph) when aluminum hydroxides are dehydrated by evacuation and/or calcination, and the surface area becomes large. The meso-pores are formed by elimination of water and the pore sizes are enlarged by partial degradation and aggregation of several pores [79]. On the other hand, well-developed boehmite generates micro-pores inside the particles during dehydration process and the surface area somewhat increases.

Pore structure of Al_2O_3 can be controlled by particles size and morphologies of the precursor phases. Boehmite having plate-like shapes, winkle sheet-like shapes, and lozenge-like shapes gives a different pore-size distribution on calcination [80]. When ammonia is added to a reaction system to obtain aluminum hydroxide gel by precipitation, Al_2O_3 derived from the gel has pores with sizes of about 2 nm which are narrowly distributed, while aluminum hydroxide precipitated by urea gives a bimodal distribution of pores of about 2 and 5 nm [81]. Ramsay et al. reported that pore structure of Al_2O_3 can be controlled by adding acids as peptization agents for boehmite [82]. Precipitates formed with 2–3 units particles are generated by adding suitable amounts of acid ($NHO_3/AlOOH \approx 2 \times 10^{-2}$) and the size of precipitates can be controlled by the amounts of acid. As a result, the pore structure of the Al_2O_3 derived from the products is

changed due to the change in the precipitate size. On the other hand, Tsay et al. reported that Al_2O_3 having small pore sizes compared with Al_2O_3 synthesized by the conventional methods is obtained by the calcination of aluminum xerogel prepared by hydrolyzing aluminum alkoxide ($Al[OCH(CH)_3C_2H_5]_3$) with a small portion of water in a non-aqueous solution [83]. Generally, the aluminum hydroxide formed from aqueous solution is composed of aggregates of small particles, but homogeneous polymeric aluminum sols are built up by the alkyl groups in a non-aqueous system. These sols shrink by calcination and make small pores.

The drying process of aluminum gel is important for controlling the pore structure of Al_2O_3. When water is substituted with methanol before drying aluminum gels, the extent of coagulation between particles decreases because the reduction of surface tension, and, as a result, pore volume of Al_2O_3 increases after final calcination [79]. Pierre et al. pointed out the importance of cohesion of the particles by the surface tension of water in the drying process [4]. They obtained a series of Al_2O_3 starting from different types of gel: gels obtained by conventional drying process evaporating water, by supercritical fluid dry process with CO_2, and by substitution of water with organic solvents after hydrolysis in excess water. All these aluminas had different pore structures.

As shown above, the pore structures (micro-, meso-pore; < 2 nm, 2~100 nm) of Al_2O_3 can be controlled by changing preparation factors: solvents, additives, and temperature.

1-3-2.   Control of pore structure in Al₂O₃ catalyst or support by forming processes

   (macro-pore, > 100 nm)

15

For heterogeneous catalysts, large pores (macro-pores > 100 nm) are favorable because diffusion of reactants and products inside the catalysts is easy. Therefore, the control of macro-pores in catalyst supports is a very importance factor to improve catalyst performance.

Generally, catalysts are molded by extrusion or pellet forming process for practical use. Aluminum hydroxide/oxyhydoxide or Al_2O_3 powders are generally used as raw materials [84]. A powder is mixed with a suitable additive and molded into a pellet followed by calcination. As this process contributes with various factors to pore structure formation, more detailed investigation is necessary for this process.

Various types of additives are used in the pellet forming process. In order to attain uniform pressure on the whole part of the pellet when pressurized, 0.3–3 wt% of graphite, poly(vinyl alcohol) or lubricants such as grease are added [85]. In addition, 3–5 wt% of binders are added to increase the strength of the pellet [86]. Sometimes, fillers such as carbon black, petroleum coke, and melamine are also added with 40–70 wt% content in order to form macropores by combustion of fillers in the calcination process [86–88]. All the materials added in this way affect the formation mode of the pore, but it is thought that fillers exert the largest influence. The added filler fills up the voids between particles, and when it is removed on calcination, it makes pores. The size of the pores formed by this process is decided by the size of the filler used.

The relationship between filler size and pore diameter has been clarified by Veselov et al. [89]. They reported that there exists an almost linear relationship between the size of the petroleum coke filler particles and the size of the pores. In addition, the quantity of added carbon affects the pore volume formed in the pellet. When 40 wt% of coke was added, the pore volume increased by 47–60 vol% compared with the case

without coke. Furthermore, with an increase in the quantity of coke with a size of *ca*. 500 nm, the size of the pores increased even up to 1500 nm. It was deduced that, therefore, coke was not equally distributed inside the pellet when the quantity of the coke increased; aggregation of coke occurred.

In the extrusion process, additives, binders, and fillers affect the strength of catalysts and formation of macro-pores as in the case of pellet forming process. The catalyst pastes used in the extrusion process show different viscosities and fluidities depending on the quantity of water added as well as the kind of additives shown above. All these factors affect the properties of the obtained products [84,89]. Walendziewski et al. reported about the change of pore structure of the Al_2O_3 obtained by using various types of extruder and fillers such as carbon black, activated carbon, and sugar [90,91]. Pore size of the obtained Al_2O_3 granule can be controlled form 3 nm to 5 nm in the meso-pore region and from 20 nm to 1250 nm in macro-pore region by choosing the content of fillers and the type of extruder devices (single/twin extruder, piston extruder, disc granulator). However, the macro-pore volume is influenced more by the type of extruder device than by the amount/kind of fillers added in the paste.

1-3-3.   *Control of pore structure by surface active agents*

Methods for the synthesis of mesoporous materials of various metal oxides (Si, Ti, Sb, Pb) using surfactants has been reported [92–95]. Yada et al. reported the preparation of aluminum-based materials having a hexagonal mesostructure by using dodecyl sulfate as a template [95]. In this reaction, the micelle structure is transformed from a lamellar structure into hexagonal one by uniformly raising the pH of the system by the hydrolysis of urea. However, these products give an amorphous Al_2O_3 due to the

17

collapse of mesostructure during calcination process, and, as a result, the mesostructured Al_2O_3 could not be obtained by this method. On the other hand, Vaudry et al. reported on the preparation of Al_2O_3 having narrow pore size distribution using an anionic surfactant [5]. However, the pore size was about 20 Å, and its control was impossible even if length of the alkyl chain of the surfactant was changed. Pinnavaia et al. reported about a method to control the pore size of Al_2O_3 by the N^oI^o (N: nonionic surfactant, I: inorganic precursor) process using polyethylene oxide [6,7].

These synthesis methods of mesoporous materials using surfactants resemble the methods of the synthesis of mesoporous silica which utilize various micelle structures derived by the surfactants in aqueous solutions [94]. In this reaction, an interaction of surfactant molecules with silicate polyanions occurs first. Then, nucleation and precipitation take place, and, at the same time, micelles with specific shapes are formed depending on the reaction condition. The mesoporous structures are built up by condensation and polymerization of silicate layers after these steps. Such a combination of surfactant and metal ion generates nuclei having a unique structure through interactions such as the van der Waals forces between organic materials and electro static forces, and finally precipitation occurs. The mode of condensation depends on temperature and reaction time, and the degree of condensation increases at high temperature and with long reaction time. In addition, since surfactants neutralize the interfacial charge between liquid and solid phase, the electric charges on the surface of inorganic frame decrease, and, therefore, precipitation occurs.

However, such synthesis methods have a limit for the preparation of mesoporous Al_2O_3. Because hydrolysis rate of aluminum alkoxide is very fast, the lamellar structure of the hydroxide is easily formed in the presence of surfactants [8].

Cabrera et al. investigated the preparation of mesoporous Al_2O_3 under an appropriate condition to control hydrolysis rate in solution to overcome this problem [96]. In this method, triethanolamine (TEA) which has a tendency to coordinate strongly with aluminum is used. Formation of stable TEA-Al^{3+} complex is derived by the removal of water from aluminum/TEA/water solution by heating. Since hydrolysis of TEA-Al^{3+} complex proceeds through a substitution mechanism, the rate is so slow that partially hydrolyzed aluminum complex can interact with surfactant molecules. In this reaction, when a large quantity of water is added to the reaction system, the reaction proceeds to the direction in which lamellar structures are preferably developed and the pore size is enlarged. The characteristic of this reaction is that the pore size of alumina can be controlled by controlling the quantity of water added.

The control of the pore structure of Al_2O_3 by the use of templates is affected by electrostatic interaction and steric factor, which control the interaction between solvent molecules, inorganic molecules, and self-assembled organic surfactants.

In views of all these backgrounds, the present work focuses on the study of pore structure of Al_2O_3 derived from the precursor synthesized by the solvothermal reaction in alcohols and on the investigation of novel route to prepare gallium-based oxides by the solvothermal reaction.

2. Scope and outline of the present thesis

As mentioned in the previous section, thermal treatments (glycothermal and alcohothermal treatments) of aluminum triisopropoxide (AIP) in organic solvents (glycols and alcohols) yielded the derivatives of boehmite, in which alkyl (or

19

hydroxyalkyl) groups were incorporated into the boehmite layers through covalent bonding; therefore, they are called alkyl derivatives of boehmite. The aluminas derived from these precusors are expected to have characteristic pore structures compared with the alumina obtained by the conventional methods because the morphologies and particle sizes of the alkyl derivatives of boehmite have completely different features from those of the other precursors. Chapter 1 describes the characteristics of the alkyl derivatives of boehmite (alkoxyalumoxane; $AlO(OH)_{1-x}(OR)_x$) synthesized by the reaction of AIP in straight-chain primary alcohols and the pore structures of the aluminas derived from them.

Chapter 2 clarifies the effects of drying process on the pore structure of aluminas. Aerogel/xerogel of aluminas was prepared by a simple method in which direct removal of the solvent from the autoclave at the end of the solvothermal reaction was involved. The alkyl derivatives of boehmite were prepared by the alcohothermal treatment of AIP and recovered as xerogel or aerogel, and the pore-textures of the alumina derived from these products were examined.

In Chapter 3, the effect of feed ratio of the reactants to the solvents on the characteristics of the products recovered as xerogel or aerogel is described. Transformation of alumina phases and the pore-textures of the alumina derived from the products are explained.

According to a molecular mechanics calculation of the alkyl derivatives of boehmite, it was found that the layered structure of the alkyl derivatives of boehmite is maintained even if the alkyl chains are partially removed [97]. These results indicate that partial removal of the alkyl chains creates voids in the alkyl layers because the alkyl chains are attached to the boehmite layers. In Chapter 4, the empirical examination on

whether the voids surrounded by alkyl chains are actually generated by the heat treatment of the alkyl derivatives of boehmite is discussed.

Chapter 5 deals with the solvothermal oxidation of gallium metal with various organic solvents, and the structure and property of the product are discussed.

Finally, the contents through Chapter 1 to Chapter 5 are summarized in General Conclusion. The future prospects of the alumina derived from the alkyl derivatives of boehmite and preparation of Ga_2O_3 by the solvothermal reaction are described.

References.

[1] P. N. Ho, S. W. Weller, *Fuel Process Tech.*, 4 (1981) 21.

[2] H. Shimada, M. Kurita, T. Sato, Y. Yoshimura, T. Kawakami, S. Yoshitomi, A. Nishijima, *Bull. Chem. Soc. Jpn.*, 57 (1984) 2000.

[3] W. C. Van Zijll Langhout, C. Ouwerkerk, K. M. A. Pronk, *Oil & Gas J.*, Dec. 1 (1980) 120.

[4] A. C. Pierre, E. Elaloui, G. M. Pajonk, *Langmuir*, 14 (1998) 66.

[5] F. Vaudry, S. Khodabandeh, M. E. Davis, *Chem. Mater.*, 8 (1996) 1451.

[6] S. A. Bagshaw, T. J. Pinnavaia, *Angew. Chem. Int. Ed. Engl.*, 35 (1996) 1102.

[7] W. Zhang, T. J. Pinnavaia, *Chem. Commun.*, (1998) 1185.

[8] S. Valange, J.-L. Guth, F. Kolenda, S. Lacombe, Z. Gabelica, *Microporous Mesoporous Mater.*, 35–36 (2000) 597.

[9] X. Zhang, F. Zhang, K.-Y. Chan, *Mater. Lett.*, 58 (2004) 2872.

[10] W.-C. Li, A.-H. Lu, W. Schmidt, F. Schüth, *Chem. Eur. J.*, 11 (2005) 1658.

[11] D. L. Trimm, A. Stainslaus, *Appl. Catal.*, 21 (1986) 21.

[12] K. Shimizu, A. Satsuma, T. Hattori, *Appl. Catal.*, *B,* 16 (1998) 319.

[13] M. D. Fokema, J. Y. Ying, *Cat. Rev. – Sci. Eng.*, 43 (2001) 1.

[14] G. L. Price, V. Kanazirev, *J. Catal.*, 126 (1990) 267–278.

[15] Y. Ono, K. Kanae, *J. Chem. Soc. Faraday Trans.*, 87 (1991) 669.

[16] C. R. Bayense, A. J. M. van der Par, J. H. C. van Hooff, *Appl. Catal.*, 72 (1991) 81.

[17] R. Roy, V. G. Hill, E. F. Osborn, *J. Am. Chem. Soc.*, 74 (1952) 719.

[18] K. Pohl, *Naturwiss.*, 55 (1968) 82.

[19] H. Bremer, B. Bogatzki, *Z. Chem.*, 8 (1968) 309.

[20] M. Inoue, T. Nishikawa, H. Otsu, H. Kominami, T. Inui, *J. Am. Ceram. Soc.*, 81

(1998) 1173.

[21] T. Chen, K. Tang, *Appl. Phys. Lett.*, 90 (2007) 051304.

[22] S.-J. Chen, X.-T. Chen, Z. Xue, L.-H, Li, X.-Z. You, *Cryst. Growth*, 246 (2002) 169.

[23] R. W. Jones, "Fundamental Principles of Sol-Gel Technology." Institute of Materials, VT (1989).

[24] C. B. Jeffrey, "Sol-Gel Science: The Physics and Chemistry of Sol-Gel Processing." Academic Press, Boston (1990).

[25] M. Inoue, "Chemical Processing of Ceramics" 2nd Ed., Taylor & Francis, Boca Raton. FL. (2005) p. 21.

[26] G. R. Patzke, F. Krumeich, R. Nesper, *Angrew. Chem. Int. Ed. Engl.*, 41 (2002) 2446.

[27] C. Wei, Y. Deng, Y.-H. Lin, C.-W. Nan, *Chem. Phy. Lett.*, 372 (2003) 590.

[28] S.-H. Yu, Y. Yang, Y.-T. Qian, M. Yoshimura, *Chem. Phys. Lett.*, 361 (2002) 362.

[29] W. S. Fyfe, M. A. Hollander, *Am. J. Sci.*, 262 (1964) 709.

[30] G. Yamaguchi, H. Yanagida, T. Fugimura, *Bull. Chem. Soc. Jpn.*, 38 (1954) 54.

[31] H. Jacobs, C. Stuve, *J. Less Common Met.*, 96 (1984) 323.

[32] A. P. Purdy, *Chem. Mater.*, 11 (1999) 1648.

[33] G. Demazeau, G. Goglio, A. Denis, A. Largeteau, *J. Phys. Condense. Mater.*, 14 (2002) 11085.

[34] H. Bialowons, M. Müller, B. G. Müller, *Anorg. Allg. Chem.*, 621 (1995) 1227.

[35] K. Wefers, C. Misra, "Oxides and Hydroxides of Alumina," Alcoa Technical Paper No.19, Alcoa Laboratories, Pittsburgh, PA (1987).

[36] S. J. Wilson, *Proc. Br. Ceram. Soc.*, 28 (1979) 281.

[37] B. C. Lippens, J. H. De Bore, *Acta Crystallogr.*, 17 (1964) 1312.

[38] I. Levin, D. Brandon, *J. Am. Ceram. Soc.*, 81 (1998) 1995.

[39] H. Ginsberg, M. Koster, *Z. Anorg. Allgem. Chem.*, 293 (1957) 204.

[40] M. Inoue, H. Tanino, Y. Kondo, T. Inui, *J. Am. Ceram. Soc.*, 72 (1989) 352.

[41] M. Inoue, M. Kimura, H. Kominami, H. Tanino, T. Inui, 72nd Annual Meeting of Chemical Society of Japan, Tokyo, March 1997, abstract no. 1BY09.

[42] N. S. Bell, S.-B. Cho, J. H. Adair, *J. Am. Ceram. Soc.*, 81 (1998) 1411.

[43] S.-B. Cho, S. Venigalla, J. H. Adair, *J. Am. Ceram. Soc.*, 79 (1996) 88.

[44] N. S. Bell, J. H. Adair, *J. Cryst. Growth*, 203 (1999) 213.

[45] M. Inoue, K. Kitamura, H. Tanino, H. Nakamura, T. Inui, *Clays Clay Miner.*, 37 (1989) 71.

[46] A. J. Fanelli, J. V. Burlew, *J. Am. Ceram. Soc.*, 69 (1986) C-174.

[47] T. Kubo, K. Uchida, *Kogyo Kagaku Zasshi*, 73 (1970) 70.

[48] M. Inoue, Y. Kondo, T. Inui, *Inorg. Chem.*, 27 (1988) 215.

[49] M. Inoue, K. Kitamura, T. Inui, *J. Chem. Technol. Biotechnol.*, 46 (1989) 233.

[50] M. Inoue, H. Kominami, T. Inui, *J. Am. Ceram. Soc.*, 73 (1990) 1100.

[51] M. Inoue, H. Otsu, H. Kominami, T. Inui, *J. Am. Ceram. Soc.*, 74 (1991) 1452.

[52] M. Inoue, H. Tanino, Y. Kondo, T. Inui, *Nippon Kagakukaishi*, (1991) 1036.

[53] M. Inoue, H. Kominami, T. Inui, *J. Mater. Sci.*, 29 (1994) 2459.

[54] M. Inoue, M. Kimura, T. Inui, *Chem. Mater.*, 12 (2000) 55.

[55] S. Winstein, E. Allred, R. Heck, R. Glick, *Tetrahedron*, 3 (1958) 88.

[56] M. Haneda, Y. Kintaichi, H. Hamada, *Appl. Catal.*, B, 20 (1999) 289.

[57] M. Haneda, H. E. Jonbert, J. C. Menezo, D. Duprez, J. Barbier, N. Bion, M. Daturi, J. Saussey, J. C. Lavalley, H. Hamada, *Phys. Chem. Chem. Phys.*, 3 (2001) 1366.

[58] Y. N. Pushkar, A. Sinitsky, O. O. Parenago, A. N. Kharlanov, E. V. Lunina, *Appl. Surf. Sci.*, 167 (2000) 69.

[59] M. Takahashi, T. Nakatani, S. Iwamoto, T. Watanabe, M. Inoue, *Appl. Catal. B: Environmental*, 70 (2007) 73.

[60] M. Yada. H, Takenaka, M. Machida, T. Kijima, *J. Chem. Soc., Dalton Trans.*, (1998) 1547.

[61] B. Cheng, E. T. Samulski, *J. Mater. Chem.*, 11 (2001) 2901.

[62] J. Zhang, F. Jiang, *Chem. Phys.*, 289 (2003) 243.

[63] J. Q. Hu, Q. Li, X. M. Meng, C. S. Lee, S. T. lee, *J. Phys. Chem., B,* 106 (2002) 9536.

[64] Z. R. Dai, Z. W. Pan, Z. L. Wang, *J. Phys. Chem., B*, 106 (2002) 902.

[65] R. Roy, V. G. Hill, E. F. Osborn, *J. Am. Chem. Soc.*, 74 (1952) 719.

[66] C. Otero Areán, M. Rodríguez Delgado, V. Montouillout, D. Massiot, *Z. Anorg. Allg. Chem.*, 631 (2005) 2121.

[67] M. Takahashi, N. Inoue, T. Takeguchi, S. Iwamoto, M. Inoue, *J. Am. Ceram. Soc.,* 89 (2006) 2158.

[68] J. Böhm, *Angew. Chem.*, 53 (1940) 131.

[69] C. Otero Areán, A. López Bellan, M. Peñarroya Mentruit, M. Rodríguez Delgado, G. Turnes Palomino, *Microporous Mesoporous Mater.*, 40 (2000) 35.

[70] M. Zinkevich, F. M. Morales, H. Nitsche, M. Ahrens, M. Rühle, F. Aldinger, *Z. Metallkd.*, 95 (2004) 756.

[71] S. E. Collins, M. A. Baltanás, A. L. Bonivardi, *J. Phys. Chem., B*, 110 (2006) 5498.

[72] M. Rodríguez Delgado, C. Otero Areán, *Z. Anorg. Allg. Chem.*, 631 (2005) 2115.

[73] B. Zheng, W. Hua, Y. Yue, Z. Gao, *J. Catal.*, 232 (2005) 143.

[74] Y. Hou, L. Wu, X. Wang, Z. Ding, Z. Li, X. Fu, *J. Catal.*, 250 (2007) 12.

[75] H. Bremer, B. Bogatzki, *Z. Chem.*, 8 (1968) 309.

[76] T. Chen, K. Tang, *Appl. Phys. Lett.*, 90 (2007) 051304.

[77] B. C. Lippen, J. J. Steggerda, "Physical and Chemical Aspects of Adsorbents and Catalyst" Ed. by B. G. Linsen, Academic Press, London (1970).

[78] H. De Souza Santos, P. K. Kiyohara, P. De Souza Santos, *Mater. Res. Bull.*, 31 (1996) 799.

[79] M. F. L. Johnson, J. Mooi, *J. Catal.*, 10 (1986) 342.

[80] T.-L. Hong, *Appl. Catal. A: General*, 158 (1997) 257.

[81] T. Kotanigawa, M. Yamamoto, M. Utiyama, H. Hattori, K. Tanabe, *Appl. Catal.*, 1 (1981) 185.

[82] J. D. F. Ramsay, S. R. Daish, C. J. Wright, *Discuss. Faraday. Soc.*, 65 (1978) 65.

[83] C. S. Tsay, C. K. Lee, A. S. T. Chiang, *Chem. Phys. Lett.*, 278 (1997) 83.

[84] A. B. Stile, "Catalyst Manufacture" Marcel Dekker, N. Y. (1983).

[85] R. Snel, *Appl. Catal.*, 12 (1984) 347.

[86] U. Hammon, M. Kotter, *Chem. Ing. Tech.*, 56 (1984) 455.

[87] D. Basmadjian, G. N. Fulford, B. I. Parsons, D. S. Montgomery, *J. Catal.*, 1 (1962) 547.

[88] K. Onuma, H. Kobayashi, M. Suzuki, *J. Jpn. Petrol. Inst.*, 27 (1984) 348.

[89] V. V. Veselov, T. A. Levanyuk, V. V. Savinykh, T. I. Kusharenko, E. T. Morgunova, *Kinet. Catal.*, 16 (1975) 868.

[90] J. Walendziewski, T. Trawczynski, *Appl. Catal.*, 96 (1993) 163.

[91] J. Walendziewski, T. Trawczynski, *Appl. Catal.*, 119 (1994) 45.

[92] D. M. Antonelli, J. Y. Ying, *Angrew. Chem.*, 34 (1995) 2014.

[93] Q. Huo, D. I. Margoles, U. Ciesla, P. Feng, F. E. Gier, P. Sieger, R. Leon, P. M. Petroff, F. Schuth, *Nature*, 368 (1994) 317.

[94] Q. Huo, D. I. Margoles, U. Ciesla, D. G. Demuth, P. Feng, F. E. Gier, P. Sieger, A. Firouzi, B. F. Chmelka, F. Schuth, G. D. Stucky, *Chem. Mater.*, 6 (1994) 1176.

[95] M. Yada, H. Hiyoshi, K. Ohe, M. Machida, T. Kijima, *Inorg. Chem.*, 36 (1997) 5565.

[96] S. Cabrera, J. Haskouri, J. Alamo, A. Beltran, S. Mendioraz, M. D. Marcos, P. Amoros, *Adv. Mater.*, 11 (1999) 379.

[97] Y. Nakazaki, M. Inoue, *J. Phys. Chem. Solids*, 65 (2004) 429.

Chapter 1

Pore structure of aluminas derived from the alkyl derivatives of boehmite

1-1 Introduction

Alumina (Al_2O_3) is most widely used because it is inexpensive and reasonably stable, and is provided with a wide range of surface areas and porosities suitable for a variety of catalyst application [1]. Preparation of alumina (or alumina-based) supports with the controlled pore structure is still an active area: Thus, many papers have been reported [2–8].

Boehmite is one of the modifications of aluminum oxide hydroxide, AlOOH, and it can be easily prepared by hydrothermal treatment of aluminum hydroxide [9]. Microcrystalline boehmite is called "pseudoboehmite" and is used as a precursor of aluminas. Although boehmite has a layered structure, intercalation of guest molecules into the boehmite layers has never been reported, presumably because of the strong hydrogen bonding between the layers. On the other hand, during the course of our long-term study on controlling the pore texture of alumina for use as catalyst supports, we found that the thermal treatment (glycothermal and alcohothermal treatments) of aluminum triisopropoxide (AIP) in organic solvents (glycols and alcohols) yielded novel derivatives of boehmite, in which the alkyl (or hydroxyalkyl) groups were incorporated into boehmite layers through the covalent bonding [10–13].

In this chapter, the pore structures of aluminas derived from the alkyl derivatives of boehmite are described.

28

1-2. Experimental

1-2-1. *Synthesis of the alkyl derivatives of boehmite*

In a Pyrex test tube serving as an autoclave liner, 130 ml of a straight-chain primary alcohol (ethanol, EtOH; 1-butanol, BuOH; 1-pentanol, PeOH; 1-hexanol, HeOH; 1-octanol, OcOH; 1-decanol, DeOH; 1-dodecanol, DDOH) and 12.5 g of aluminum triisopropoxide (AIP) were placed, and the test tube was then placed in a 300 ml autoclave. In the gap between the autoclave wall and the test tube was placed an additional 30 ml of the alcohol. The autoclave was thoroughly purged with nitrogen, heated to 300 ℃ at a rate of 2.3 ℃ /min, and held at that temperature for 2 h. After the mixture was cooled to room temperature, the resulting precipitate was washed by repeated of agitation with methanol followed by centrifuging and decantation, and, finally, air-dried. The obtained product was calcined at various temperatures by heating at a rate of 10 ℃ /min and holding at these temperatures for 30 min in a furnace in static air.

These products were designated by "A" followed by the abbreviation of the name of the medium used in the alcohothermal treatment and calcination temperature in degree Celsius in parentheses. The original samples will be specified by a term, "as-syn", in parentheses.

1-2-2. *Characterization*

Powder X-ray diffraction (XRD) was measured on a Shimadzu XD-D1 diffractometer using CuKα radiation and a carbon monochromator. The nitrogen adsorption isotherms were measured at liquid-nitrogen temperature by using a volumetric gas-sorption system, Quantachrome Autosorb-1. The alumina samples were
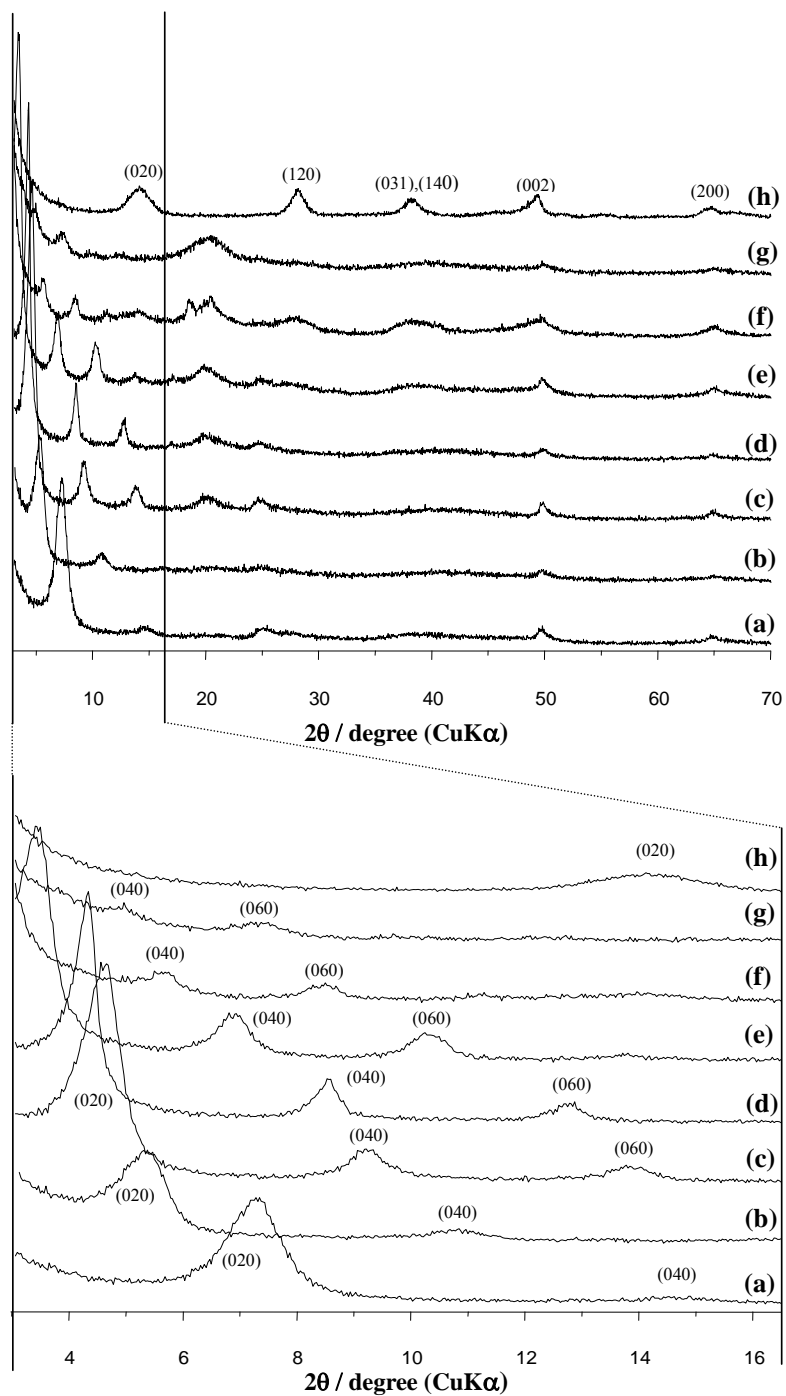
Fig. 1-1. XRD patterns of pseudoboehmite (h) and the products (a–g) obtained by the reaction of AIP in alcohols: a, AEtOH(as-syn); b, ABuOH(as-syn); c, APeOH(as-syn); d, AHeOH(as-syn); e, AOcOH(as-syn); f, ADeOH(as-syn); g, ADDOH(as-syn).

previously outgassed at 300 ºC for 30 min. Surface areas were calculated by applying the BET method to the adsorption data, taking the average area occupied by a nitrogen molecule as 0.162 nm^2. Pore size distributions were calculated from the desorption branch of the nitrogen adsorption isotherm by the BJH method. Infrared spectra were obtained on a JASCO FT/IR-470 Plus spectrophotometer using the usual KBr-pellet technique with 128 integration times. Simultaneous thermogravimetric (TG) and differential thermal (DTA) analyses were performed on a Shimadzu DTG-50 analyzer: a weighed (ca. 20 mg) sample was placed in the analyzer, and then heated at a rate of 10 ºC/min. Morphologies of the products were observed with a scanning electron microscope (SEM), Hitachi S-2500X.

1-3. Results and discussion

1-3-1. Alkyl derivatives of boehmite obtained by the solvothermal method

The XRD patterns of the products are shown in Fig. 1-1. For comparison, the XRD pattern of pseudoboehmite is also given in the figure. The XRD peaks at the high angle side (2θ = 50º and 65º) are related to the lattice parameters, *a* and *c*, of pseudoboehmite (200 and 002 planes), and they could be indexed on the basis of a boehmite structure [12,13]. The 020 plane peak of the products shifted toward the lower-angle side with an increase in the carbon number of the alcohols used as the solvents (Fig. 1-1), suggesting that the alkyl groups derived from the solvent alcohols are incorporated between the boehmite layers. In the XRD patterns of ADeOH(as-syn) and ADDOH(as-syn), the peak due to 020 plane was not clearly seen. The alkyl chains of the decyl and dodecyl groups are so long that the diffraction peaks for the 020 plane
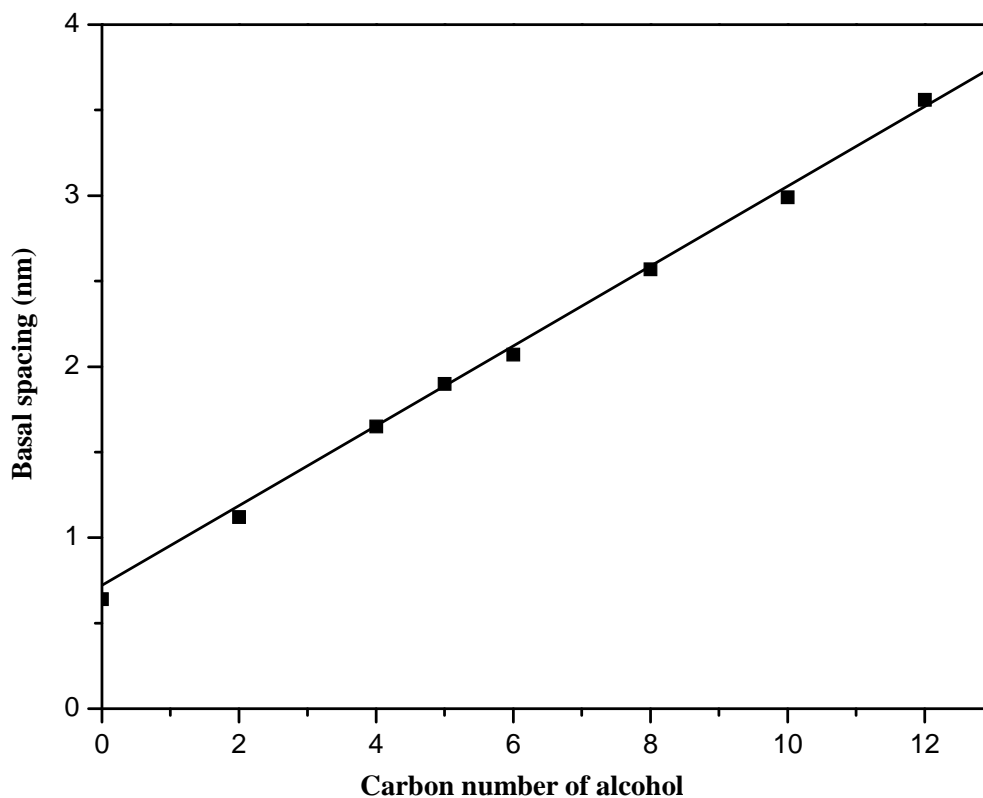
Fig. 1-2. Interlayer spacing of the products obtained by the reaction of aluminum triisopropoxide in straight-chain primary alcohols. For the datum for carbon number zero the basal spacing of pseudoboehmite (microcrystalline boehmite) is plotted. However, it must be noted that boehmite layers in boehmite are held together with each other by a strong hydrogen bondings, whereas in the bilayer structure of the alkyl derivatives of boehmite, the alkyl layers attached to the two adjacent boehmite layers are linked together by van der Waals force. Therefore, the basal spacing of pseudoboehmite is slightly smaller than the y-intercept obtained by extrapolation of the data for the basal spacings of the alkyl derivatives of boehmite.
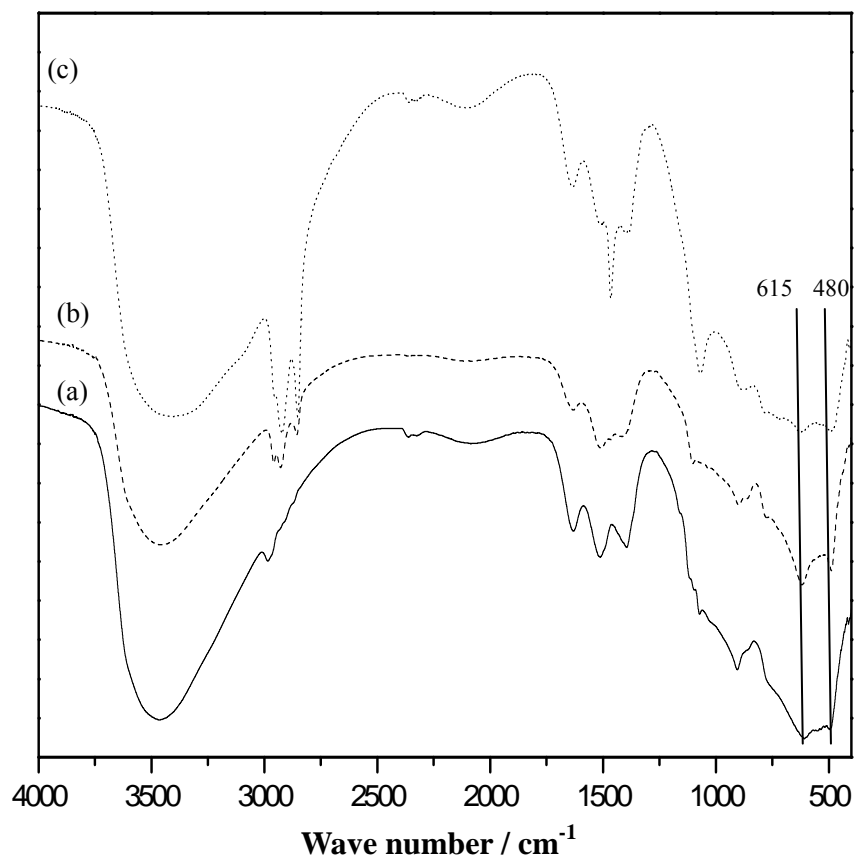
Fig. 1-3. IR spectra of the products obtained by the reaction of AIP
in alcohols: a, AEtOH(as-syn); b, AHeOH(as-syn); c,
ADDOH(as-syn).
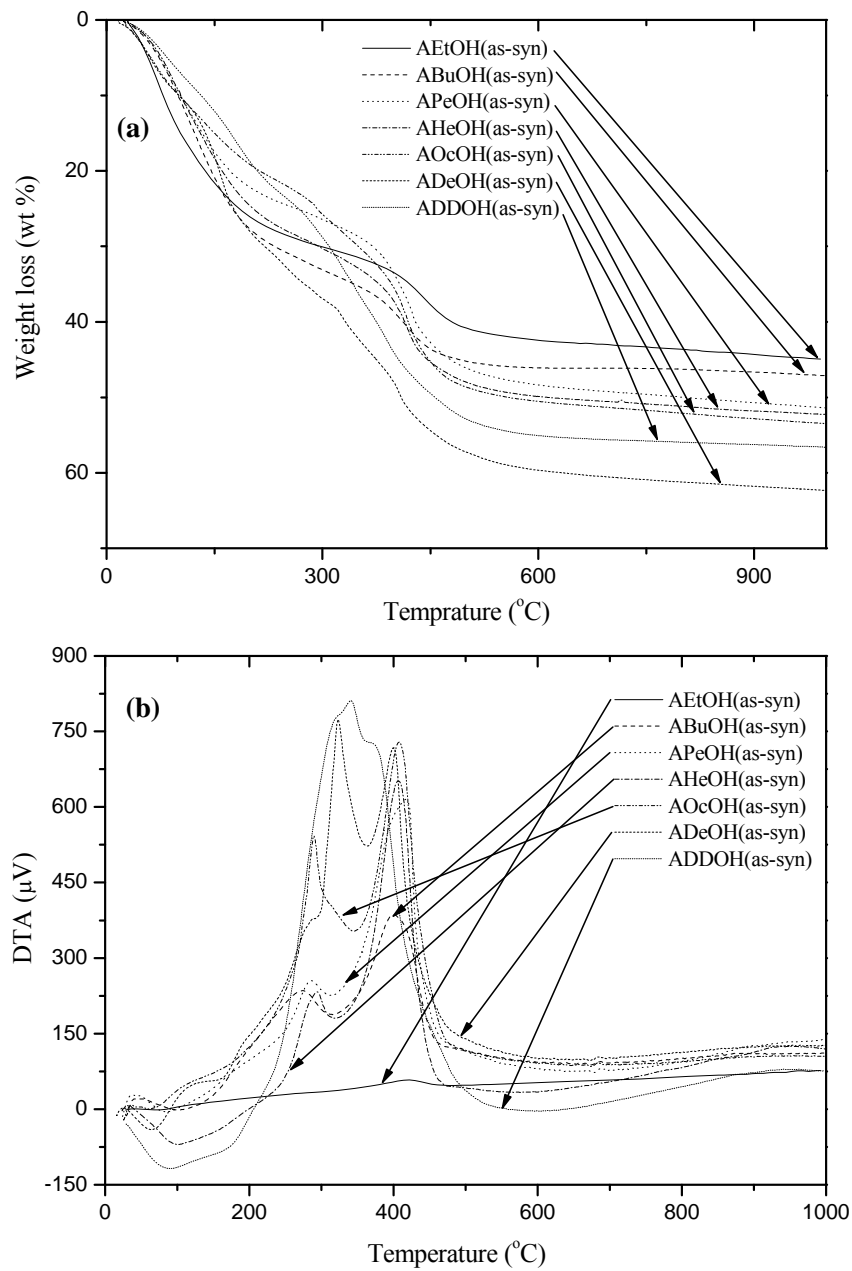
Fig. 1-4. Thermal analyses of the products obtained by the reaction of AIP in the alcohols specified in the figure in a 40 ml/min flow of dried air at a heating rate of 10 ºC /min: a, TG; b, DTA.

(basal plane) of ADeOH and ADDOH appeared at $2\theta < 3°$. However, they exhibited 040 and 060 diffraction peaks (these peaks are 2nd and 3rd order diffraction peaks of the basal plane), and therefore the position of the 020 diffraction peak can be calculated precisely from these peaks, which clearly shows the low-angle shift of the 020 diffraction peak. To clarify these points, 040 and 060 diffraction peaks are indexed in Fig. 1-1. A linear increase of basal spacing with an increase in the carbon number of the solvents was observed (Fig. 1-2), which is an incontestable evidence for the incorporation of the alkyl groups derived from the solvent alcohols.

In the IR spectra of the products shown in Fig. 1-3, bands characteristic of the boehmite layers are seen at around 615 and 480 cm^{-1} [14–16], suggesting that the products had the layer structure of boehmite. Bands due to the incorporated organic moieties were also noted at 3000–2850 cm^{-1} (ν_{CH}).

Figure 1-4 shows the results for thermal analyses of the products. A large weight decrease is seen around 100 and 400 $°C$ for all of the samples. Judging from the DTA profiles of the products, it is shown that one endothermic and two exothermic processes took place at around 100, 300 and 400 $°C$, respectively. The first process is attributed to the desorption of physisorbed water/methanol and the second and third processes are caused by the combustion of the alkyl moieties incorporated between the boehmite layers. Collapse of the boehmite layers yielding amorphous alumina seems to take place simultaneously with the third process. However, the endothermic response due to the collapse of boehmite layer was not observed because of the large exothermic effect of combustion. Because the molecular weight of ethanol is small as compared to other alcohols used in this study, the intensity of the exothermic peak as well as the total weight decrease was smallest among the samples. The exothermic peak shifted slightly

Table 1-1 Summary of the thermal analysis of the alkyl derivatives of boehmite obtained by the solvothermal method.

Sample	Weight ratio (BD^a/Al_2O_3)	Ignition temperature (^oC)	Molecular fomular[b]
AEtOH	1.25	425	$AlO(OH)_{0.86}(OEt)_{0.14}$
ABuOH	1.25	402	$AlO(OH)_{0.89}(OBu)_{0.11}$
APeOH	1.51	417	$AlO(OH)_{0.76}(OPe)_{0.24}$
AHeOH	1.36	407	$AlO(OH)_{0.89}(OHe)_{0.11}$
AOcOH	1.51	408	$AlO(OH)_{0.85}(OOc)_{0.15}$
ADeOH	1.41	400	$AlO(OH)_{0.91}(ODe)_{0.09}$
ADDOH	1.66	373	$AlO(OH)_{0.85}(ODD)_{0.15}$

a: Alkyl derivatives of boehmite.

b: Empirical formulas, $AlO(OH)_{1-x}(OR)_x$ were calculated from ignition losses determined by TG analyses for the products; Et, CH_3CH_2-; Bu, $CH_3(CH_2)_3$-; Pe, $CH_3(CH_2)_4$-; He, $CH_3(CH_2)_5$-; Oc, $CH_3(CH_2)_7$-; De, $CH_3(CH_2)_9$-; DD, $CH_3(CH_2)_{11}$-
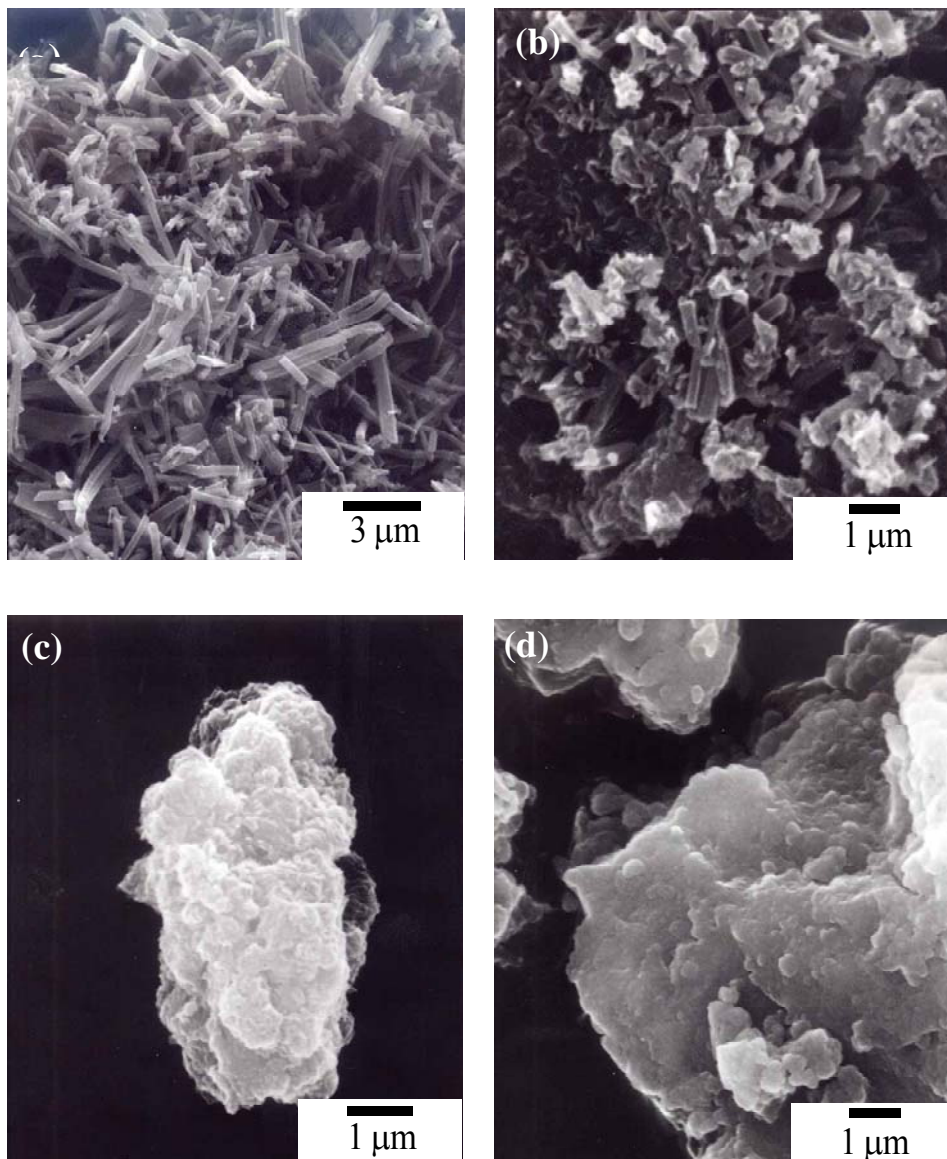
Fig. 1-5. Scanning electron micrographs of the products: a, AEtOH(as-syn); b, APeOH(as-syn); c, AHeOH(as-syn); d, ADDOH(as-syn).
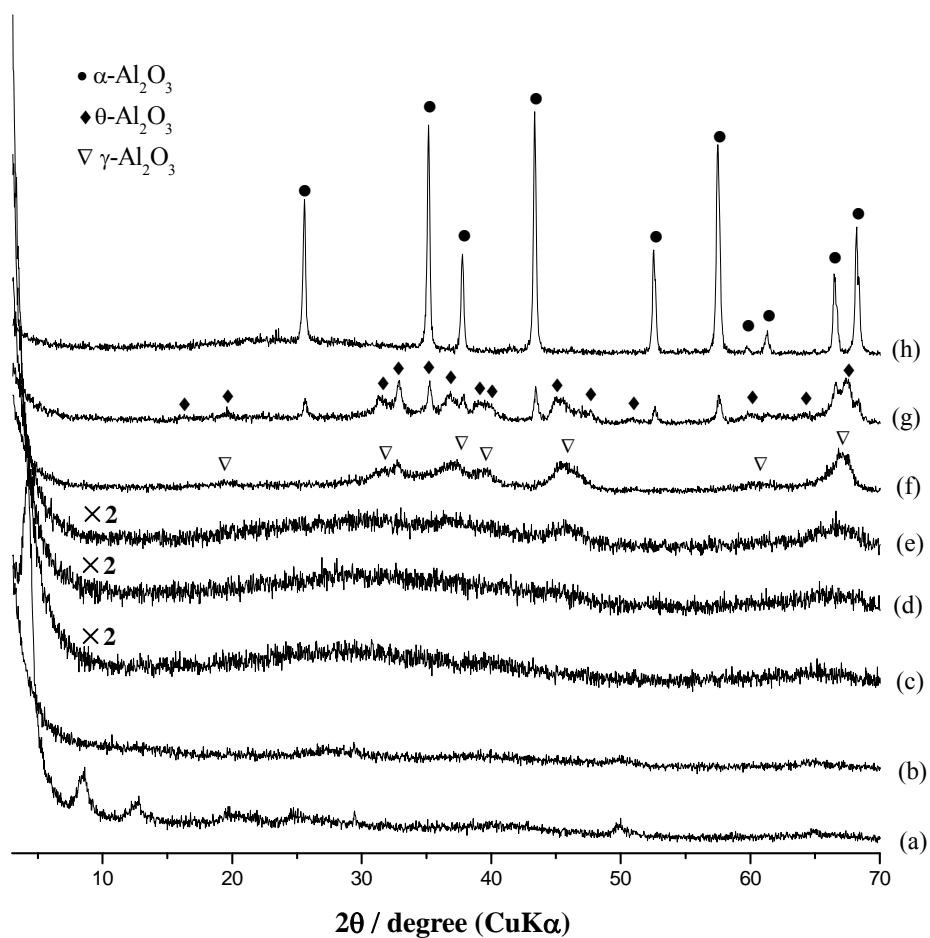
Fig. 1-6. XRD patterns of aluminas obtained by the calcinaton of the hexyl derivative of boehmite at various temperatures in air: a, 300 ℃; b, 400 ℃; c, 500 ℃; d, 600 ℃; e, 800 ℃; f, 1000 ℃; g, 1100 ℃; h, 1200 ℃.

toward a lower temperature region when a long chain alcohol was used (AEtOH(as-syn); 425 ºC, AHeOH(as-syn); 407 ºC, ADDOH(as-syn); 373 ºC). This result may be attributed to the fact that the octane numbers of alcohols having short alkyl chains are higher than those of alcohols having long alkyl chains [17]. The results of the thermal analyses of the products obtained by the reaction of AIP in primary alcohols are summarized in Table 1-1. All these results are consistent with the fact that the alkyl moieties are incorporated between the boehmite layers. Note that a linear correlation was found between the basal spacing of the alkyl derivative of boehmite and carbon number of the alkyl group (Fig. 1-2) in spite of the fact that the alkyl population in the boehmite layers was varied (Table 1-1). Since the alkyl groups are attached to the oxygen atoms in the boehmite layers, distribution of location of alkyl chains is not homogeneous, and therefore the most crowded part of the assembly of the alkyl chains determines the basal spacing [11, 18, 19].

1-3-2. Morphological aspects

The scanning electron micrographs of the products are shown in Fig. 1-5. Particles of the product obtained in ethanol (AEtOH(as-syn)) had a rod shape. On the other hand, particles of APeOH(as-syn) had irregular shapes but rod shape particles were also seen together with the irregularly-shaped particles. AHeOH(as-syn) and ADDOH(as-syn) were composed of large aggregate particles having irregular shapes.

1-3-3. Calcined product.

Phase transformation of the alkyl derivatives of boehmite was investigated and Fig. 1-6 shows the transformation of AHeOH as the representative results. AHeOH
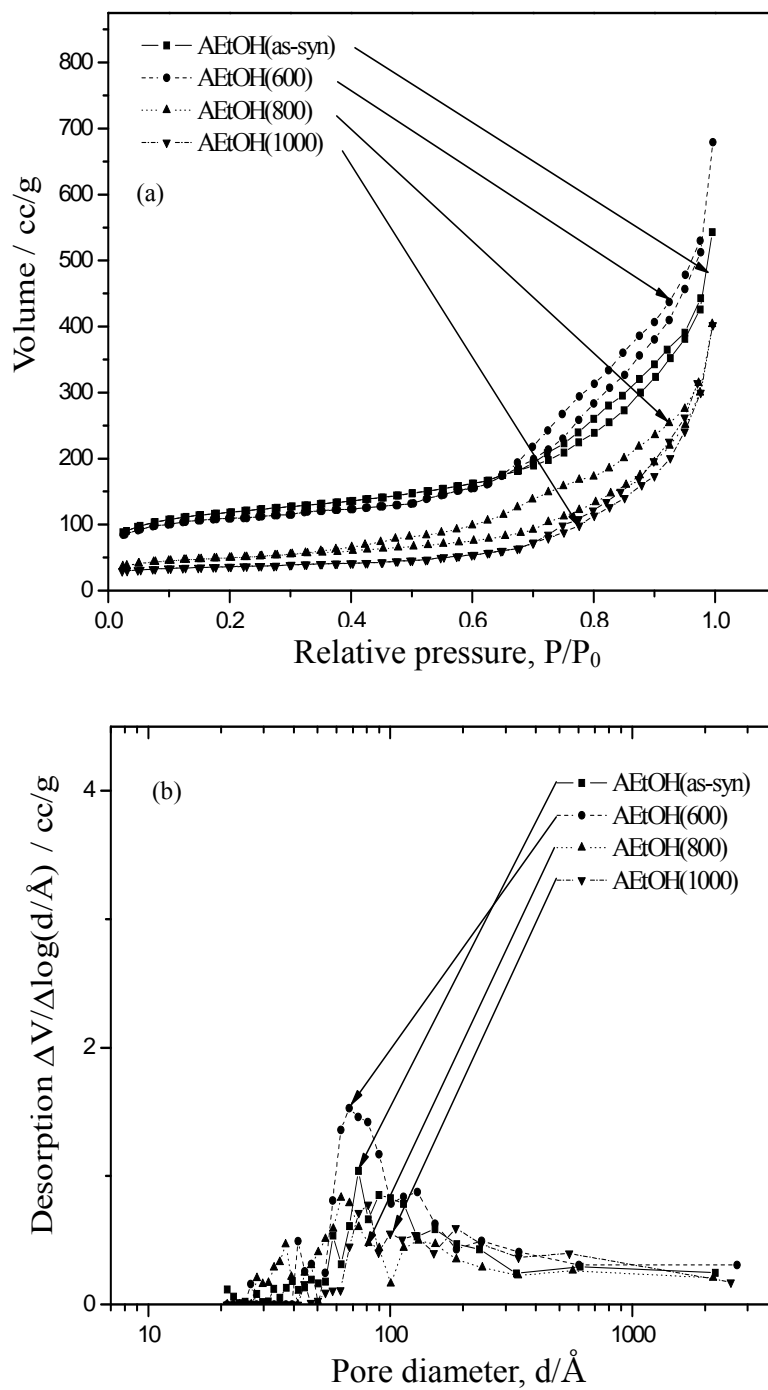
Fig. 1-7. Nitrogen adsorption isotherms (a) and pore-size distribution (b) of the aluminas obtained by the calcinaton of ethyl derivative of boehmite at various temperatures.
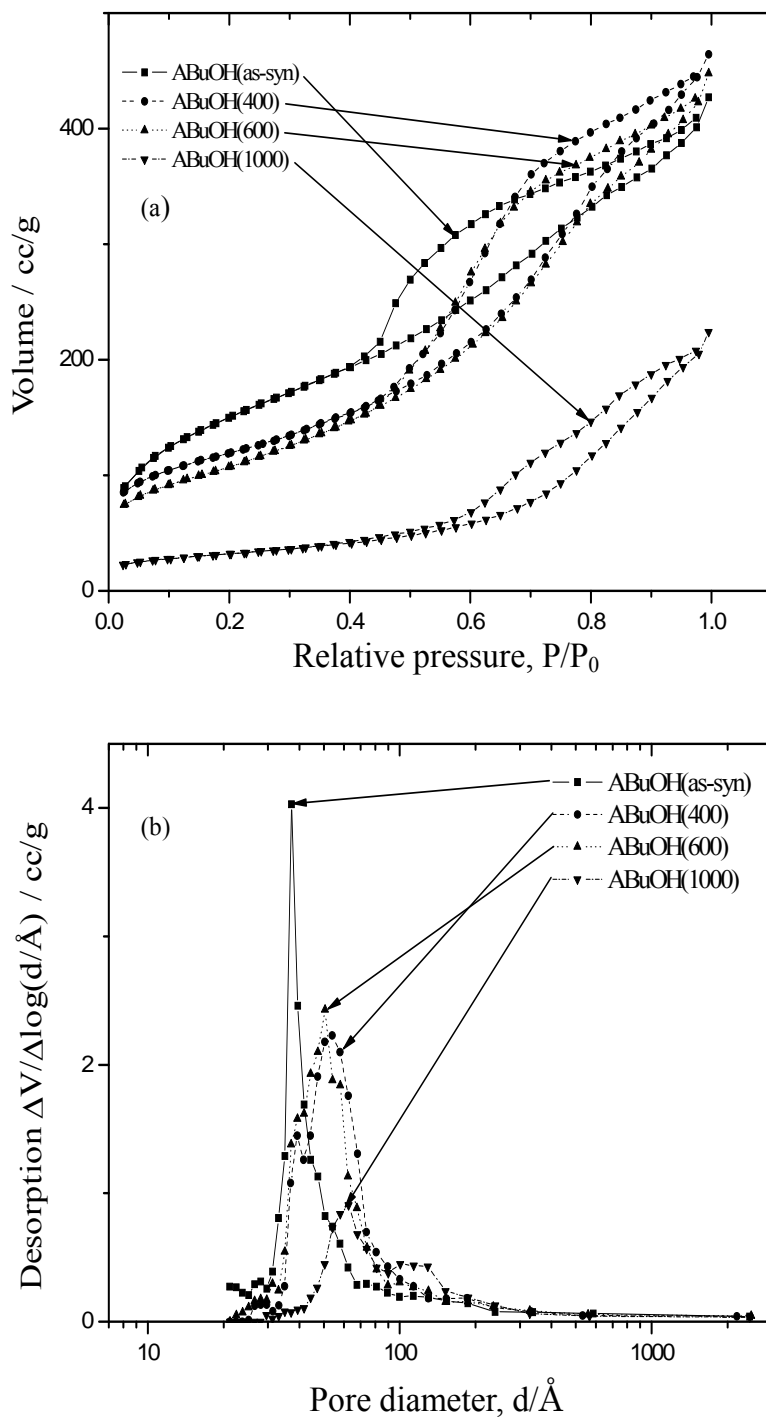
Fig. 1-8. Nitrogen adsorption isotherms (a) and pore-size distribution (b) of the aluminas obtained by the calcinaton of butyl derivative of boehmite at various temperatures.

maintained the boehmite structure at 300 °C and was converted to amorphous alumina at 400 °C. The γ-phase appeared by calcination in air at 800 °C for 30 min. The sample calcined at 1000 °C was composed of θ- and α-phases. The α-single phase was obtained by calcination at 1200 °C.

All of the other alkyl derivatives of boehmite were converted into γ-alumina through an amorphous phase by calcination at 1000 °C in air, and their XRD patterns were essentially identical irrespective of the solvents used.

1-3-4.   Pore structure of alumina derived from alkyl derivatives of boehmite

Nitrogen adsorption isotherms, and pore size distribution curves of some the products are shown in Figs. 1-7−1-9 and *t*-plots of all the products examined in this chapter are given in Fig. 1-10.

Although the aluminas derived from the ethyl derivative of boehmite exhibited rather complex N_2-adsorption isotherms (Fig. 1-7a), the *t*-plots (Fig. 1-10a) derived from the isotherms can be divided into 5 segments. At low *t* (statistical thickness; 0−3 Å) region (corresponding to low partial pressure of nitrogen), the plot seems to have a rather steep slope going through the origin, although only a few data points are available. In the second segment (3−7 Å), the slope decreased. The slope increased in the third segment (7−12 Å) and decreased again in the forth segment (12−18 Å) with a final increase at higher *t* region (>18 Å; fifth segment). The decrease of the slope from the first to the second segment is a typical phenomenon seen for microporous materials and is explained by micropore filling. It was reported that calcination of well-crystallized boehmite gives alumina having micropores with a slit-shape [20,21]. The crystallite sizes of the present products were relatively large, and much larger than
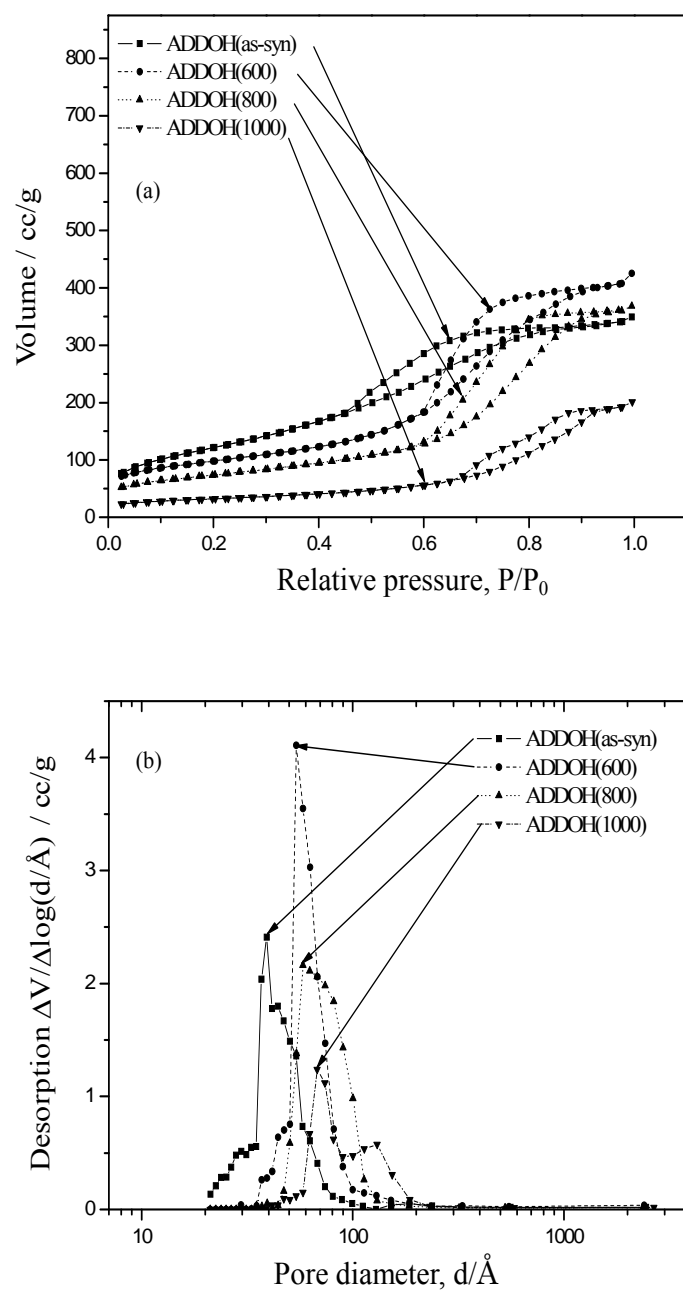
Fig. 1-9. Nitrogen adsorption isotherms (a) and pore-size distribution (b) of the aluminas obtained by calcinaton of the dodecyl derivative of boehmite at various temperatures.

pseudoboehmite usually obtained in aqueous systems. Therefore, the boehmite layer structure seems to give slit-shaped micropores on calcination. Hysteresis loop observed in the isotherms (Fig. 1-7a) supports the presence of slit-shaped pores in the AEtOH(600).

The increase in the slope at the middle partial pressure region (third segment) can be explained by capillary condensation of adsorbate molecules into mesopores. Gradual decrease in the slope in the third and forth segments suggests that the pore size distributed widely, which is verified by the pore-size distribution curve calculated by the BJH method (Fig. 1-7b). These pores seem to be formed in the rod-shaped pseudomorphous particles (ethyl derivatives of boehmite). The difference between the true densities of γ-alumina and the ethyl derivative of boehmite makes this pore. The large slope in the fifth segment indicates the presence of macropores, which can be also recognized from the pore-size distribution curve shown in Fig. 1-7b. Since the pore size is in the order of the size of rod-shaped particles, these pores are formed between pseudomorphous rod-shaped particles.

Partial formation of microporous structure of AEtOH(as-syn) is due to the elimination of a part of the alkyl groups during the drying stage prior to the N_2-adsorption measurement. Calcination of the product developed micro- and meso-pores because of the elimination of ethyl groups and collapse of the boehmite layer structure. Significant increase in mesopore volume is apparent. Further increase in the calcination temperature caused a significant decrease in micropore volume while mesopore volume was slightly decreased. This result suggests that the primary particles of alumina separated by micropores are easily sintered by heat treatment. On the other hand, macropores formed between the rod-shaped particles were not affected by
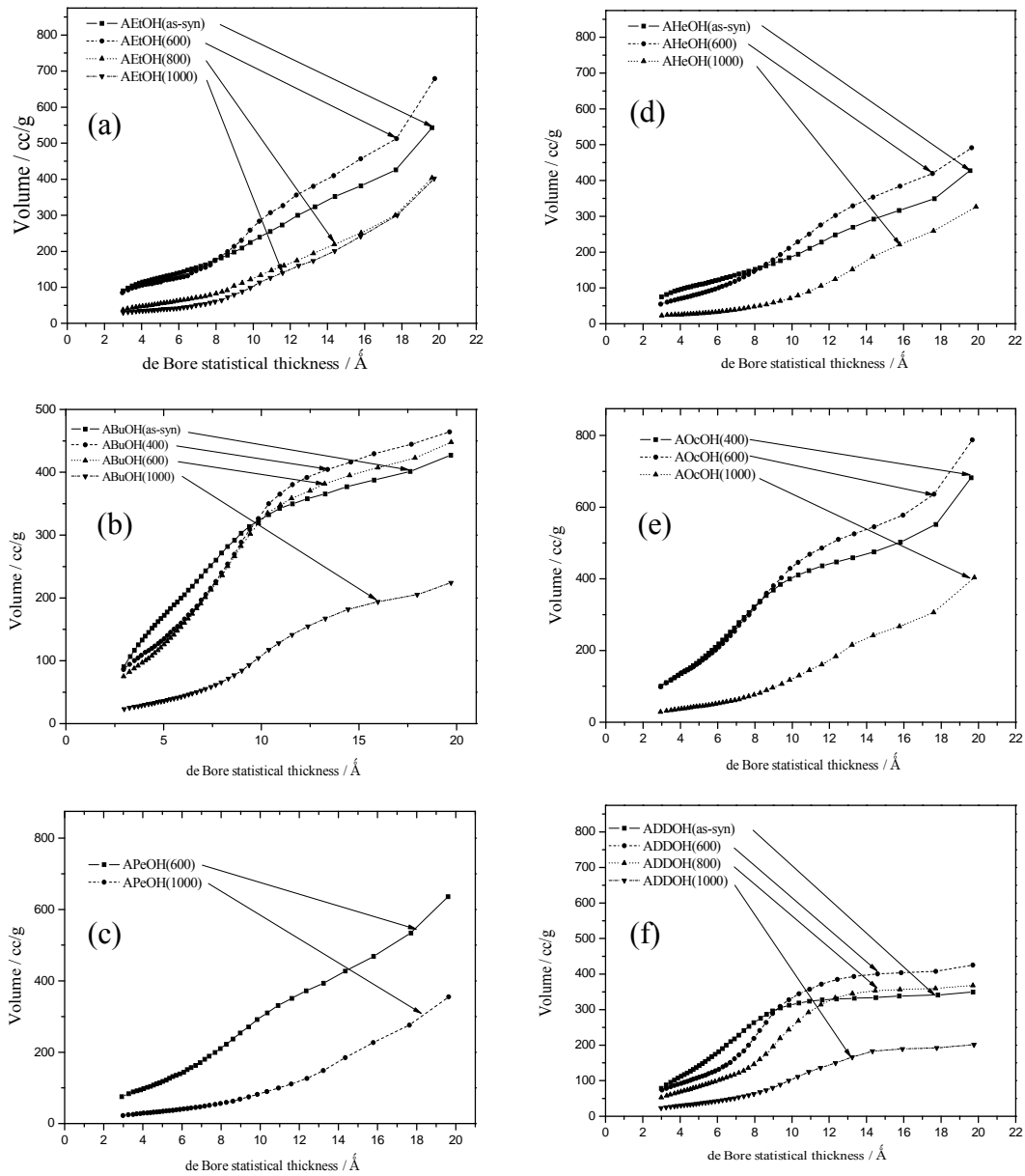
Fig. 1-10. *t*-Plots of the aluminas obtained by calcinaton of the alkyl derivatives of boehmite at various temperatures: (a) ethyl derivative boehmite; (b) butyl derivative boehmite; (c) pentyl derivative boehmite; (d) hexyl derivative boehmite; (e) octyl derivative boehmite; (f) dodecyl derivative boehmite.

45

calcination. This can be recognized by essentially identical slopes in the fifth segment and also by the pore-size distribution curves.

The aluminas derived from ABuOH showed *t*-plots (Fig. 1-10b) different from those obtained from AEtOH. The decrease in the slope from the first to second segments was not seen, indicating that the micropores were not present in the samples. The increase in the slope from the second to third segment was significant and third and forth segments are clearly distinguished, indicating that the pore size distributed in a narrow range, which is verified by the pore-size distribution curve (Fig. 1-8b). Macropores were not recognized. Hysteresis loop of these products suggests that tubular pores with narrow constriction were formed (Fig. 1-8a).

Nitrogen adsorption isotherms of AOcOH exhibited a similar tendency with ABuOH. However, an abrupt increase in the slope at high *t* region (fifth segment) was observed in AOcOH (Fig. 1-10e), indicating that macropores were present in these samples.

As for APeOH(600) and AHeOH(600), micropores were not recognized and the first and second segments are merged into one line going through the origin (Figs. 1-10c and 1-10d). This result can be explained by the boehmite layers separated by long alkyl groups. The forth and fifth segments are also merged. Usually the slope at high *t* region (forth segment) corresponds to the outer surface area after mesopores are filled by adsorbate molecules by capillary condensation. However, this is not the case because the slope at this region is much larger than the slope at low *t* region (the first segment; corresponding to the total surface area). Therefore, pores are formed between the irregularly-shaped particles (Fig. 1-5c), and the size of these pores distributes widely from meso- to macro- pore region.

Table 1-2 Physical properties of the alumina obtained by calcination of alkyl derivatives of boehmite at various temperatures.

Sample	Calcination Temp. (^{o}C)	Surface area (m^2/g)	Pore volume (cm^3/g)	mode pore size (nm)
AEtOH	as syn.	389	0.74	7.4
	600	346	1.02	6.8
	800	167	0.64	6.3
	1000	117	0.64	8.0
ABuOH	as syn.	543	0.63	3.7
	400	414	0.73	5.0
	600	390	0.73	5.1
	1000	112	0.37	5.8
APeOH	600	364	1.0	5.0
	1000	105	0.56	11.0
AHeOH	as syn.	389	0.47	9.0
	600	392	0.69	6.8
	1000	119	0.51	15.4
AOcOH	400	530	1.1	3.7
	600	513	1.27	5.0
	1000	136	0.65	6.2
ADeOH	as syn	444	0.71	3.7
	400	592	1.3	3.7
	600	469	1.2	4.2
	1000	157	0.76	6.2
ADDOH	as syn.	392	0.54	3.9
	600	338	0.69	5.4
	800	258	0.59	5.8
	1000	111	0.32	6.8

The most significant difference between the t plots of AHeOH(1000) and ADDOH(1000) is found in the slope at higher t region (Fig. 1-10f). Since the slope for ADDOH(1000) is smaller than the slope at low t region, the former corresponds to the outer surface area of the irregularly-shaped particles shown in Fig. 1-5d. The particles size was so large that the space between these particles is not recognized as pores by the nitrogen adsorption method.

The pore sizes of the aluminas derived from ADDOH(as-syn) can be assessed either by closure points of the hysteresis in the isotherms (Fig. 1-9a), by the regions of the third segments in the t-plots (Fig. 1-10f), or by the pore-size distribution curves (Fig. 1-9b). All the data suggest that the pore size increased with the increase in the calcination temperature. However, the increase in the pore size with the increase in the calcination temperature is much smaller than that for the ordinary aluminas derived from pseudoboehmite and crystalline aluminum hydroxides [22]. This indicates robustness of the pore structure of the alumina derived from the dodecyl derivative of boehmite, which is attributed to the well-developed layer structure of the precursor due to the strong interaction between the alkyl groups. Table 1-2 summarized the physical properties of the products.

1-4. Conclusions

The alumina derived from the ethyl derivative of boehmite had a broad pore-size distribution, while the pore-size of the aluminas obtained from the alkyl derivatives of boehmite with long alkyl chains distributed in a narrow range in the mesopore region. The mode pore diameter of the latter aluminas increased with an increase in calcination temperature (as-syn., 39 Å; 600 °C, 54 Å; 800 °C, 58 Å; 1000 °C,

68 Å; for ADDOH), but narrow pore-size distribution was maintained even after calcination at high temperatures. These results indicate that van der Waals interaction between the alkyl chains facilitated the formation of the boehmite layers having a fewer number of defects, and that the collapse of the well-developed boehmite layers gave aluminas with narrow pore-size distributions.

References

[1] D.L. Trimm, A. Stanislaus, *Appl. Catal*. 21 (1986) 215.

[2] A.C. Pierre, E. Elaloui, G.M. Pajonk, *Langmuir* 14 (1998) 66.

[3] F. Vaudry, S. Khodabandeh, M.E. Davis, *Chem. Mater*. 8 (1996) 1451.

[4] S.A. Bagshaw, T.J. Pinnavaia, *Angew. Chem. Int. Ed. Engl*. 35 (1996) 1102.

[5] W. Zhang, T.J. Pinnavaia, *Chem. Commun*. (1998) 1185.

[6] S. Valange, J.-L. Guth, F. Kolenda, S. Lacombe, Z. Gabelica, *Microporous Mesoporous Mater*. 35-36 (2000) 597.

[7] X. Zhang, F. Zhang, K.-Y. Chan, *Mater. Lett*. 58 (2004) 2872.

[8] W.-C. Li, A.-H. Lu, W. Schmidt, F. Schüth, *Chem. Eur. J*. 11 (2005) 1658.

[9] A. Ionescu, A. Allouche, J.-P. Aycard, M. Rajzmann, F. Hutschka, *J. Phys. Chem. B* 106 (2002) 9359.

[10] M. Inoue, H. Kominami, T. Inui, *J. Am. Ceram. Soc*. 73 (1990) 1100.

[11] M. Inoue, M. Kimura, T. Inui, *Chem. Mater*. 12 (2000) 55.

[12] M. Inoue, Y. Kondo, T. Inui, *Inorg. Chem*. 27 (1988) 215.

[13] M. Inoue, H. Tanino, Y. Kondo, *T. Inui, Clays Clay Miner*. 39 (1991) 151.

[14] J.J. Fripiat, H. Bosmans, P.G. Rouxhet, *J. Phys. Chem*. 71 (1967) 1097.

[15] M.C. Stegmann, D. Vivien, C. Mazieres, *Spectrichim. Acta, Part A* 29A (1973) 1653.

[16]. A.B. Kiss, G. Keresztury, L. Farkas, *Spectrochim. Acta. Part A* 36A (1980) 653.

[17] Y. Yacoub, R. Bata, M. Gautam, *Proc. Instn. Mech. Engrs. Part A* 212 (1998) 363.

[18] Y. Nakazaki, M. Inoue, *J. Phys. Chem. Solids* 65 (2004) 429.

[19] M. Kobayashi, S.-W. Kim, S. Iwamoto, M. Inoue, *J. Phys. Chem. Solid* 69 (2008) 1367.

[20] J.H. de Boer, B.C. Lippens, *J. Catal*. 3 (1964) 38.

[21] B.C. Lippens, J.H. de Boer, *J. Catal*. 4 (1965) 319.

[22] T. Inui, T. Miyake, Y. Takegami, *J. Jpn. Petrol. Inst*. 25 (1983) 242.

Chapter 2

Surface and Pore Structure of Alumina Derived from Xerogel/Aerogel

2-1. Introduction

In the Chapter 1, it is described that alumina obtained by the calcination of the alkyl derivatives of boehmite had quite a large pore diameter and pore volume, and the pore texture of alumina could be controlled by the choice of alcohols used as the solvents in the solvothermal reaction.

Various preparation methods have been reported to control the porosity of catalyst supports. Drying processes affect pores texture of the products because the surface tension of liquids present between primary particles aggregates them at the drying stage. Aerogel is obtained from a wet gel (or sol) prepared by a precipitation method such as an alkoxide process followed by drying with supercritical fluid, and it has a pore structure distinctly different from xerogel obtained from the wet gel by evaporation of the solvents. Many papers have discussed the pore structures of aerogel and xerogel [1−10]. The xerogel alumina usually has mesopores with a narrow pore−size distribution while the aerogel alumina has macroporous structures [1].

Many efforts have been made to improve the properties of aerogel and xerogel and most of the researches have used wet-gels prepared by alkoxide processes [9, 8]. However, several steps are needed to obtain aerogel or xerogel from the alkoxide

process. Therefore, in this chapter, the preparation of aerogel or xerogel by a simple procedure is discussed. The strategy is to directly dry the gel obtained in the solvothermal reaction in an autoclave by removing the solvent at the end of the reaction. By this method, aerogel or xerogel can be obtained simply by using only the reaction vessel. Thus, the alkyl derivatives of boehmite were prepared by the alcohothermal treatment of AIP and recovered as xerogel or aerogel and the pore-textures of the aluminas derived from the products were examined in this chapter.

2-2. Experimental

2-2-1. Synthesis of the alkyl derivatives of boehmite

Five alcohols, ethanol (EtOH, bp. 78.3 $^{\circ}$C, T_c. 240.9 $^{\circ}$C), 1-butanol (BuOH, bp. 117.7 $^{\circ}$C, T_c. 289.9 $^{\circ}$C), 1-hexanol (HeOH, bp. 157.5 $^{\circ}$C, T_c. 337.2 $^{\circ}$C), 1-octanol (OcOH, bp. 195 $^{\circ}$C, T_c.379.4 $^{\circ}$C) and 1-dodecanol (DDOH, bp. 259 $^{\circ}$C, T_c. 405.9 $^{\circ}$C) were used as the solvents for the solvothermal reaction. In a Pyrex test tube serving as an autoclave liner, AIP (12.5 g) and n-alcohol (130 ml) were placed, and the test tube was then placed in a 300 ml autoclave equipped with two valves, one of which was connected to a Liebig condenser of the stainless steel tubing. In the gap between the autoclave wall and the test tube was placed an additional 30 ml of n-alcohols. The autoclave was purged with nitrogen, heated to 300 $^{\circ}$C at a rate of 2.3 $^{\circ}$C/min, and held at 300 $^{\circ}$C for 2 h. The product was recovered by the xerogel preparation method reported previously [11]: After the solvothermal reaction, the valve of the autoclave was carefully opened to remove the organic vapor by flash evaporation while keeping the autoclave temperature at 300 $^{\circ}$C. The products were obtained directly as bulky solids. The obtained product was calcined at desired temperatures by heating at a rate of 10

°C/min and holding at that temperature for 30 min in static air in a furnace.

These products were designated by "A", the abbreviation for the medium used, and calcination temperatures in degree Celsius in parentheses. The original samples were specified by a term, "assyn".

2-2-2. Characterization.

Powder X-ray diffraction (XRD) patterns were recorded on a Shimadzu XD-D1 diffractometer using CuKα radiation and a carbon monochromator. Simultaneous thermogravimetric and differential thermal analyses (TG-DTA) were performed on a Shimadzu DTG-50 analyzer: A weighed amount (ca. 20 mg) of the sample was placed in the chamber of the analyzer, dried in a 40 ml/min flow of dried air until no further weight decrease was observed, and then heated at a rate of 10 °C/min in the same gas flow. Morphologies of the products were observed with a scanning electron microscope (SEM), Hitachi S-2500X. Nitrogen adsorption isotherms were measured at liquid-nitrogen temperature by the usual constant-volume method on a Quantachrome Autosorb-1 gas-sorption system; samples were previously outgassed at 300 °C for 30 min. Surface areas were calculated by applying the BET method to the adsorption data, taking the average area occupied by a nitrogen molecule as 0.162 nm^2. Pore-size distribution was calculated from the desorption branch of the isotherm by the BJH method. Infrared spectra were obtained on a JASCO FT/IR-470 Plus spectrophotometer using the usual KBr-pellet technique.

2-3. Results and discussion

2-3-1. Aerogel or xerogel obtained by direct removal of the solvent

The alkyl derivatives of boehmite were prepared by the solvothermal reaction of AIP with various alcohols, and were recovered as xerogel/aerogel. The XRD patterns of the products are shown in Fig. 2-1. For comparison, the XRD pattern of pseudoboehmite is also given in the figure. All the products except ADDOH(assyn) exhibited two XRD peaks at 50° and 65° 2θ, each of which is related the lattice parameters, *a* and *c*, of the boehmite structure (002 and 200 planes), respectively. The observed XRD pattern could be explained on the basis of the boehmite structure [12]. However, the interlayer spacing of (020) plane was much larger than that of the authentic boehmite and the peak gradually shifted to the lower angle side with an increase in carbon number of *n*-alcohols used as the solvents. These results indicate that the alky groups derived from the solvent alcohols are incorporated between the boehmite layers.

ADDOH(assyn) exhibited a different XRD pattern, which is attributed to γ-Al_2O_3. This result was obtained because dodecyl derivative of boehmite formed by the solvothermal reaction was converted to γ-Al_2O_3 during evaporation of 1-dodecanol; as this solvent has a high boiling point and requires a very long time of 120 min to be eliminated completely at 300 $^{\circ}$C, thermolysis of boehmite derivative to γ-Al_2O_3 occurs at the later stage of evaporation where there is only a small amount of the solvent. Evaporation of EtOH, BuOH, HeOH and OcOH requires short time of 10, 30, 40, 50, respectively.

The IR spectra of the products are given in Fig. 2-2. The authentic boehmite shows characteristic bands at 770, 651 and 492 cm^{-1} due to the vibration modes of the
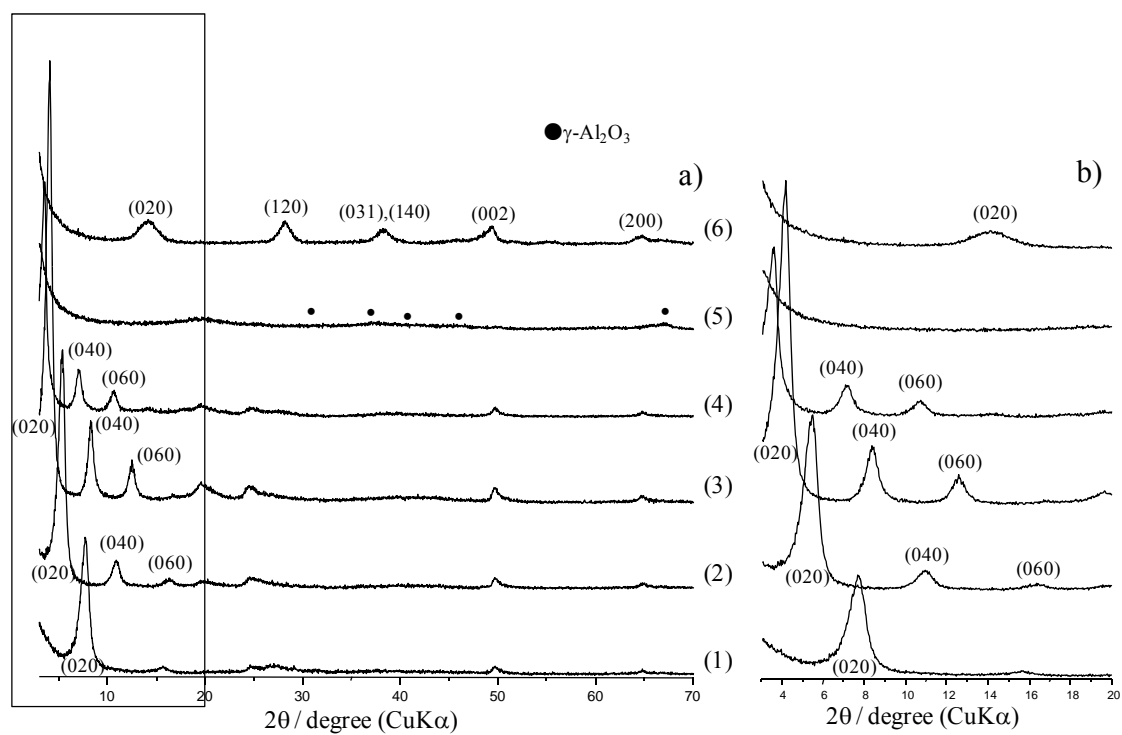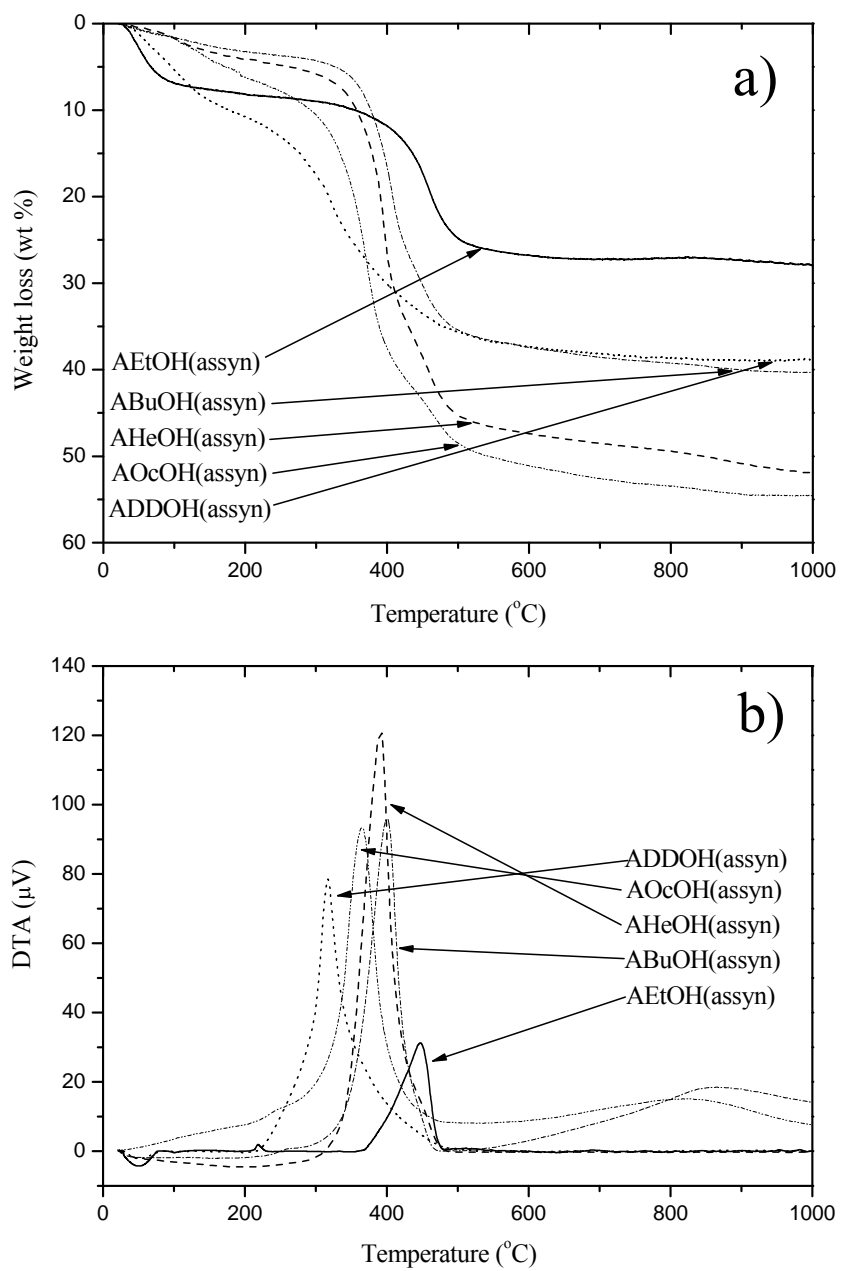
Fig. 2-1. X-ray diffraction patterns of the products recovered as xerogel/aerogel after solvothermal reaction of AIP in various alcohols: 1, AEtOH(assyn); 2, ABuOH(assyn); 3, AHeOH(assyn); 4, AOcOH(assyn); 5, ADDOH(assyn); 6, Pseudoboehmite.
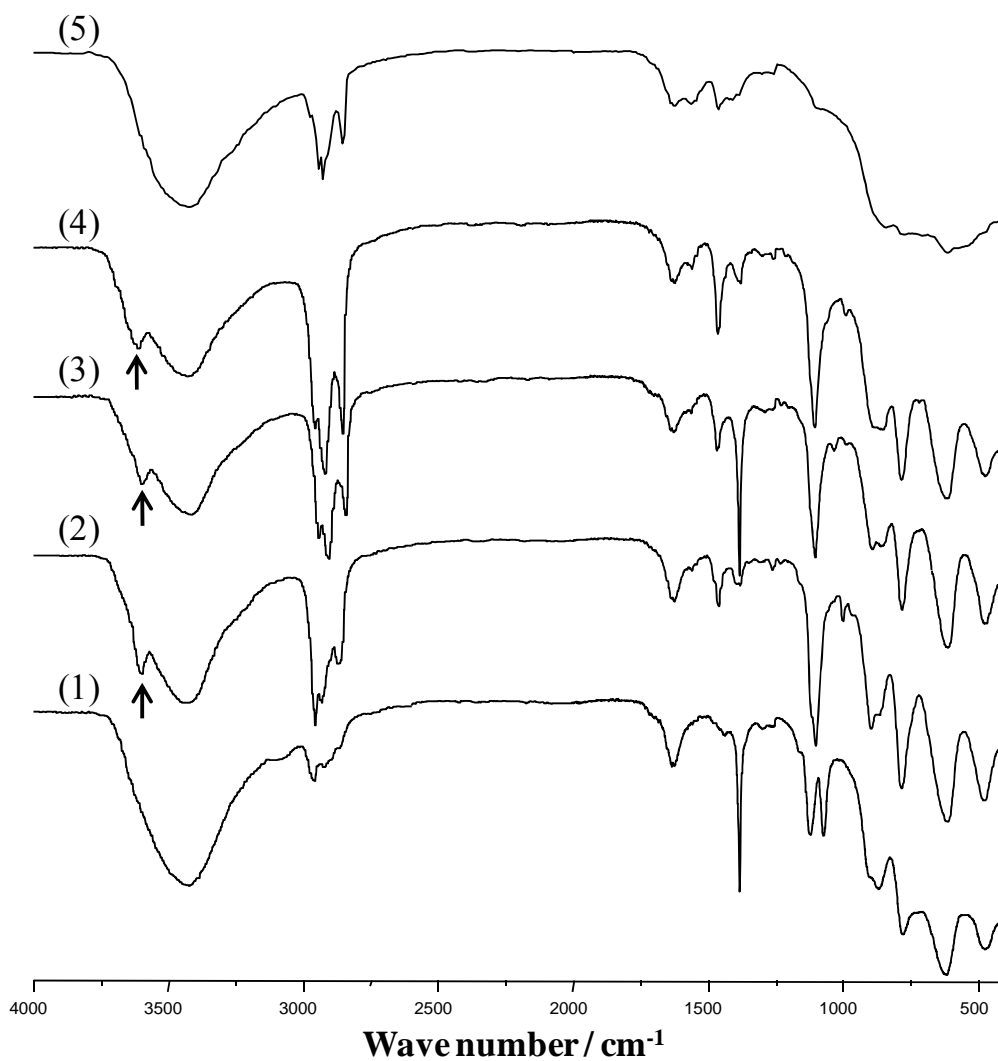
Fig. 2-2. IR spectra of the products recovered as xerogel/aerogel after solvothermal reaction of AIP in various alcohols: 1, AEtOH(assyn); 2, ABuOH(assyn); 3, AHeOH(assyn); 4, AOcOH(assyn); 5, ADDOH(assyn). The peaks indicated by arrows are due to the isolated OH groups remaining in the boehmite layers.

boehmite layers [13]. The present products showed these bands at around 780, 620 and 480 cm^{-1}. In ADDOH(assyn) whose XRD pattern is due to γ-Al$_2$O$_3$, a small amount of the undecomposed boehmite derivative seems to be present because of the presence of weak absorption bands due to the boehmite structure. Absorption bands due to the alkyl groups originated from the solvent used for the reaction were observed at around 3000–2800 (vCH), 1468 (δCH$_2$), 1390 (δCH$_3$) and 1115 (vCO) cm^{-1}. The bands characteristic of the hydrogen bonding between two adjacent boehmite layers (v_{as}OH, 3295 cm^{-1}; v_sOH, 3092 cm^{-1} for well crystallized boehmite) were not observed, but stretching vibration mode of isolated OH groups was clearly observed at 3603 cm^{-1} (indicated by the arrows in the figure). This band was not recognized in the research results described in Chapter 1, presumably because of the difficulty in removing water molecules by the usual drying procedure adopted in the previous work. Because the area occupied by an alkyl group attached to the boehmite layer is larger than that occupied by one OH group on the boehmite layer, only a part of OH groups on the boehmite layer are substituted with OR groups, and, therefore, isolated OH groups remain on the boehmite layers.

Fig. 2-3 shows the results of the thermal analyses of the products. The samples exhibited weight decreases at around 100 and around 400 ^{o}C, which were accompanied by endothermic and exothermic responses, respectively, in DTA. The endothermic process at around 100 ^{o}C is attributed to the desorption of physisorbed water. In Chapter 1, we reports that alkyl derivatives of boehmite exhibited two weight loss processes at around 300 (exothermic) and 400 ^{o}C (endothermic) due to combustion of the alkyl groups (exothermic) and collapse of the boehmite layers yielding amorphous alumina (endothermic), respectively. However, in the present samples, the combustion

Fig. 2-3. TG/DTA profiles of the products recovered as xerogel/aerogel after solvothermal reaction of AIP in various alcohols: a, TG; b, DTA.
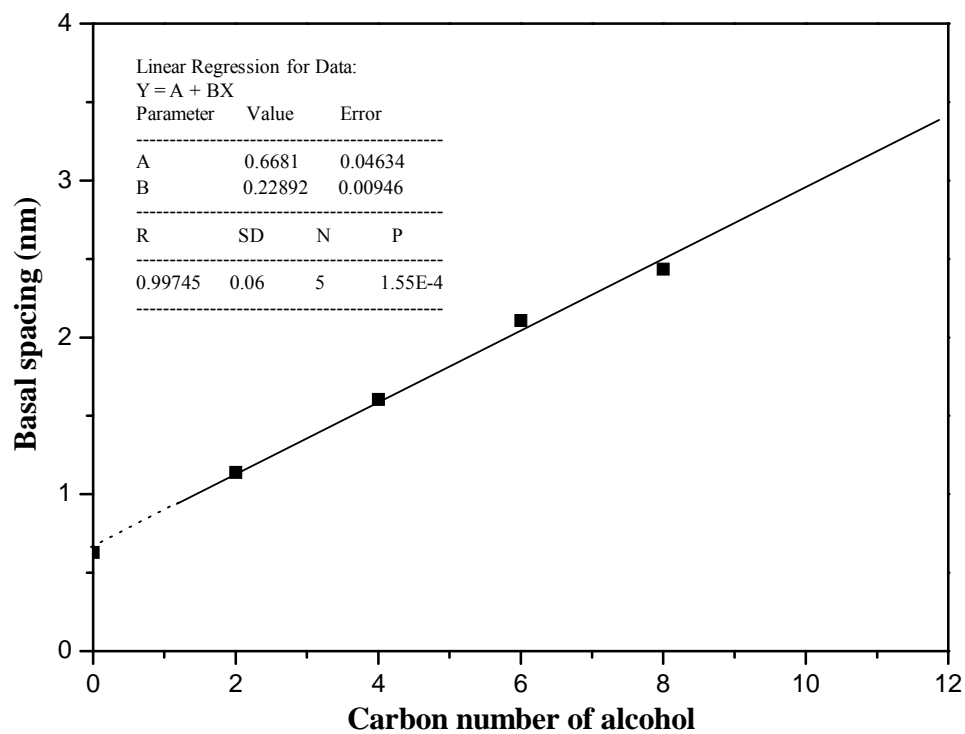
Fig. 2-4. Interlayer spacing of the aerogel/xerogel obtained by the reaction of aluminum triisopropoxide in straight-chain primary alcohols.

of the alkyl groups took place at a higher temperature and only one weight decrease process was observed at around 400 $^{\circ}$C. The endothermic response due to collapse of the boehmite layers was not observed even when the heating rate was decreased to 2 $^{\circ}$C/min. The increase in combustion temperature of the alkyl chains seems to be caused by an increase of crystallinity of the alkyl derivative of boehmite. Combustion of the alkyl groups incorporated between the well developed boehmite layers requires higher temperatures than that of the alkyl moieties incorporated between poorly crystallized boehmite layers because the former process requires long diffusion paths for oxygen molecule.

Because the molecular weight of ethanol is small as compared with other alcohols used in this study, the intensity of the exothermic peak as well as the total weight decrease is smallest among the samples.

ADDOH(assyn) showed an exothermic DTA process at lower temperature (317 $^{\circ}$C) as compared to other samples. This exothermic phenomenon is attributed to combustion of the alkyl groups remaining on the surface of γ-Al$_2$O$_3$ and/or in the alkyl derivative of boehmite (as detected by the IR spectrum). The results of the thermal analyses of the products are summarized in Table 2-1.

The basal spacing (i.e., spacing of the 020 plane of boehmite structure) of the present products calculated from XRD data is shown in the Fig. 2-4. The steady increase in the layer spacing with slope of 2.29 Å/CH$_2$ was observed. When the alkyl groups form a bilayer of fully extended (i.e., all-trans) alkyl chains, the tilt angle of the alkyl chain with respect to the boehmite layer can be calculated to be 64.4° on the basis of typical methylene repetition distance of 1.27 Å/CH$_2$ for all-trans polymethylene. Theoretically calculated tilt angle of alkyl groups with respect to the boehmite layer is

Table 2-1. Thermal analysis of the products recovered as xerogel/aerogel in the solvothermal reaction of AIP in n-alcohols.

Sample	Weight ratio (BD^a/Al_2O_3)	Ignition temperature (^{o}C)	Molecular fomular[b]
AEtOH (assyn)	1.25	446	$AlO(OH)_{0.21}(OEt)_{0.79}$
ABuOH(assyn)	1.56	400	$AlO(OH)_{0.48}(OBu)_{0.52}$
AHeOH(assyn)	1.84	392	$AlO(OH)_{0.51}(OHe)_{0.49}$
AOcOH(assyn)	1.79	365	$AlO(OH)_{0.53}(OOc)_{0.47}$
ADDOH(assyn)	-	317	$Al_2O_3^{C}$

a: Alkyl derivatives of boehmite.

b: Empirical formulas, $AlO(OH)_{1-x}(OR)_x$ were calculated from ignition losses determined by the TG analysis of the products; Et, CH_3CH_2-; Bu, $CH_3(CH_2)_3$; He, $CH_3(CH_2)_5-$; Oc, $CH_3(CH_2)_7$

c: Deduced from the XRD pattern

59.2°. This value is in good agreement with the value calculated from the basal spacing versus carbon number plot result shown in Chapter 1 (tilt angle, 60.5°). As for the present products, although the tilt angle (64.4°) calculated from the basal spacing vs carbon number plot is larger than that calculated in the result described in Chapter 1, this result maybe due to the fact that the present products have larger population of alkyl groups in the space between boehmite layers. These results together with the lack of IR bands due to the hydrogen bonding between two adjacent boehmite layers suggest that the alkyl groups derived from the solvent alcohols are incorporated between the boehmite layers.

The results obtained from XRD, IR and thermal analyses suggest that the present products (except ADDOH) had well-developed boehmite structures as compared with the product recovered by washing with methanol reported in chapter 1 [16]. Since the present products were obtained as xerogel/aerogel by removal of organic solvents at the reaction temperature, this process seems to be effective to increase the crystallinity by stacking the boehmite layers.

2-3-2. Calcined products.

The phase transformation of the products was investigated and the results are shown in Fig. 2-5. In the case of the products having well-developed boehmite structure (i.e., the products other than ADDOH), collapse of the boehmite structure yielded an amorphous alumina, from which γ-Al_2O_3 crystals began to be developed from 800 °C. Transformation into θ-Al_2O_3 started at 1000 °C. Transformation into α-Al_2O_3 was not completed even after calcination at 1200 °C, and XRD pattern due to θ-Al_2O_3 was observed in these samples. AEtOH(1200) preserved the θ-Al_2O_3 structure, although
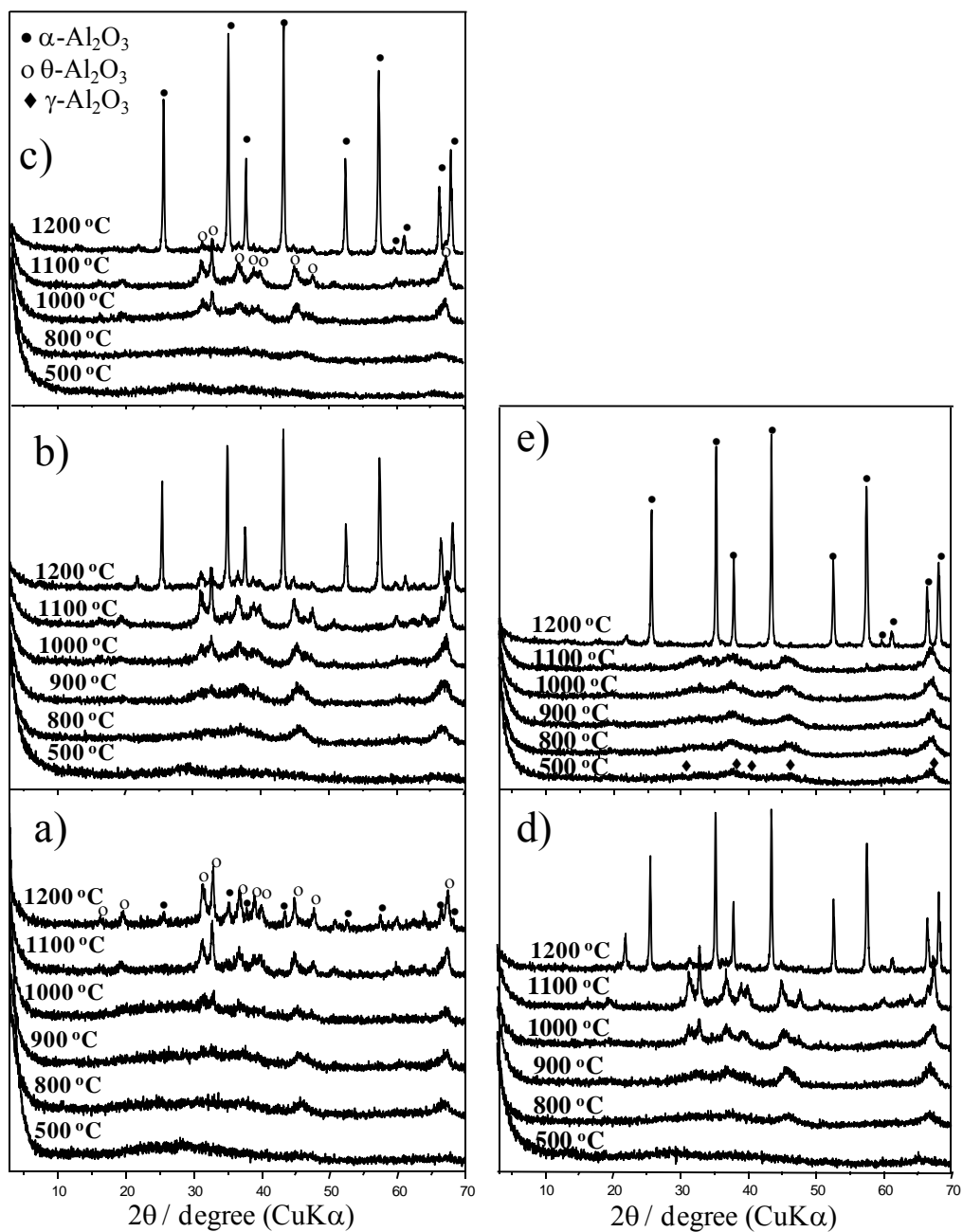
Fig. 2-5. X-ray diffraction patterns of the aluminas derived from xerogel/aerogel of the alkyl derivative of boehmite by calcination at temperatures specified in the figure: a, AEtOH; b, ABuOH; c, AHeOH; d, AOcOH; e, ADDOH.
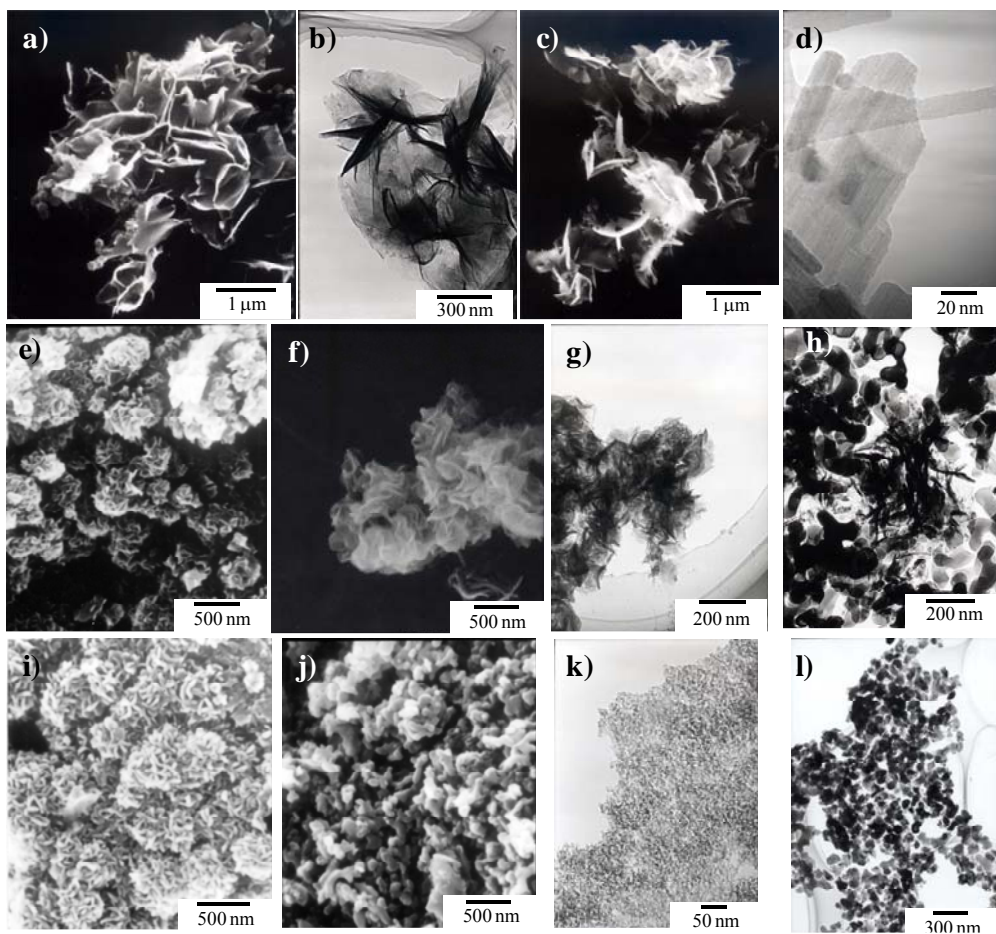
Fig. 2-6. SEM (a, c, e, f, i and j) and TEM (b, d, g, h, k and l) images of the products: a and b, AEtOH(assyn); c and d, AEtOH(1200); e, ABuOH(assyn); f and g, AHeOH(assyn); h, AHeOH(1200); i, AOcOH(assyn); j, AOcOH(1200); k, ADDOH(assyn); l, ADDOH(1200).

some peaks due to α-Al_2O_3 were observed in the XRD pattern. On the other hand, calcination of ADDOH(assyn) which was predominantly composed of γ-Al_2O_3 contaminated with a small amount of the dodecyl derivative of boehmite preserved the γ-Al_2O_3 structure at 1100 ^{o}C. However, θ-Al_2O_3 phase was not developed and γ-Al_2O_3 was directly converted into α-Al_2O_3 at 1200 ^{o}C. Retardation of the transformation into α-Al_2O_3 for the samples having well-developed boehmite structure is caused by excessive growth of the θ-Al_2O_3 structure. Because the θ-Al_2O_3 phase is thermodynamically more stable than γ-Al_2O_3, growth of the former phase retards the development of α-Al_2O_3. It is generally accepted that transformation of metastable alumina phases into α-Al_2O_3 starts to occur by sintering at the contact points between primary particles, and it is reported that the kinetic of the transformation of metastable aluminas into α-Al_2O_3 can be restrained by controlling particle morphology to minimize the contact points between primary particles, fibrous morphology being desired [14]. The result that transformation of AEtOH into α-Al_2O_3 was suppressed suggests that alumina derived from AEtOH has a smaller number of contact points between primary particles as compared with other samples. Because this product was recovered by the removal of the solvent in a super-critical state, the dried product has large voids filled with air. ABuOH(assyn) was also recovered as an aerogel and a fairly large portion of θ-Al_2O_3 remained in the sample calcined at 1200 ^{o}C, while the other samples (solvents larger than BuOH) were obtained from wet gels by evaporation of subcritical state solvents and have α-form after 1200 ^{o}C calcination. This result shows that, aerogel flocculated less firmly than xerogel.
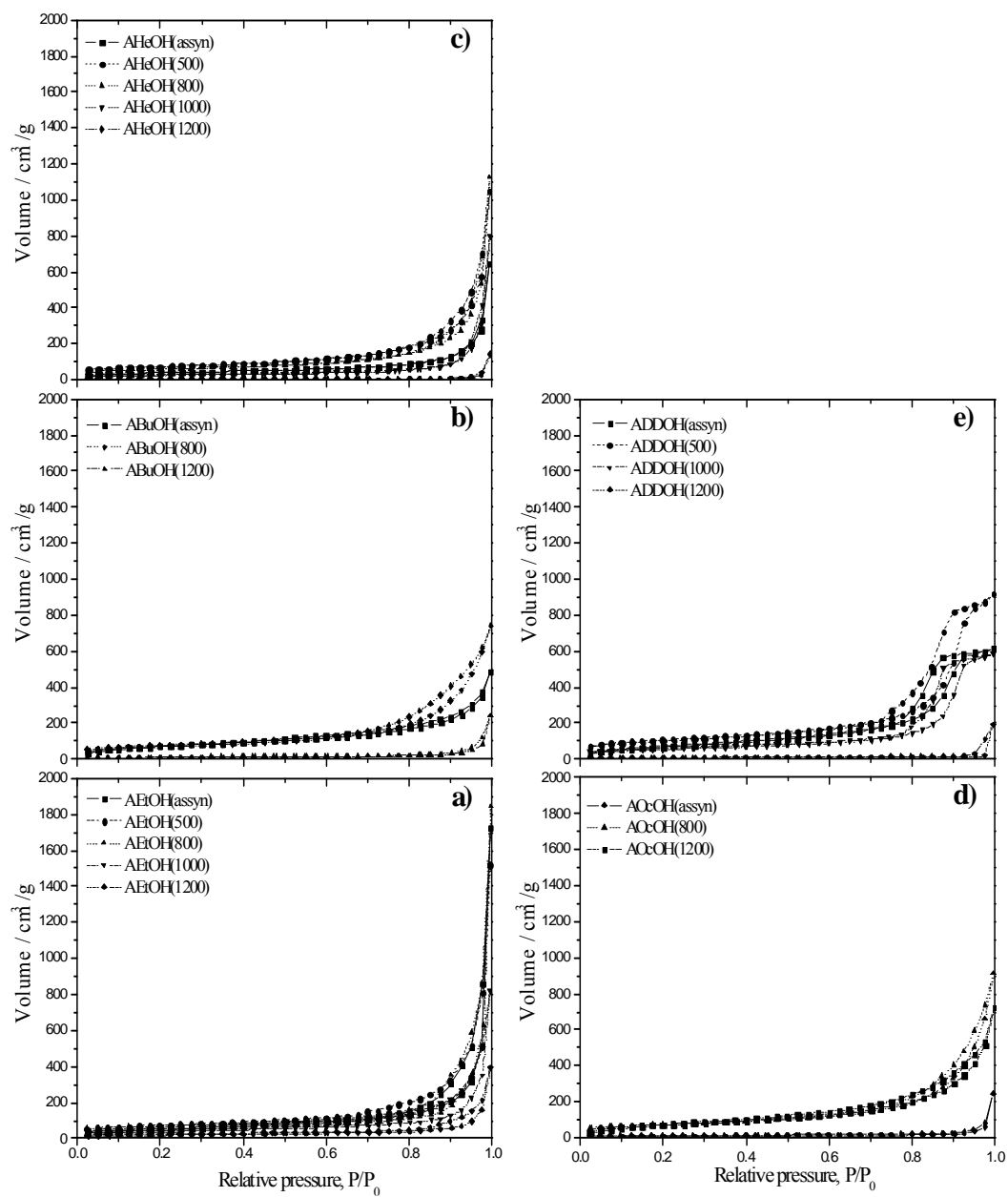
Fig. 2-7. Nitrogen adsorption isotherm of the products recovered as xerogel/aerogel (assyn) after solvothermal reaction of AIP in solvents specified in the figure and alumina obtained by calcination thereof in air at temperatures specified in the figure: a, AEtOH; b, ABuOH; c, AHeOH; d, AOcOH; e, ADDOH.

2-3-3. Morphological aspects.

Morphologies of the products are shown in Fig. 2-6. The products having well-developed boehmite were composed of plate like particles (Figs. 2-6a, b, e–g and i) and similar morphology was observed for the glycol derivative of boehmite. The plate-like structure was developed well in AEtOH(assyn) (Figs. 2-6a and b), and this morphology was maintained even after calcination at 1200 ^{o}C (Figs. 2-6c and d). In the case of the other samples calcined at 1200 ^{o}C, the vermicular morphological characteristic of α-Al$_2$O$_3$ particles were observed (Figs. 2-6h, j and l). These results indicate that plate structures suppress the transformation rate to α-Al$_2$O$_3$. ADDOH(assyn) was composed of particles less than 10 nm and plate-like particles were not observed (Fig. 2-6k). Each α-Al$_2$O$_3$ particle obtained by calcination at 1200 ^{o}C was rather small and a fairly large surface area was preserved for ADDOH (8 m^2/g) even after calcination at 1300 ^{o}C (Table 2-2).

2-3-4. Pore textures of the products.

The nitrogen adsorption isotherms of the products and aluminas obtained by calcination thereof are shown in Fig. 2-7. The products having a well-developed boehmite structure showed similar isotherms. The hysteresis loops can be classified to type H-3 [15], which can be explained by the presence of slit-shaped pores formed between well-developed plate-like particles of the boehmite derivatives (Figs. 2-6a–g, i and j).

On the other hand, ADDOH showed an N$_2$ adsorption isotherm different from those of other samples. The hysteresis of the isotherms belongs to H-1 type [15], which can be explained by porous materials made of agglomerates or compacts of
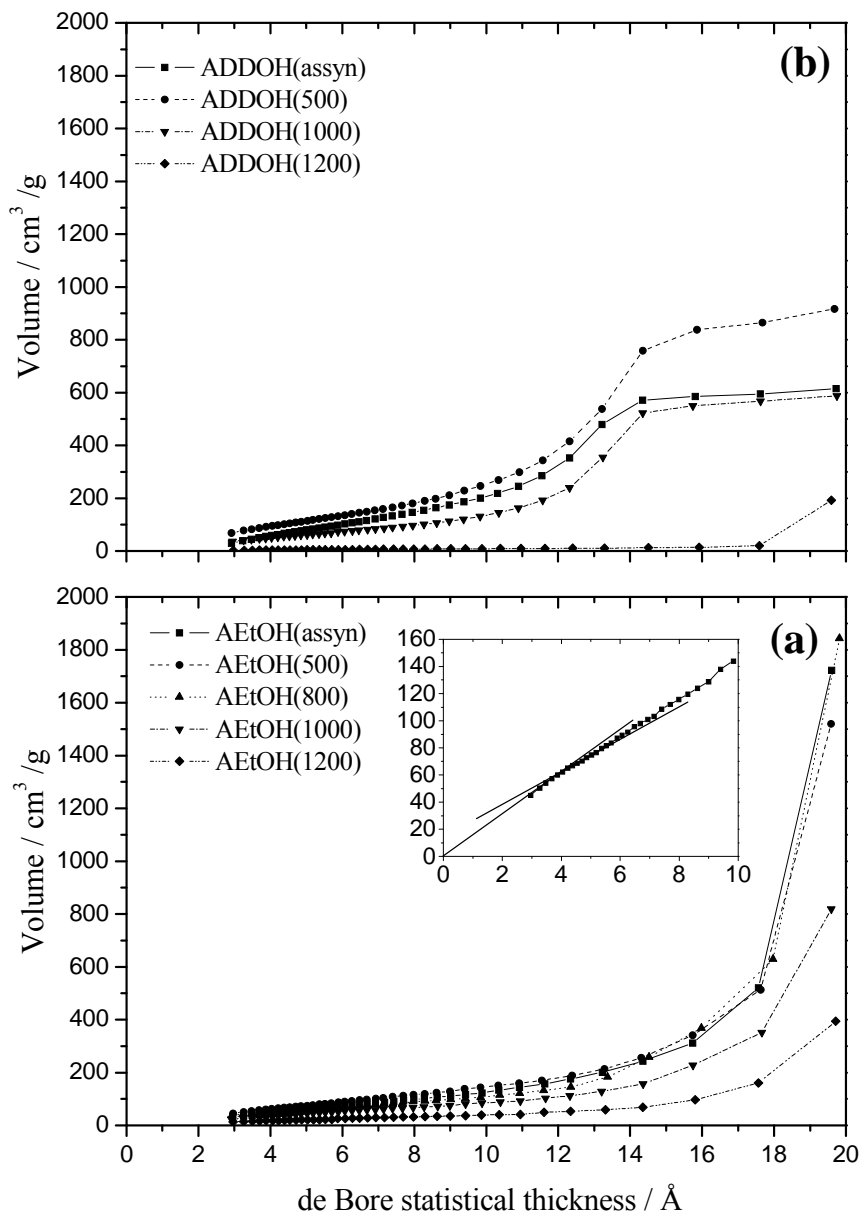
Fig. 2-8. *t*-Plots of the products recovered as xerogel/aerogel after solvothermal reaction of AIP: a, AEtOH; b, ADDOH. Inset figure (a) shows the expanded plot for AEtOH(500).
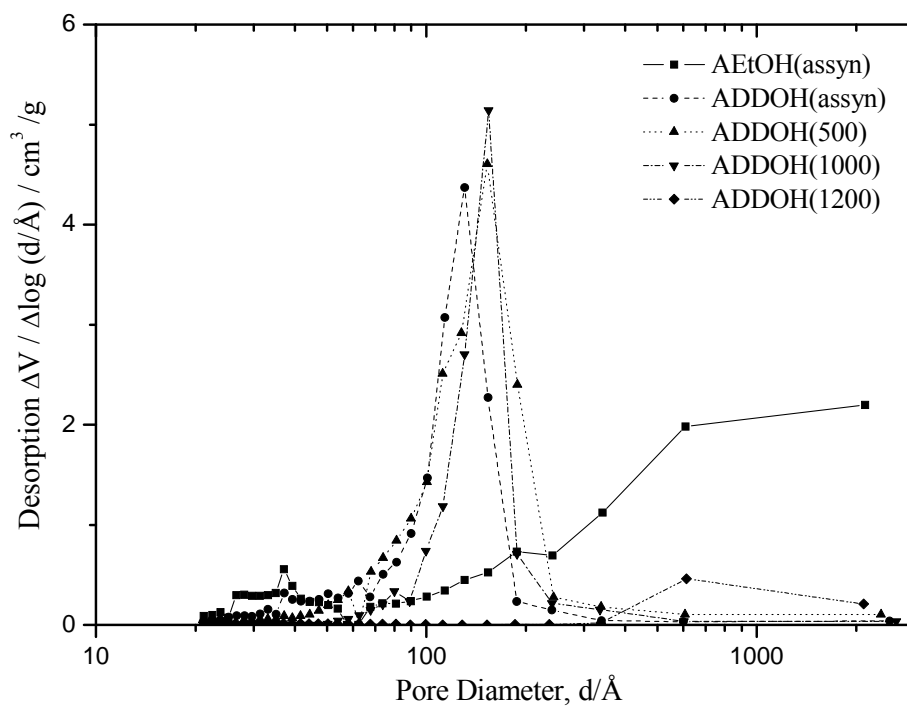
Fig. 2-9. Pore-size distribution of the products recovered as xerogel/aerogel after solvothermal reaction in the solvents specified in the figure.

approximately uniform spheres having a narrow size distribution. AEtOH(assyn) which was composed of well developed plate-like particles (Figs. 2-6a-d) showed larger nitrogen uptakes (larger pore volume) than the other samples (Table 2-2), indicating that capillary condensation of nitrogen took place between well-developed plate-like particles.

The t-plot of AEtOH(assyn) can be divided into two segments (Fig. 2-8a). In the first segment at the lower t region, the plots went through the origin. In the second segment at the high-t-region the slope of the t-plot increased. The increase in the slope in the second segment is due to capillary condensation of nitrogen into meso- and macro-pores, suggesting this sample had pores whose sizes are larger than those can be assessed by the nitrogen adsorption method. In the t-plots of AEtOH(500), a slight decrease in the slope was observed at mid-t-region, which is explained by micropore filling. This result indicates that the formation of amorphous alumina by the collapse of boehmite layers is associated with formation of micropores. The amount of nitrogen adsorbed on the aluminas decreased with the increase in calcination temperature. Since transformation from metastable alumina phase to α-Al_2O_3 was retarded, AEtOH(1200) had a relatively large surface area and pore volume (Table 2-2).

The t-plot of ADDOH(assyn) showed a tendency completely different from those of the other samples (Fig. 2-8b). The t-plot of ADDOH(assyn) can be divided into 4 segments. In the first segment, (low t region) the slope has a rather steep slope going through the origin. In the second segment, the slope of the t-plot slightly decreased and a large increase in the slope was observed at the med-t-region (third segment) and the slope decreased at high-t-region. The slight decrease in the slope between the first and second segments is due to the micropore filling, suggesting that this sample had

71

Table 2-2. Physical properties of the products recovered as xerogel/aerogel after solvothermal reaction of AIP.

Sample	Calcination temperature (°C)	Bulk density (g/cm^3)	surface area (m^2/g)	Pore volume (cm^3/g)	Mode pore diameter (nm)
AEtOH	assyn	0.11	177	2.6	213
	500	0.13	232	2.21	209
	800	0.1	195	2.56	299
	1000	0.14	141	1.16	210
	1200	0.11	66	0.56	250
ABuOH	assyn	0.1	266	0.69	4
	800	0.15	241	1.1	154
	1200	0.21	28	0.36	239
AHeOH	assyn	0.16	132	1.02	229
	500	0.12	243	1.6	60
	800	0.1	199	1.73	61
	1000	0.11	80	1.24	34
	1200	0.23	7	0.23	227
AOcOH	assyn	0.09	278	1.09	15
	800	0.12	255	1.35	15
	1200	0.22	28	0.35	252
ADDOH	assyn	0.39	265	0.98	13
	500	0.24	355	1.35	15
	1000	0.27	193	0.88	16
	1200	0.44	14	0.28	61
	1300	0.45	8	0.28	231

micropores. The large increase in the slope between the second and third segments is due to capillary condensation, and relatively narrow third segment region suggests that the pore-size distributed in a narrow range. The narrow pore size distribution was actually verified in the pore size distribution curves (Fig. 2-9). The product was composed of small primary particles with the size less than 10 nm (Fig. 2-6k), and the voids formed between the primary particles corresponded to the pores in meso region. Although this product completely converted into α-alumina at 1200 ^{o}C, the particles size was about 100 nm (Fig. 2-6l) which is relatively small as compared with α-Al_2O_3 obtained by ordinary methods.

2-4. Conclusions

Aerogel or xerogel was directly obtained by drying the gel obtained by the solvothermal reaction in an autoclave by removing the solvent at the end of the reaction. The products, alkyl derivatives of boehmite, had higher crystallinity than the products recovered by the conventional drying process. Aluminas derived from these products had large pore volumes (AEtOH(800), 2.56 cm^3/g; ABuOH(800), 1.1 cm^3/g; AHeOH(800), 1.73 cm^3/g; AOcOH(800), 1.35 cm^3/g; ADDOH(500), 1.35 cm^3/g). For AEtOH which was recovered as an aerogel, transformation into α-Al_2O_3 was retarded even after calcination at 1200 ^{o}C and θ-Al_2O_3 was mainly observed.

References

[1] G. Tournier, M. Lacroix-Repellin, G.M. Pajonk, Preparation of Catalysts IV (Studies in Surface Science and Catalysis, Vol. 31) (Elsevier, Amsterdam, 1987) 333.

[2] R. Tleimat-Mazalji, D. Bianchi, G. M. Pajonk, Appl. Catal. A: General, 101 (1993) 339.

[3] T. Skapin, E. Kemnitz, Catal. Lett., 40 (1996) 241.

[4] H. Hirashima, C. Kojima, H. Imai, J. Sol-Gel Sci. Thecnol., 8 (1997) 843.

[5] T. Horiuchi, L. Chen, T. Osaki, T. Mori, Catal. Lett., 72 (2001) 77.

[6] A. G. Sault, A. Martino, J. S. Kawola, E. Boespflug, J. Catal., 191 (2000) 474.

[7] A. F. Popa, L. Courthéoux, E. Gautron, S. Rossignol, C. Kappenstein, Eur. J. Inorg. Chem., (2005) 543.

[8] L. Courthéoux, F. Popa, E. Gautron, S. Rossignol, C. Kappenstein, J. Non-Cryst. Solids, 350 (2004) 113.

[9] E. Elaloui, A. C. Pierre, G. M. Pajonk, J. Catal., 166 (1997) 340.

[10] Y. De Hazan, G. E. Shter, Y. Cohen, C. Rottman, D. Avnir, G. S. Grader, J. Sol-Gel Sci. Thecnol., 14 (1999) 233.

[11] S. Iwamoto, K. Saito, K. Kagawa, M. Inoue, Nano Lett.,1 (2001) 417.

[12] M. Inoue, H. Tanino, Y. Kondo, T. Inui, Clays Clay Miner., 39 (1991) 151.

[13] A.B. Kiss, G. Keresztury, L. Farkas, Spectrochim. Acta., 36A (1980) 653.

[14] J. A. Schwarz, C. Contescu, A. Contescu, Chem. Rev., 95 (1995) 477.

[15] F. Rouquerol, J. Rouquerol, K. Sing, Adsorption by Powders and Porous Solids Principles, Methodology and Applications (Academic Press, San Diego, CA, 1999).

[16] S.-W. Kim. S. Iwamoto and M. Inoue, J. Porous Mater., in press.

Chapter 3

Effects of Feed Ratio on the Pore Structure of Alumina derived from alkyl derivatives of boehmite obtained by the Solvothermal Reaction

3-1. INTRODUCTION

Preparation of the aerogel/xerogel by directly drying a gel obtained by the solvothermal reaction in an autoclave by removing the solvent at the end of reaction is shown in Chapter 2. Transformation into Al_2O_3 from these aerogel/xerogel products was controlled by the kinds of used solvents in the reaction. These Al_2O_3 thus obtained had a relatively large pore volume which was in 1.35−2.56 cc/g range. The kinds of n-alcohols used in the reaction affected the phase, morphology, and surface structure of the obtained alumina. This result indicates that expanded volume of solvents at reaction temperature (300 ^{o}C) remains with void in products by removal of solvents at reaction temperature and these voids contribute to increase pore volume in final product.

In this chapter, to obtain alumina having large pore volume by expansion of products volume in autoclave, the solvothermal reaction of various feed ratio of reactants in autoclave having total volume 300 ml have been tried. Among the n-alcohols, ethanol and 1-hexanol were used as solvent and pore-textures of alumina derived from the products obtained by the controlled feed ratio in solvothermal reaction were investigated.

3-2. EXPERIMENTAL

3-2-1. Synthesis of the alkyl derivatives of boehmite

In a Pyrex test tube serving as an autoclave liner, prescribed amounts of ethanol (EtOH) or 1-hexanol (HeOH) and AIP were charged, and the test tube was then placed in a 300-ml autoclave equipped with two valves, one of which was connected to a Liebig condenser of stainless steel tubing. In the gap between the autoclave wall and the test tube was placed an additional 30 ml of the reaction solvent. The autoclave was purged with nitrogen, heated to 300 ^{o}C at a rate of 2.3 ^{o}C/min, and held at 300 ^{o}C for 2 h. The product was recovered by a xerogel preparation method reported previously [1]: After the solvothermal reaction, the valve of the autoclave was slightly opened to remove the organic vapor while keeping the autoclave temperature at 300 ^{o}C. The products were obtained directly as bulky solids. For comparison, the product which was formed under the same reaction conditions as mentioned above was recovered by a washing process with methanol after the assemble was cooled to room temperature. The obtained products were calcined at various temperatures by heating at 10 ^{o}C/min and holding at that temperature for 30 min in a static air in an electric furnace.

The products recovered as aerogel by the removal of supercritical ethanol were designated by "AA" and the products recovered as xerogel by the removal of subcritical hexanol is called "AX", while the product recovered by the washing process with methanol was expressed as "AM". These abbreviations were further accompanied by an abbreviation for the medium used in the alcohothermal treatment, quantities of AIP (gram)-solvent (milliliter) used for the reaction, and calcination temperatures in degree Celsius in parentheses. The original samples are specified by a term, "assyn", in parentheses. Note that the surface tension of a liquid at a temperature near its critical

point has a quite small value; therefore, coagulation of the product particles due to the surface tension of the liquid remaining between the particles at the drying stage was avoided.

3-2-2. Charaterization

Powder X-ray diffraction (XRD) was measured on a Shimadzu XD-D1 diffractometer using CuKα radiation and a carbon monochromator. The crystallite size was estimated by the Scherrer equation. Simultaneous thermogravimetric and differential thermal analyses (TG-DTA) were performed on a Shimadzu DTG-50 analyzer: A weighed amount (ca. 20 mg) of the sample was placed in the analyzer, dried in a 40 ml/min flow of dry air until no further weight decrease was observed, and then heated at a rate of 10 $^{\circ}$C/min in the same gas flow. Morphologies of the products were observed with a scanning electron microscope (SEM), Hitachi S-2500X, and a transmission electron microscope (TEM), Hitachi H-800, operated at 200 kV. The TEM specimen was prepared by dipping a microgrid in a solution in which samples are dispersed. Nitrogen adsorption isotherms were measured at the liquid-nitrogen temperature by the usual constant-volume method on a Quantachrome Autosorb-1 gas-sorption system and samples were previously outgassed at 300 $^{\circ}$C for 30 min. Surface areas were calculated by applying the BET method to the adsorption data, taking the average area occupied by a nitrogen molecule as 0.162 nm^2. Pore-size distribution was calculated from the desorption branch of the nitrogen adsorption isotherm by the BJH method. Infrared spectra were obtained on a JASCO FT/IR-470 Plus spectrometer using the usual KBr-pellet technique. Temperature-programmed desorption (TPD) of NH_3 and CO_2 was measured using a fixed-bed flow reactor. After

the samples were pretreatment at 500 $^{\circ}$C in a helium flow for 1 h, the samples were exposed to a reaction gas composed of 100 % NH_3 or CO_2 at 50 $^{\circ}$C for 1 h. Then, the sample was purged with a 100 ml/min flow of helium for 1 h. The temperature was raised to 500 $^{\circ}$C at a rate of 10 $^{\circ}$C/min in the same helium flow with continuously analyzing the effluent gases from the reactor with a Q-mass spectrometer.

3-3. RESULTS AND DISCUSSION

3-3-1. Effect of the feed ratio of the reactant to solvent.

The XRD patterns of the products obtained by the solvothermal reaction of AIP in ethanol/1-hexanol under various feed ratios of the reactant to the solvent are shown in Fig. 3-1. AAEt(12.5-70)-(assyn) showed a low intensity peak due to basal planes of the ethyl derivative of boehmite and the boehmite structure was only poorly developed. When the feed ratio of AIP to ethanol was increased, the XRD pattern of the product (AAEt(12.5-50)-(assyn)) showed a diffraction peak at $2\theta = 42.6^{\circ}$. This peak corresponds to the prohibited 321 diffraction of the spinel structure and clearly indicates the formation of χ-Al_2O_3 [2-4]. χ-Alumina is a modification of transition aluminas and is a dehydrated phase of gibbsite ($Al(OH)_3$). It has been generally believed that χ-Al_2O_3 can only be prepared by dehydration of gibbsite, but we reported that thermal decomposition of AIP in non-polar solvents such as toluene yielded χ-Al_2O_3 [5, 6]. In the present case, because the amount of ethanol used for the reaction was insufficient to react with AIP, the intermediate phase seemed to thermally decompose to χ-Al_2O_3 before developing the structure of the ethyl derivative of boehmite. To elucidate the reaction mechanism, solvothermal reactions of AIP in branched-chain alcohols (isobutyl
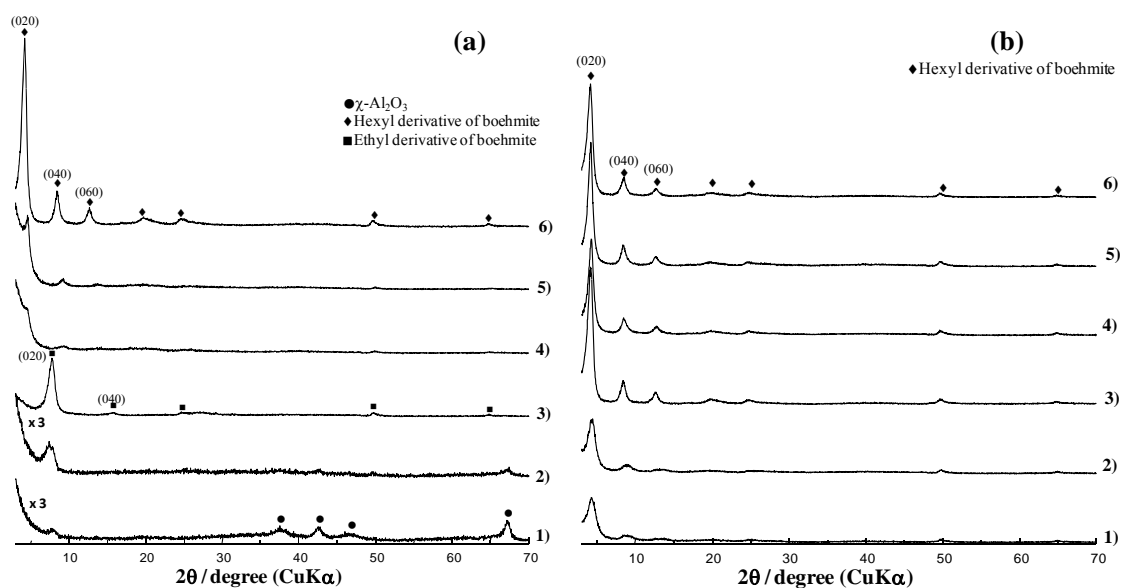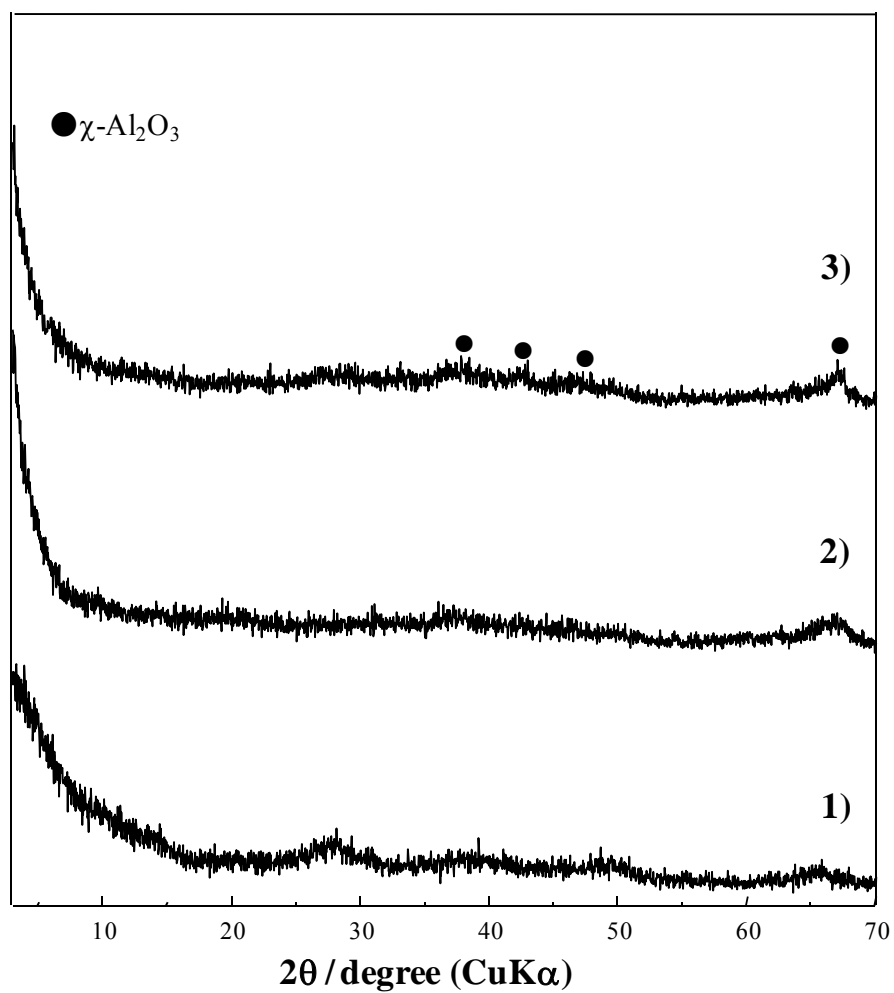
Fig. 3-1. X-ray diffraction patterns of the products.

(a) Products obtained by the direct drying process.

1), AAEt(12.5-50)-(assyn); 2), AAEt(12.5-70)-(assyn); 3), AAEt(12.5-130)-(assyn); 4), AXHe(12.5-50)-(assyn); 5), AXHe(12.5-70)-(assyn); 6), AXHe(12.5-130)-(assyn).

(b) Products obtained by washing with metahnol.

1), AMHe(12.5-50)-(assyn); 2), AMHe(12.5-70)-(assyn); 3), AMHe(12.5-130)-(assyn); 4), AMHe(3-50)-(assyn); 5), AMHe (3-70)-(assyn); 6), AMHe (3-130)-(assyn).

Fig. 3-2. X-ray diffraction patterns of the products obtained by
solvothermal reaction of AIP in: 1), isobutyl alcohol;
2), 2-ethyl-1-hexanol; 3), 2-propanol.

alcohol and 2-ethyl-1-hexanol) and in a secondary alcohol (isopropyl alcohol) were examined, and XRD patterns of the products are given in Fig. 3-2. The reactions yielded amorphous/χ-Al$_2$O$_3$ phases but alkyl derivatives of boehmite were not formed. These results indicate that van der Waals interaction between the alkyl chains is the prime factor for the formation of the alkyl derivative of boehmite. Note that the reaction of aluminum 2-butoxide in 2-butanol was examined by Fanelli and Burlew [7]. They expected that water formed by dehydration of the alcohol hydrolyzes the alkoxide and found well-crystallized boehmite was formed. In the present work, well-crystallized boehmite was not detected in the product of the reaction of AIP in 2-propanol. Further work is required to find the reason for this discrepancy.

In Fig. 3-3, the crystallite sizes of the hexyl derivative of boehmite calculated on the basis of the half-height width of 040 peak ($2\theta = 8.4°$) are plotted against the AIP/hexanol ratio. With the decrease in this ratio, the layer structure of the product developed well. In other words, sufficient crystal growth does not occur in the presence of a large amount of AIP in the hexanol solution. During the reaction, alkoxyl exchange takes place between AIP and hexanol yielding aluminum hexoxide and 2-propanol. This reaction is reversible, and when the AIP/solvent ratio is large, the number of 2-propoxy groups remaining in the coordination sphere of aluminum is also large. Thermal decomposition of the intermediate gives the layer structure of boehmite; however, the presence of 2-propyl groups in n-alkyl layers weakens van der Waals interaction between the alkyl groups, leading to the suppression of boehmite layer formation. In fact, with the increase in AIP/hexanol ratio, the 020 peak slightly shifted to the higher angle side, indicating that the closest packing of the alkyl chains was not achieved when a large amount of 2-propyl groups was present in the intermediate.
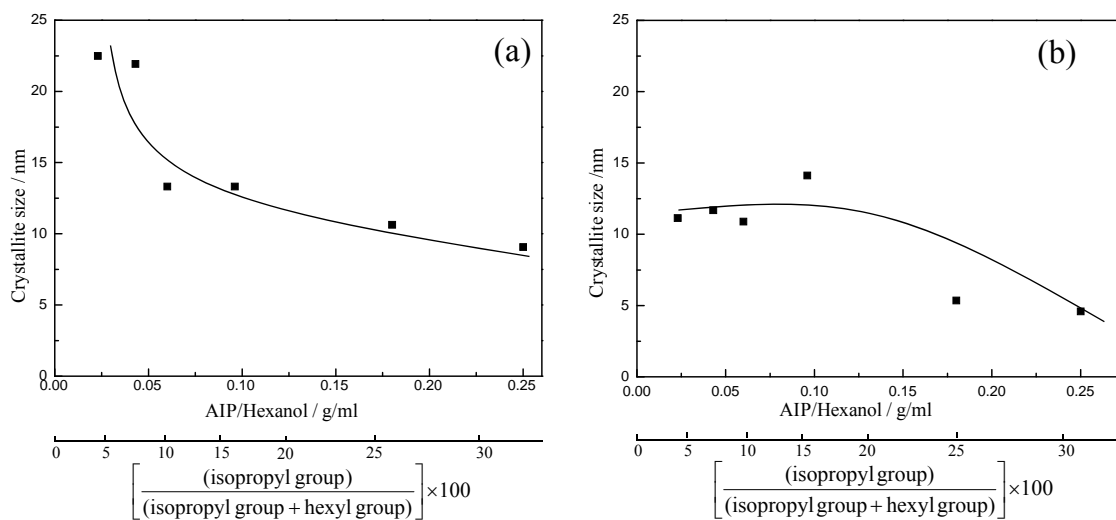
Fig. 3-3. Crystallite size of the hexyl derivative of boehmite vs. AIP/hexanol ratio:(a) results for AXHe products, (b) results for AMHe products.

The XRD patterns of the hexyl derivative of boehmite obtained by a conventional process (after the reaction, the products were recovered by repeated cycles of agitation with methanol, centrifuging, and decantation) are shown in Fig. 3-1b. The effect of AIP/hexanol ratio on the crystallite size of the product is shown in Fig. 3-3b. Change in crystallinity of the products showed the same tendency as in the case of the xerogel products, but crystallites of the products recovered by the conventional method did not develop well at low AIP/hexanol region as compared with the xerogel products. This result indicates that the stacking of boehmite layers takes place more efficiently during the evaporation of the solvent in the product recovery process of the xerogel method [8].

The IR spectra of the products are given in Fig. 3-4. The bands at ~3400 cm^{-1} and 1630 cm^{-1} observed in all the products can be assigned to the stretching and bending vibration modes of adsorbed water [9]. Absorption bands due to the alkyl groups originated from the solvent used for the reaction were observed at 3000–2800 (νCH), 1468 (δCH$_2$), 1384 (δCH$_3$) and around 1100 (νCO) cm^{-1}. In well-crystallized boehmite, the bands characteristic of hydrogen bonding between two adjacent boehmite layers are observed at 3295 (ν_{as}OH) and 3092 (ν_sOH) cm^{-1} [10, 11]. These bands, however, were not observed in the present products, but stretching vibration mode of isolated OH groups was observed at 3594 cm^{-1} in some of the products. In the alkyl derivatives of boehmite, only a part of the OH groups on the boehmite layer are substituted with the OR groups because the area occupied by an alkyl group attached to the boehmite layer is larger than that occupied by a hydroxyl group, and therefore isolated OH groups remained on boehmite layers. The AXHe products (the products recovered as xerogels) showed a relatively sharp absorption band due to the isolated OH groups as compared
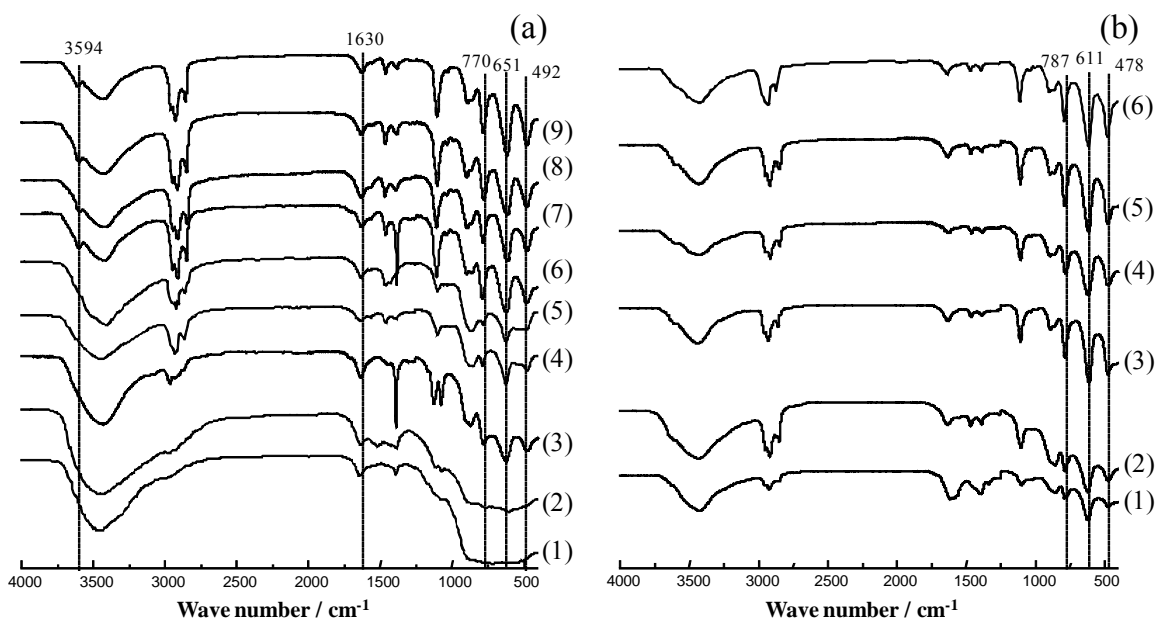
Fig. 3-4. IR spectra of the products.

(a) Products recovered by the direct drying process.

1), AAEt(12.5-50)-(assyn); 2), AAEt(12.5-70)-(assyn); 3), AAEt(12.5-130)-(assyn); 4), AXHe(12.5-50)-(assyn); 5), AXHe(12.5-70)-(assyn); 6), AXHe(12.5-130)-(assyn); 7), AXHe(3-50)-(assyn); 8), AXHe(3-70)-(assyn); 9), AXHe(3-130)-(assyn).

(b) Products recovered by washing with methanol.

1), AMHe(12.5-50)-(assyn); 2), AMHe(12.5-70)-(assyn); 3), AMHe(12.5-130)-(assyn); 4), AMHe(3-50)-(assyn); 5), AMHe (3-70)-(assyn); 6), AMHe (3-130)-(assyn).

with the AMHe products. For the latter products, the band due to the isolated OH groups was not clearly observed presumably because of the difficulty in removing water molecules adsorbed on the products by the usual drying procedure. Boehmite shows characteristic bands at 770, 651 and 492 cm^{-1}. The first and second bands are assigned to stretching vibration modes of Al-O and the last one, to the bending mode of AlO$_6$ [12, 13]. The IR spectrum of the AAEt(12.5-70)-(assyn) showed weak absorption peaks at around 787, 611 and 478 cm^{-1} due to the structural vibrations of boehmite layers, but AAEt(12.5-50)-(assyn) showed a broad band at <1000 cm^{-1}, which is a typical absorption band for transition aluminas, indicating that AAEt(12.5-50)-(assyn) does not have a boehmite structure. AXHe(12.5-70)-(assyn) exhibited the bands due to the boehmite structure and intensities of these bands increased with the decrease in the AIP/hexanol ratio. This result accords with the XRD results.

3-3-2. Thermal analyses of the products.

Fig. 3-5 shows the results for thermal analyses of the products. All of the samples exhibited a weight decrease at around 400 ^{o}C, which was associated with an exothermic (400 ^{o}C) response in DTA. AAEt(12.5-70)-(assyn) and AAEt(12.5-50)-(assyn) showed a weight decrease at around 100 ^{o}C due to desorption of adsorbed species and only a slight weight decrease was observed at around 400 ^{o}C, suggesting that only a small amount of the alkyl groups are incorporated in these samples. The thermal analysis of AXHe(12.5-70)-(assyn) and AXHe(12.5-50)-(assyn) showed other exothermic processes at around 240 and 330 ^{o}C besides the exothermic weight loss at ~400 ^{o}C. These peaks seem to be due to combustion of the alkyl groups
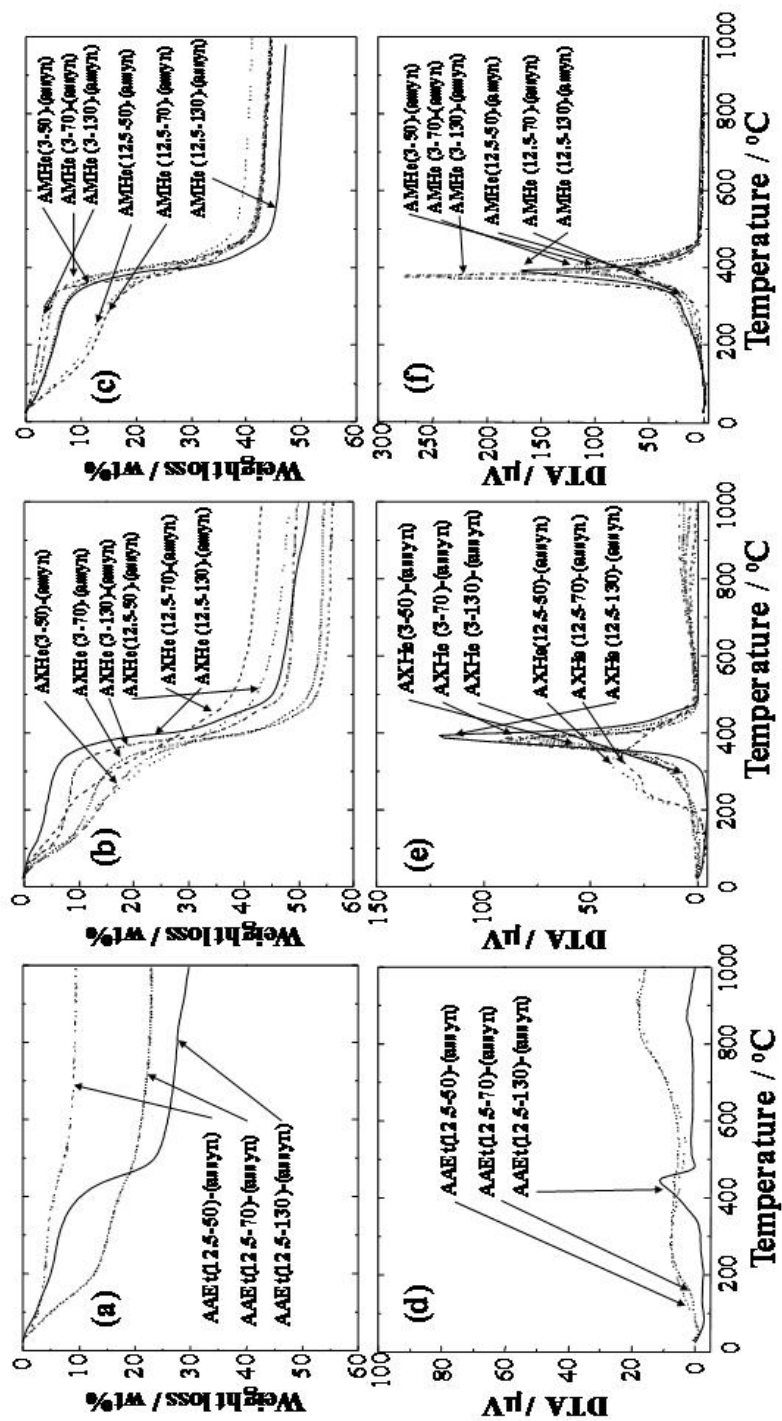
Fig. 3-5. TG (a–c) and DTA (d–f) profiles of the products recovered by aerogel/xerogel method (a, b, d and e) and by washing with methanol (c and f).

Table 3-1. Summary of thermal analysis of the products.

Sample	Weight ratio (BD^a/Al_2O_3)	Ignition temperature (°C)	Molecular fomula[b]
AXHe(12.5-130)	1.84	392	$AlO(OH)_{0.51}(OHe)_{0.49}$
AXHe(12.5-70)	1.42	243, 334, 404	$AlO(OH)_{0.85}(OHe)_{0.15}$
AXHe(12.5-50)	1.43	243, 321, 405	$AlO(OH)_{0.85}(OHe)_{0.15}$
AXHe(3-130)	1.78	379	$AlO(OH)_{0.66}(OHe)_{0.34}$
AXHe(3-70)	1.84	385	$AlO(OH)_{0.61}(OHe)_{0.39}$
AXHe(3-50)	1.78	385	$AlO(OH)_{0.66}(OHe)_{0.34}$
AMHe(12.5-130)	1.74	393	$AlO(OH)_{0.7}(OHe)_{0.3}$
AMHe(12.5-70)	1.51	397	$AlO(OH)_{0.87}(OHe)_{0.13}$
AMHe(12.5-50)	1.45	397	$AlO(OH)_{0.91}(OHe)_{0.09}$
AMHe(3-130)	1.74	380	$AlO(OH)_{0.7}(OHe)_{0.3}$
AMHe(3-70)	1.71	394	$AlO(OH)_{0.72}(OHe)_{0.28}$
AMHe(3-50)	1.64	403	$AlO(OH)_{0.77}(OHe)_{0.23}$

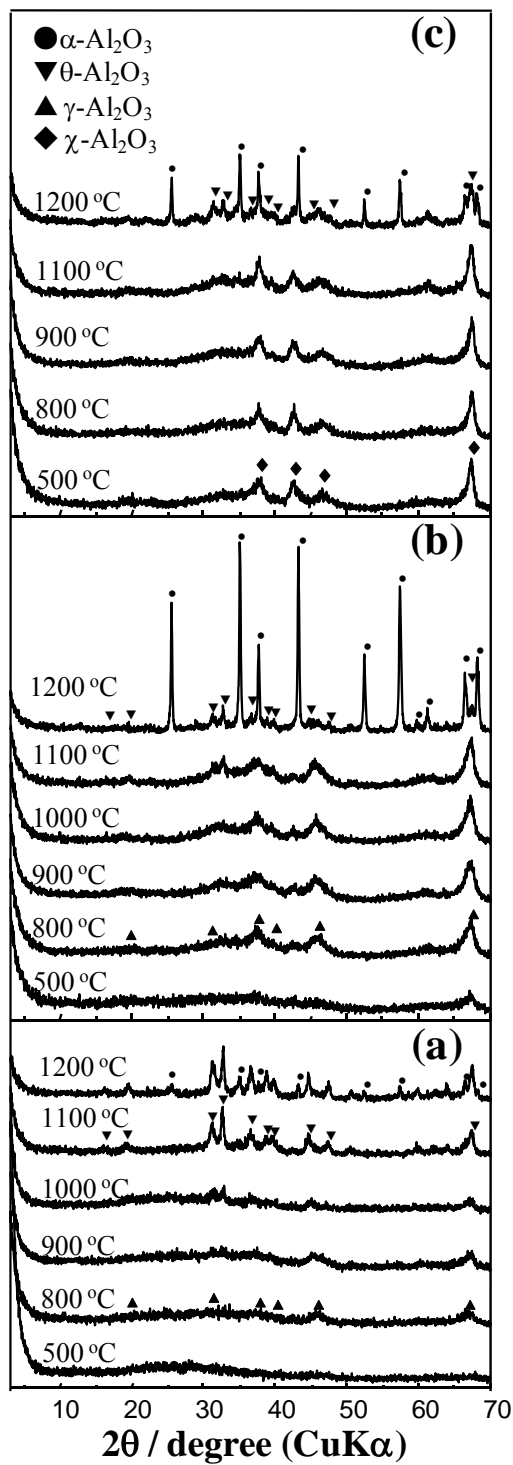[a] Alkyl derivatives of boehmite.

[b] Empirical formulas, $AlO(OH)_{1-x}(OR)_x$, were calculated from ignition losses determined by TG analysis of the products. "He" means the hexyl group.

present in the defect sites of poorly-crystallized boehmite layers. Similar thermal decomposition behavior was observed in the AMHe products. The results of thermal analysis of the products are summarized in Table 3-1. The empirical formula of the hexyl derivative of boehmite calculated from ignition losses are also shown in the table. The alkyl population in the boehmite layer (x value) has a tendency to increase with the increase in the crystallinity of the product.

3-3-3. Calcined products.

The XRD patterns of the phases developed from the aerogels are shown in Fig. 3-6. AAEt(12.5-130) was converted to an amorphous phase at 500 $^{\circ}$C, and γ-Al$_2$O$_3$ appeared at 800 $^{\circ}$C. Transformation into θ-Al$_2$O$_3$ started at 1000 $^{\circ}$C. The θ-Al$_2$O$_3$ structure was preserved at 1200 $^{\circ}$C, although some peaks due to α-Al$_2$O$_3$ were also observed in the XRD pattern. AAEt(12.5-70) showed a similar transformation sequence. However, γ-Al$_2$O$_3$ structure was developed well compared with AAEt(12.5-130) in the low temperature range (500–800 $^{\circ}$C), and only a small amount of θ-Al$_2$O$_3$ was formed at 1100 $^{\circ}$C, while α-Al$_2$O$_3$ was developed well at 1200 $^{\circ}$C. These results indicate that poorly-developed γ-Al$_2$O$_3$ structure facilitates the formation of θ-Al$_2$O$_3$ and the presence of low-temperature transition alumina facilitates the transformation into α-Al$_2$O$_3$. Since transformation of γ- to θ-Al$_2$O$_3$ and θ- to α-Al$_2$O$_3$ requires activation energies, high energy level of the starting materials (i.e., low crystallinity and low-temperature transition alumina) caused low activation energies, thus facilitating the transformation.

On the other hand, AEtOH(12.5-50)-assyn (χ-Al$_2$O$_3$; Fig. 6c) maintained its structure even after calcination at 1100 $^{\circ}$C, and partially converted to α-Al$_2$O$_3$ by

88

Fig. 3-6. XRD patterns of the aluminas derived from aerogels of the ethyl derivative of boehmite by calcination at the temperature specified in the figure: (a), AAEt(12.5-130); (b), AAEt(12.5-70); (c), AAEt(12.5-50).
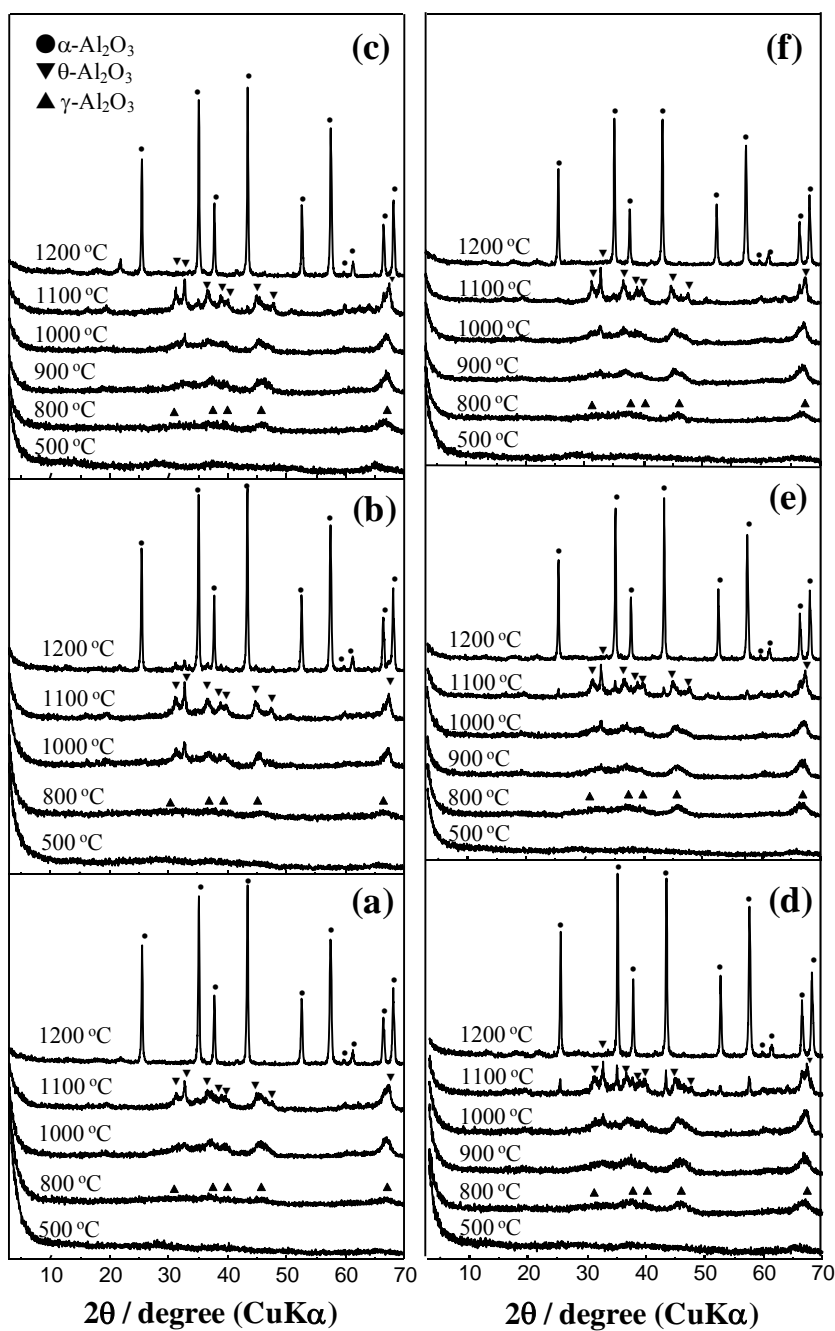
Fig. 3-7. XRD patterns of the aluminas derived from: (a), AXHe(12.5-50); (b), AXHe(12.5-130); (c), AXHe(3-50); (d), AMHe (12.5-50); (e), AMHe(12.5-130); (f), AMHe(3-50); by calcination at temperatures specified in the figure.

calcination at 1200 ^{o}C. χ-Al$_2$O$_3$ obtained by the dehydration of gibbsite transforms into a high-temperature transition alumina, κ-Al$_2$O$_3$, at around 800 ^{o}C [2, 3]. However, the present χ-Al$_2$O$_3$ sample required a much higher temperature to transform into more stable phase. In general, gibbsite obtained from bauxite by Bayer process contains a significant amount of Na$^+$ ions, which can not be eliminated by thermal treatment. Therefore, the thus-formed χ-Al$_2$O$_3$ has a low crystallinity and has many defects in the structure. These defects in the χ-Al$_2$O$_3$ matrix facilitate the formation of κ-Al$_2$O$_3$. On the other hand, the present sample was obtained by thermal decomposition of AIP in an alcohol, and, therefore, foreign ions such as Na$^+$ are absent in the χ-Al$_2$O$_3$ matrix; therefore, formation of high-temperature transition alumina is suppressed.

Acid/base properties of the present products and the χ-Al$_2$O$_3$ samples obtained by thermal dehydration of commercially available gibbsite samples (B73, C-301) were compared by NH$_3$- and CO$_2$-TPD profiles (Fig. 3-10). AAEt(12.5-50)-(800) (χ-Al$_2$O$_3$) exhibited a NH$_3$ desorption peak at 300 ^{o}C while AXHe(12.5-50)-(800) (γ-Al$_2$O$_3$) showed a peak at ~200 ^{o}C: The acid strength of the former sample is much stronger than the latter. However, these two samples had quite low acid-densities. On the other hand, χ-Al$_2$O$_3$ obtained by thermal dehydration of gibbsite exhibited a large NH$_3$ desorption peak at 250 ^{o}C. Since these alumina samples have low crystallinities, surface defect sites may have acted as Lewis acid sites. The CO$_2$-TPD profiles showed a small CO$_2$ desorption peak at a low temperature range (around 100 ^{o}C) and the peak shape was almost the same for all the products examined (Fig. 3-10b). Therefore, base sites on the surface of these aluminas have similar properties.

The samples of the hexyl derivative of boehmite showed thermal transformation sequence similar to that observed for AAEt(12.5-70) (Fig. 3-7). When AMHe and
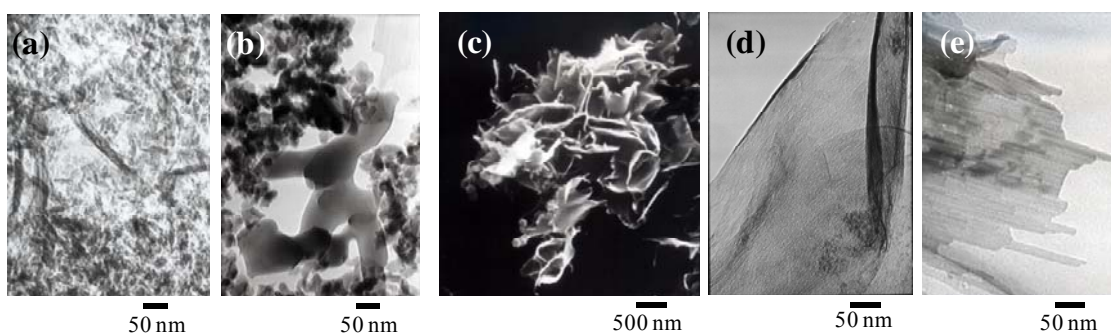
Fig. 3-8. SEM (c) and TEM (a, b, d and e) images of the products recovered as aerogels and aluminas derived therefrom: (a), AAEt(12.5-50)-(assyn); (b), AAEt(12.5-50)-(1200). (c) and (d), AAEt(12.5-130)-(assyn); (e), AAEt(12.5-130)-(1200).
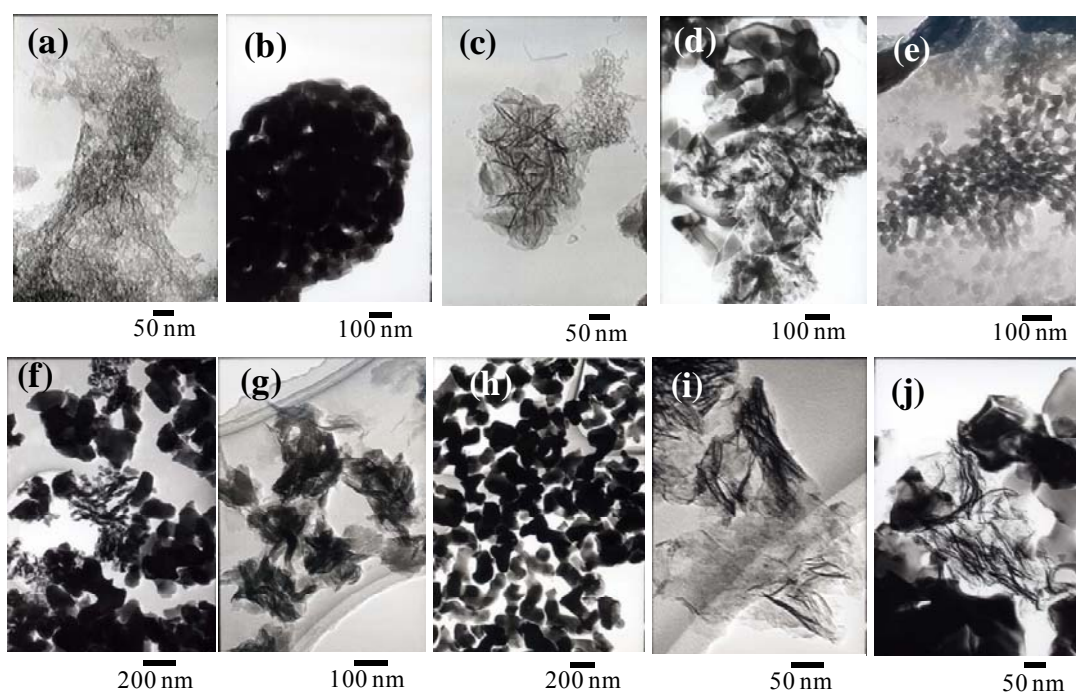
Fig. 3-9. TEM images of the hexyl derivative of boehmite and alumina derived therefrom: (a), AXHe(12.5-50)-(assyn); (b), AXHe(12.5-50)-(1200); (c), AXHe(12.5-130)-(assyn); (d), AXHe(12.5-130)-(1200); (e), AXHe(3-130)-(assyn); (f), AXHe(3-130)-(1200); (g), AMHe(12.5-130)-(assyn); (h), AMHe(12.5-130)-(1200); (i), AMHe(3-50)-(assyn); (j), AMHe(3-50)-(1200).
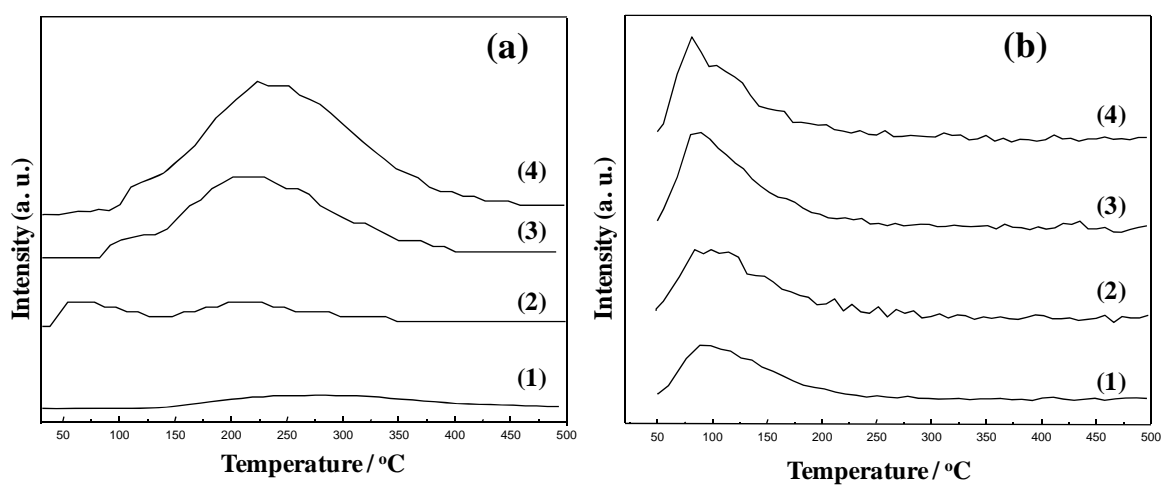
Fig. 3-10. NH$_3$- (a) and CO$_2$-TPD profiles (b): (1), AAEt(12.5-50)-(800); (2), AXHe(12.5-50)-(800); (3), χ-alumina obtained by calcination of Sumitomo C-301 at 800 ^{o}C; (4), χ-alumina obtained by calcination of Nippon Light Metal B73 at 800 ^{o}C.

AXHe samples are compared, formation of α-Al_2O_3 started at lower temperature in the former samples: A small amount of α-Al_2O_3 was clearly detected in AMHe samples calcined at 1100 ^{o}C. Since AMHe samples had larger bulk densities than AXHe samples (Table 3-3) because of compaction during the drying process, the former samples had a larger number of contact points between particles, which act as nucleation sites for α-Al_2O_3 [14], thus facilitating transformation into α-Al_2O_3.

3-3-4. Morphologies.

Morphologies of the products are shown in Figs. 3-8 and 3-9. The products having well-developed boehmite structures were composed of aggregates of randomly oriented plate-like particles (Figs. 3-7c, 3-7d, 3-8c, 3-8g, and 3-8i). The morphology of AMHe samples was similar to that of AXHe samples, and both the samples were composed of small plate-like particles (Fig. 3-8c). On the other hand, the plate-like structure was developed well in AAEt(12.5-130)-(assyn) (Figs. 3-7c and 3-7d), and this morphology was maintained even after calcination at 1200 ^{o}C (Fig. 3-7e). These results indicate that the plate structure suppresses the transformation into α-Al_2O_3. In the case of the other samples calcined at 1200 ^{o}C, a vermicular morphology characteristic of α-Al_2O_3 particles was observed.

3-3-5. Pore texture of the products.

The nitrogen adsorption isotherms of the products obtained in ethanol can be divided into two types. AAEt(12.5-130) showed an abrupt increase of adsorption volume at high relative pressure region (Fig. 3-11a), which can be explained by
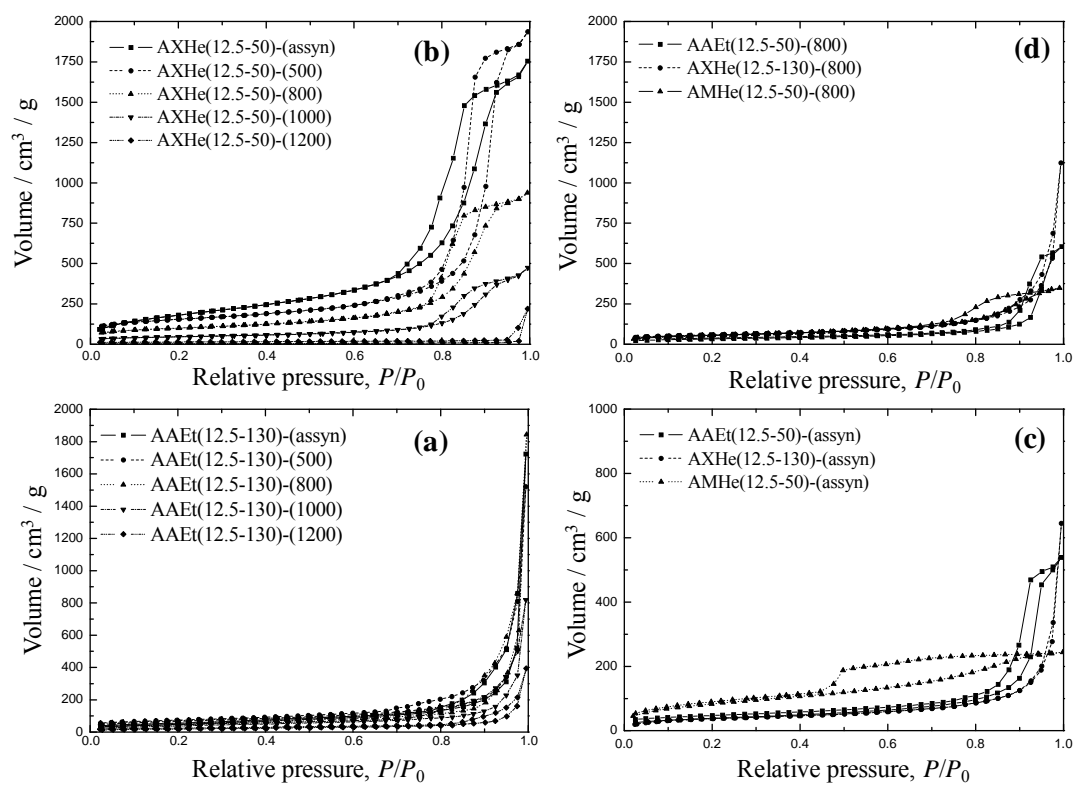
Fig. 3-11. Typical nitrogen adsorption isotherms (a and b) and *t*-plots (c and d) of the products and aluminas obtained by the calcination thereof.

capillary condensation of nitrogen taken place between well-developed sheet-like particles.

AAEt(12.5-70) and AAEt(12.5-50) showed completely different nitrogen isotherms (Fig. 3-11c). The hysteresis loops of the isotherms of these samples belong to H-1 type [15], which can be explained by the presence of porous materials made of agglomerates or compacts of approximately uniform spheres having a narrow size distribution.

The mode pore diameters of these samples together with other surface properties are surmmarized in Table 3-2. AAEt(12.5-130) showed a broad pore size distribution in the macropore-region, while AAEt(12.5-50) had narrow pores (24 nm) with a narrow pore size distribution. The pore volume of AAEt(12.5-130) was fairly large (1.16–2.6 cm^3/g), but AAEt(12.5-70) and AAEt(12.5-50) had relatively small pore volumes (Table 3-2). These results indicate that the formation of randomly oriented plate particles is important for creation of large pore volumes.

The products obtained by the solvothermal reaction in 1-hexanol showed the isotherms of three types. AXHe(12.5-130) showed an isotherm similar to that of AAEt(12.5-130). However, the pore volume of the former sample was smaller than that of the latter (Table 3-3) because the sheet-like structure did not develop well in the former sample. The shapes of isotherm and hysteresis loop of AXHe(12.5-50) were similar to those of AAEt(12.5-50), but the surface area and pore volume (587 m^2/g and 3.24–1.55 cm^3/g) of AXHe(12.5-50) were much larger than those of AAEt(12.5-50) (Table 3). When AXHe(12.5-50) and AXHe(12.5-130) are compared, the former sample had a larger surface area and pore volume. This result indicates that the development of layered structure of the alkyl derivative of boehmite rather decreases the surface area

Table 3-2. Physical properties of the products recovered as aerogels after solvothermal reaction of AIP in ethanol and aluminas obtained by calcination thereof.

Sample	Calcination temperature (^{o}C)	Bulk density (g/cm^3)	surface area (m^2/g)	Pore volume (cm^3/g)	Average pore[a] diameter (nm)	Mode pore diameter (nm)
AAEt(12.5-130)	assyn	0.11	177	2.6	59	~210
	500	0.13	232	2.21	38	~210
	800	0.1	195	2.56	53	~300
	1000	0.14	141	1.16	33	~210
	1200	0.11	66	0.56	34	~250
AAEt(12.5-70)	assyn	0.3	217	0.76	14	11
	500	0.32	178	0.87	20	13
	800	0.34	135	0.73	22	13
	1000	0.34	119	0.72	24	15
	1200	0.44	26	0.29	45	61
AAEt(12.5-50)	assyn	0.47	136	0.8	24	24
	500	0.35	138	0.92	27	24
	800	0.44	116	0.88	30	24
	1000	0.45	101	0.86	34	34
	1200	0.41	51	0.56	44	34

[a] Caculated from surface area and pore volume assuming the cylindrucal pore with a uniform diameter.

Table 3-3. Physical properties of the hexyl derivative of boehmite and aluminas obtained by calcination thereof.

Sample	Calcination temperature (°C)	Bulk density (g/cm³)	surface area (m²/g)	Pore volume (cm³/g)	Average pore[a] diameter (nm)	Mode pore diameter (nm)
AXHe(12.5-130)	assyn	0.16	132	1.02	31	~230
	500	0.12	243	1.6	26	~240
	800	0.1	199	1.73	35	~210
	1000	0.11	80	1.24	62	~230
	1200	0.23	7	0.23	131	~230
AXHe(12.5-70)	assyn	0.12	739	2.17	12	9
	500	0.13	514	2.33	18	11
	800	0.22	336	1.29	15	10
	1000	0.25	153	0.82	21	10
	1200	0.46	11	0.34	124	~220
AXHe(12.5-50)	assyn	0.08	587	2.89	20	13
	500	0.09	348	3.24	37	16
	800	0.13	345	1.55	18	11
	1000	0.24	157	0.77	20	10
	1200	0.39	12	0.33	110	~210
AXHe(3-130)	assyn	0.50	179	0.25	6	4
	500	0.31	233	0.69	12	7
	800	0.32	179	0.62	14	8
	1000	0.34	116	0.63	22	9
	1200	0.56	11	0.07	25	-
AXHe(3-50)	assyn	0.52	176	0.20	5	4
	800	0.34	223	0.54	10	4
	1000	0.34	124	0.50	16	8
	1200	0.57	17	0.03	7	-
AMHe(12.5-130)	assyn	0.42	165	0.45	11	4
	800	0.37	207	1.24	24	13
	1000	0.35	131	0.92	28	19
	1200	0.52	12	0.39	130	~230
AMHe(12.5-50)	assyn	0.35	302	0.36	5	2
	800	0.37	194	0.53	11	5
	1000	0.36	119	0.45	15	7
	1200	0.60	13	0.02	6	-

[a] Caculated from surface area and pore volume assuming the cylindrucal pore with a uniform diameter.

and pore volume of the alumina derived therefrom. This is because the development of the layer structure means the formation of thick layers. Therefore, synthesis of the alkyl derivative of boehmite having a poorly developed boehmite structure by controlling the AIP/solvent ratio is essential for the synthesis of alumina having a large surface area and pore volume.

On the other hand, AMHe(12.5-50) showed a N_2 adsorption isotherm different from those of the samples mentioned above and exhibited a hysteresis loop of type H-4 (Fig. 3-11c) [15], which is explained by narrow slit-shaped pores. This type of isotherm was also observed for the other AMHe products and AXHe products synthesized by using a small quantity of AIP. These products suffered from compaction during the drying stage or had well-developed layer structures. Therefore, slit-shaped pores are formed between the layers or inside of thick layers of the alkyl derivative of boehmite. Calcination of these samples at 800 ^{o}C changed the shape of the hysteresis loop from H-4 to H-1 type, suggesting that collapse of the layers structure of boehmite derivatives and development of γ-Al_2O_3 structure caused elimination of narrow slit-shaped pores.

3-4. CONCLUSIONS

The effect of feed ratio (AIP/alcohol) on the physical properties of the aerogel/xerogel was investigated. The feed ratio affected the crystallinity of the alkyl derivatives of boehmite formed. The increase in AIP/alcohol ratio decreased crystallite size of alkyl derivatives of boehmite because the presence of 2-propyl groups in the intermediate disturbs the development of the layer structure of the boehmite derivative. The product obtained by the solvothermal reaction in ethanol with a large AIP/alcohol (0.25) was χ-Al_2O_3. Morphologies of the products were also affected by the feed ratio.

The transformation of the products having a well developed layer structure to α-Al_2O_3 was retarded and the morphology was maintained. Alumina derived from the products having poorly developed layer structure had large pore volumes and surface areas (AXHe(12.5-50), 1.16–3.24 cm^3/g).

REFERENCES

[1] S. Iwamoto, K. Saito, K. Kagawa, M. Inoue, *Nano Lett.* 1 (2001) 417.

[2] W.H. Gitzen, Alumina as a Ceramic Material (American Ceramic Society, Columbus, OH, 1970).

[3] G.W. Brindley, J.O. Choe, *Am. Mineral.* 46 (1961) 771.

[4] I. Levin, D. Brandon, *J. Am. Ceram. Soc.* 81 (1998) 1995.

[5] M. Inoue, H. Kominami, T. Inui, *J. Am. Ceram. Soc.* 75 (1992) 2597.

[6] M. Inoue, H. Kominami, T. Inui, *J. Am. Ceram. Soc.* 79 (1996) 793.

[7] A.J. Fanelli, J.V. Burlew, *J. Am. Ceram. Soc.* 69 (1986) C-174.

[8] S.-W. Kim, S. Iwamoto, M. Inoue, *J. Porous Mater.* in press.

[9] A.D. Cross, An introduction to practical IR spectroscopy 2nd ed. (Butterworth, London, 1964).

[10] K.A. Wickersheim, G.K. Korpi, *J. Chem. Phys.* 43 (1965) 579.

[11] J.J. Fripat, H. Bosmans, P.G. Rouxhet, *J. Phys. Chem.* 71 (1967) 1097.

[12] D. Mazza, M. Vallino, G. Busca, *J. Am. Ceram. Soc.* 75 (1992) 1929.

[13] P. Mcmillan, B. Pirious, *J. Non. Cryst. Solids* 53 (1982) 279.

[14] J.A. Schwarz, C. Contescu, A. Contescu, *Chem. Rev.* 95 (1995) 477.

[15] F. Rouquerol, J. Rouquerol, K. Sing, Adsorption by Powders and Porous Solids–Principles, Methodology and Applications (Academic Press, San Diego, CA, 1999).

Chapter 4

Generation of Voids in the Alkyl Layers of the Alkyl Derivative of Boehmite by Heat Treatment and Adsorption Behavior of the Voids

4-1. Introduction

Recently, materials having molecular frameworks attract much attention in the nanotechnology fields, and voids surrounded by molecules are also paid attention [1]. These voids have unique characteristics concerning molecular condensation, molecular stress and so on [2], and therefore these voids open new possibilities for use as gas storages [3] and reaction media [4].

Many organic derivatives of layered inorganic materials have been reported [5–9]. As mentioned in the previous chapters, the solvothermal reaction of aluminum isopropoxide in *n*-alcohols yielded the alkyl derivatives of boehmite having a layered structure [10]. Molecular mechanics calculation suggests that the layered structure of alkyl derivatives of boehmite is maintained even if alkyl chains are partially removed. The calculation predicted that partial removal of the alkyl chains creates voids in the alkyl layers because the alkyl chains are attached to the boehmite layers [11]. In this chapter, it is descibed whether the voids surrounded by the alkyl chains are actually generated by heat treatment of the alkyl derivative of boehmite.

4-2. Experimental

4-2-1. Synthesis of the alkyl derivatives of boehmite

In a Pyrex test tube serving as autoclave liner, 80 mL of 1-decanol (Wako) and 7.0 g of aluminium isopropoxide (AIP, Nacalai Tesuque) were placed, and the test tube was set in a 200 mL autoclave. An additional 35 mL of 1-decanol was placed in the gap between the autoclave wall and the test tube. The autoclave was purged with N_2, heated to 300 ºC at a rate of 2.5 ºC min^{-1}, and held at that temperature for 4 h. After the assembly was cooled to room temperature, the resulting precipitates were washed by repeated cycles of agitation with methanol, centrifugiation, and decantation and then air-dried. It is noted that a small-quantity bottle of AIP was purchased and used up in a couple of days; the use of fresh AIP is crucial for the reaction.

Heat treatment of the products was carried out in a fixed-bed flow reactor. The product (0.2 g) was placed in a quartz reactor, heated in an inert gas (He) flow (60 mL min^{-1}) to the reaction temperature at a rate of 10 ºC min^{-1}, and held at that temperature for prescribed periods.

4-2-2 Charaterization

The properties of the samples were characterized by powder X-ray diffraction (XRD), thermogravimetric (TG), and N_2-adsorption techniques. The XRD patterns were obtained on a Shimadzu XD-D1 diffractorometer using CuKα radiation and a carbon monochromator. The TG analysis was performed on a Rigaku TAS8110 thermogravimeter: A weighed amount (ca. 30 mg) of the sample was placed in the heating chamber, and heated at a rate of 10 ºC/min in a 40 ml/ min flow of Ar or air. Nitrogen adsorption isotherm was determined using a volumetric sorption system, Yuasa
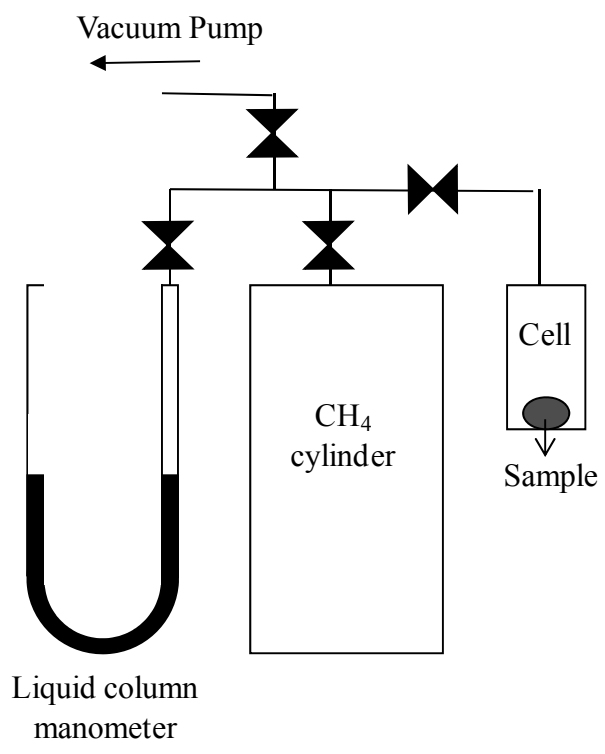
Fig. 4-1. Apparatus methane adsorption for measurement.

Ionics Autosorb-1. Pore size distribution was calculated from the adsorption branch of the nitrogen adsorption isotherm using the BJH method.

3-2-3 Methane adsorption test

Methane adsorption capacity was measured by a device of our own composition as illustrated in Fig. 4-1. Methane gas was applied to the sample holder at equiblium pressure of 35 atm and methane adsorption capacity of the sample was calculated from the volume of methane gas which came out of the device at the atmosphere pressure.

4-3. Results and Discussion

4-3-1. TG and XRD analyses of the products

The reaction of the aluminum alkoxide in 1-decanol yielded the decyl derivative of boehmite [6]. The result of the thermal analysis of the product in an Ar flow is shown in Fig. 4-2. The thermogravimetric profile showed sharp weight decreases at around 330 and 400 °C. The former weight decrease is due to the removal of the organic moieties incorporated between the boehmite layers, and the latter to the collapse of the boehmite layers yielding an amorphous alumina. This result showed that the starting temperature for the removal of the decyl groups is about 310 °C.

The XRD patterns of the samples suffered heat treatment in He at 310 °C for varying periods are shown in Fig. 4-3. The XRD patterns of the samples revealed that heating caused higher angle shift and broadening of the low-angle peaks ($2\theta = 6°$) due to the layer structure of the samples. This peak shift suggested that interlayer spacing of the products became slightly narrow by the heat treatment.
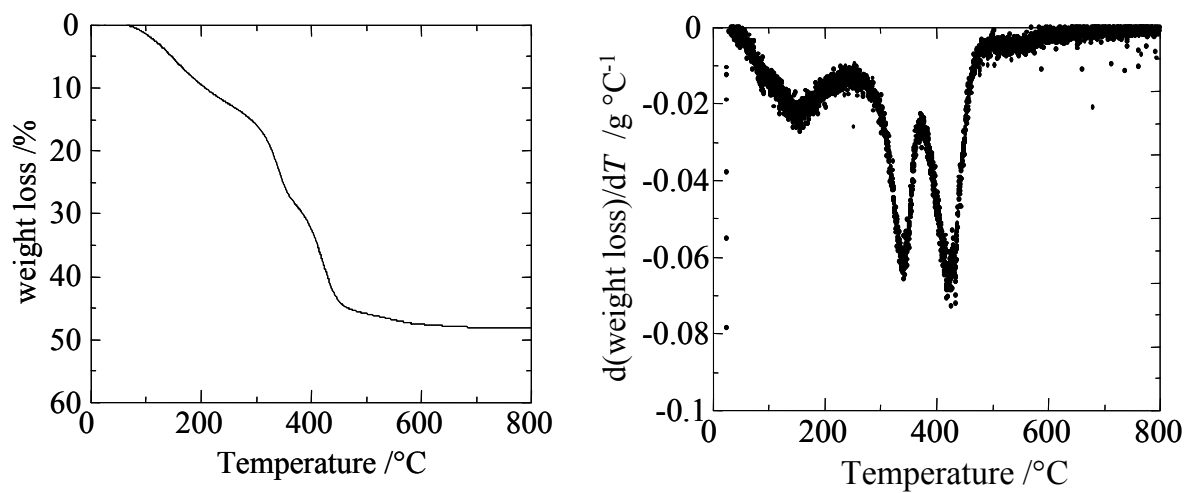
Fig. 4-2. Weight loss (left) and it differential profile (right) during the thermal analysis of the decyl derivative of boehmite in He.
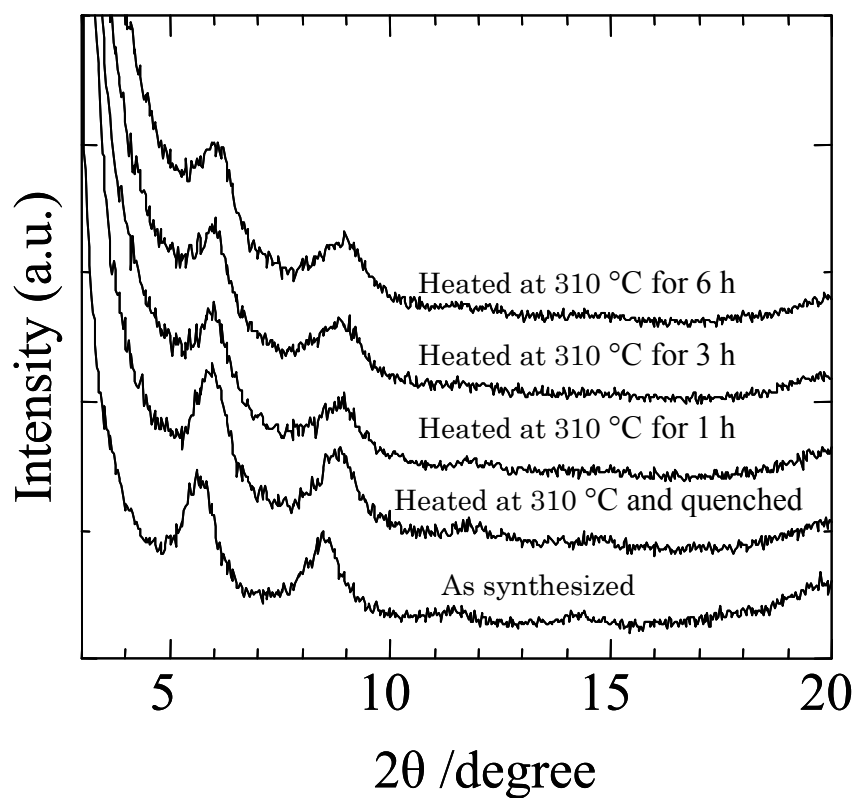
Fig. 4-3. XRD patterns and BET surface area of the decyl derivatives of boehmite heated at 310 °C for varying periods in He.

4-3-2. N$_2$ adsorption measurements of the products

The N$_2$ adsorption isotherms of the products are shown in Fig. 4-4. Hysteresis loops were observed for all the products heated for varying periods, and they are assigned as H4 type (IUPAC classification), indicating that the products had slit shaped pores. Essentially the identical hysteresis shape suggests that their pore structure was not changed by heat treatment. The products heated for 3 h had the largest N$_2$ adsorption capacity. However, prolonged heat treatment of the product (6 h) resulted in a decrease in N$_2$ adsorption capacity indicating that a partially collapse of the boehmite layers occurred. The pore size distribution (Fig. 4-4, right) showed that the pores ranging from 2 to 10 nm increased their volume by the heat treatment.

4-3-3. Physical properties and methane adsorption capacity of the products

The physical properties of the samples are summarized in Table 4-1. The *X* value for the empirical formula, $AlO(OH)_{(1-X)}(OC_{10}H_{21})_X$, was calculated from the weight loss on ignition observed by the TG analysis. The *X* value decreased from 0.304 to 0.173 by prolonged heat treatment. The interlayer spacing calculated from the XRD pattern was not decreased significantly. Since the number of alkyl chains between boehmite layers decreased significantly, the relative alkyl chains density in boehmite layers significantly decreased. The tilt angle of the alkyl chains of the untreated product with respect to the boehmite layer was calculated to be 60.5 ° on the basis of typical methylene repeated distance of 1.27 Å/CH$_2$ for all trans polymethylene [10,13]. The thickness of the boehmite layers including van der Waals distance between two alkyl layers due to bilayer arrangement of alkyl groups between the adjacent boehmite layers was calculated to be 9.0 Å from the y-intercept of the plot
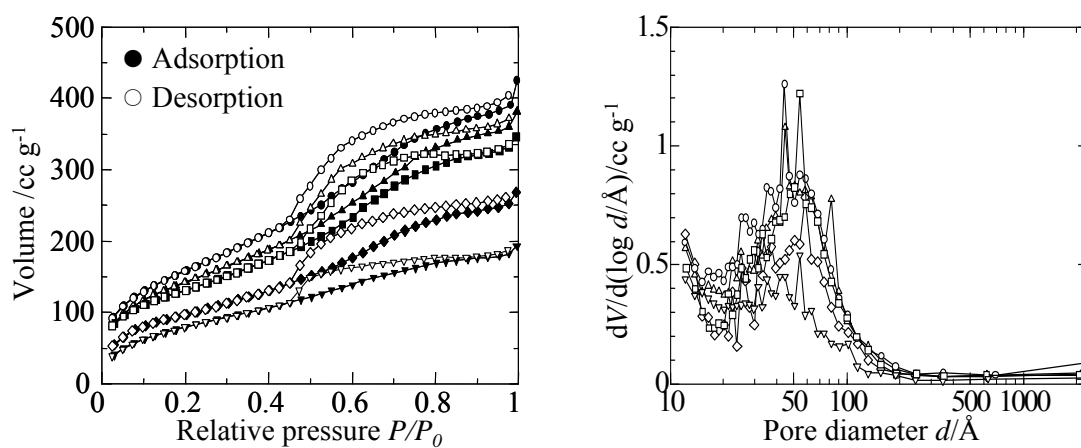
Fig. 4-4. N$_2$ adsorption isotherm (left) and pore size distribution (adsorption, right) of the decyl derivatives of boehmite heated in He (for ♦: 0 h, ▲: 1 h, ●: 3 h, ■: 6 h at 310 °C. ▼: as synthesized). All samples were preheated at 250 °C for 0.5 h. Closed symbol: adsorption. Opened symbol: desorption.

Table 4-1. The physical properties of the decyl derivatives of boehmite suffered heat treatment in He.

Temparature (°C)	Time (h)	Weight loss[a] (%)	X-value[b]	Interlayer spacing[c] (nm)	Relative alkyl chains density in boehmite layers[d]	Tilt angle of alkyl chain with respect to the boehmite layer[e] (degree)
-	-	-	0.304	3.11	1.000	60.5
310	0	7.10	0.252	2.99	0.877	55.4
310	1	10.6	0.226	2.95	0.801	53.8
310	3	14.9	0.195	2.95	0.692	53.8
310	6	17.9	0.173	2.95	0.613	53.8

a: Calculated from TG analysis.

b: The X value of empirical formula, $AlO(OH)_{(1-X)}(OC_{10}H_{21})_X$ was calculated from the weight ignition loss determined by TG analysis.

c: Calculated from XRD pattern.

d: Ratio of alkyl chain density in the boehmite layers of the heated sample to that of the sample without heat treatment was calculated from the layer spacing and X-value of the sample, assuming that the area of a layer did not change.

e: A steady increase in interlayer spacing with a slope of 2.21 Å/CH_2 was observed [10]. The interlayer spacing of decyl derivatives of boehmite was 22.1 Å, and so the length of boehmite layer was 9.0 Å. The tilt angle was calculated as $\sin^{-1}${(basal spacing - 9.0)/2/the length of decyl chains} on the basis of typical methylene repeated distance of 1.27 Å/CH_2 for an all trans polymethylene.

[10]. From this value the tilt angle of the alkyl chains of the products heated for 0 h, 1 h, 3 h, and 6 h with respect to the boehmite layer can be calculated to be 55.4 °, 53.8 °, 53.8 °, and 53.8 ° [10]. The layer structure of the alkyl derivatives of boehmite is maintained by the van der Waals interaction of the neighboring alkyl chains covalently bonded to the same boehmite layers. For an ordinary intercalation compound, partial removal of alkyl chains caused a decrease in tilt angle to obtain more van der Waals interaction. However, in the present case, the alkyl chains could not move, and therefore the alkyl chain cannot lean to the boehmite layers beneath a certain degree of the tilt angle because the decrease in the tilt angle cause the increase in repulsion between the alkyl chains.

The adsorption characteristics are summarized in Table 4-2. The BET surface area increased by heat treatment. The c value is a constant in the BET equation, which is defined by the ratio of equilibrium constants for the adsorption at the first layer to that for the adsorption at the second or higher layers. Since the ordinary BET plot gives such as small y-intercept that the c value can not be determined precisely. Therefore, $1/(v(1-x))$ was plotted against $(1-x)/x$ according to the following equation derived from the BET equation [12]:

$$1/(v(1-x))=1/v_m+(1/v_mc)(1-x)/x$$

where x, v, and v_m represent relative pressure (P/P_0), adsorption capacity of the sample at given relative pressure, and monolayer adsorption capacity of the sample, respectively. The BET surface area can be calculated by the above equation assuming the area occupied by the one molecule of adsorbate (N_2).

Relatively small c value indicates that the surface of the sample had less hydrophilic nature. The c value gradually decreased with prolonging hold time up to 3 h,

112

Table 4-2. The adsorption characteristics and methane adsorption capacity of the decyl derivatives of boehmite heated in He.

Temparature (°C)	Time (h)	BET surface area[a] (cm²/g)	c-value[b]	Pore volum (cm³/g)	Pore volume per an aluminum atom[c] (×10⁻²³ cm³/Al)	Volume of removed alkyl chains[d] (×10⁻²³ cm³)	Methane adsorption capacity[e] (wt%)
-	-	305	-	0.243	4.14	-	-
310	0	357	76.9	0.310	5.06	1.20	1.13
310	1	495	73.7	0.440	7.34	1.80	1.26
310	3	582	65.2	0.477	7.54	2.52	1.66
310	6	471	108	0.411	6.24	3.03	1.40

a: Preheated at 250 °C for 0.5 h.

b: Constant number of BET formula.

c: Calculated from the X-value and the pore volume.

d: Calculated from the X-value and volume of an alkyl chains that was calculated from crystal structure of polyethylene and was 2.08×10^{-22} cm³ [14].

e: The samples were preheated at 100 °C for 1 h. After methane gas was applied to the cells with the products at 35 atm, methane adsorption capacity was calculated from the volume of methane gas which came out from the cell under atmospheric pressure.

suggesting that heat treatment caused the formation of more hydrophobic surface. The increase in hydrophobic nature indicates that the ratio of surface area formed between the alkyl chains to that of the boehmite layers increased. On the other hand, heating for 6 h caused an increase of the c value, indicating that excessive heat treatment caused the formation of hydrophilic surface. Pore volume calculated from t-plot increased by heat treatment. Pore volume per an aluminum atom was calculated from the X-value and the pore volume, and volume of alkyl chains removed by heat treatment per an aluminum atom was calculated from the X-value on the basis of volume of an alkyl group which was calculated from the crystal structure of polyethylene [14] as 2.32×10^{-22} cm^3. The volume of removed alkyl chains per an aluminum atom was a major part of difference between the pore volume per an aluminum atom of heated sample and that of untreated sample, indicating that the increase of pore volume was due to the removal of alkyl chains.

Methane has a tendency to adsorb to hydrophobic surface, and methane adsorption capacity of the sample increased with prolonged heat treatment up to 3 h, indicating that the surface area having hydrophobic nature increased (see Table 4-2).

The change of N_2 adsorption capacity was caused by two contributing factors, which were the change of weight and pore volume of the products. As shown in Table 4-1, the weight loss of the product kept at 310 °C for 6 h was 17 %, suggesting that pore volume in the boehmite layers had the largest effect on the change of N_2 adsorption capacity.

When the heating time was prolonged from 3 h to 6 h, the decreases in the N_2 adsorption capacity, the BET surface area, and the methane adsorption capacity were caused by the partial collapse of the boehmite layers as shown in Fig. 4-4. From these

results, it was concluded that the voids in the alkyl layers of the alkyl derivatives of boehmite were generated by the heat treatment when the layer structure was maintained.

4-4. CONCLUSION

The solvothermal reaction of aluminum isopropoxide in 1-decanol yielded the decyl derivative of boehmite $[AlO(OH)_{(1-X)}(OC_{10}H_{21})_X]$. This product belongs to a class of intercalation compounds where the guest moieties are covalently bonded to the host inorganic (boehmite) layers. The alkyl chains in the boehmite layers were partially removed by heat treatment in a He flow. The XRD, TG, and N_2 adsorption measurement showed that the voids surrounded by the alkyl chains were generated by the heat treatment. When the decyl derivative of boehmite was heated at 310 ºC for 3 h in a He flow, the voids attained the largest volume, but prolonged heat treatment resulted in the partial collapse of the boehmite layers leading to a smaller void volume.

References

[1] T. K. Maji, R. Matsuda, S. Kitagawa, *Nature Mater.*, 6 (2007) 142.

[2] S. Takamizawa, E. Nakata, T. Saito, T. Akatsuka, *Inorg. Chem.*, 44 (2005) 1362.

[3] R. Matsuda, R. Kitaura, S. Kitagawa, Y. Kubota, R. V. Belosludov, T. C. Kobayashi, H. Sakamoto, T.Chiba, M. Takata, Y. Kawazoe, Y. Mita, *Nature,* 436 (2005) 238.

[4] R. Nishio, M. Sugiura, S. Kobayashi, *Org. Lett.*, 7 (2005) 4831.

[5] T. Kubo, K. Uchida, K. Tsubohashi, and F. Hashimi, *Kog. Kagaku Zasshi,* 73 (1970) 75.

[6] S. Yamanaka, *Inorg. Chem.*, 15 (1976) 2811.

[7] J. J. Tunney and C. Detellier, *Chem. Mater.*, 5 (1993) 747.

[8] M. Inoue, H. Kominami, and T. Inui, *J. Chem. Soc. Dalton Trans.*, (1991) 3331.

[9] M. Inoue, M. Tanino, H. Kondo, Y. Inui, *J. Am. Ceram. Soc.*, 72 (1989) 352.

[10] M. Inoue, M. Kimura, T. Inui, *Chem. Mater.*, 12 (2000) 55.

[11] Y. Nakazaki, M. Inoue, *J. Phys. Chem. Solids,* 65 (2004) 429.

[12] T. Keii, T. Takagi, S. Kanetaka, *Anal. Chem.*, 33 (1961) 1965.

[13] A. I. Kitaigogoroskii, "Molecular Crystals and Molecules", (Academic Press, N. Y., 1973, p 48).

[14] C. W. Bunn, *Trans. Faraday Soc.*, 35 (1939) 482.

Chapter 5

Solvothermal Oxidation of Gallium Metal in Various Organic Solvents

5-1. Introduction

Gallium oxide (Ga_2O_3) is one of the 13 group metal oxides and has five polymorphs: α, β, γ, δ and ε [1]. Gallium oxide-based catalysts are also known to be active for various catalytic processes [2–10]. As mentioned in General Introduction, it is now generally believed that crystal structures of Ga_2O_3 is similar to that of Al_2O_3, and, especially, γ-form having a defect spinel structure is of particular interest because of its high surface area suitable for catalyst uses. However, as pointed out in General Introduction, synthesis of this phase is not an easy task because prolonged contact of the hydroxide gel particles with water causes the formation of GaOOH-like phase having a diaspore-type structure, which is a precursor of α-Ga_2O_3. To overcome this problem, an ethanol solution (50 vol%) of concentrated aqueous ammonia is added to a solution of gallium nitrate in ethanol at room temperature [11], and this procedure is followed by most of the recent studies [12–16] for the synthesis of γ-Ga_2O_3. Only few preparation methods other than that mentioned above have been reported [17–20]. Therefore, development of other synthetic procedures is highly desired. Among the various synthetic methods to prepare γ-Ga_2O_3, the solvothermal reaction starting from Ga metal has an advantage, because GaOOH-like phase having a diaspore-type structure is not

formed by this reaction. Solvothermal oxidation of metals has been examined: Aluminum metal is oxidized by straight-chain primary alcohols with a carbon number as high as 12, yielding the alkyl derivatives of boehmite, and the basal spacing of the product linearly increases with the increase in the carbon number of the alcohol [21,22]. When cerium metal tips with the superficial layers of oxide are allowed to react in 2-methoxyethanol at 250–300 $^{\circ}$C, a colloidal solution containing 2–3 nm-sized CeO_2 particles is obtained after the removal of coarse ceria particles originating from the superficial layers [23].

In this chapter, solvothermal oxidation of gallium metal with various aminoalcohols at 300 $^{\circ}$C is discussed. The structure and property of the products will be discussed.

5-2. Experimental

5-2-1. Synthesis method.

Commercially available gallium metal (Kanto Chemical) was used without further purification. In a Pyrex test tube serving as autoclave liner, 130 ml of an aminoalcohol and a piece of gallium metal were placed, and the test tube was then placed in a 300 ml autoclave. In the gap between the autoclave wall and the test tube was placed an additional 30 ml of the solvent. The autoclave was thoroughly purged with nitrogen, heated to the desired temperature (300 °C) at a rate of 2.5 °C/min and held at that temperature for a desired period (2–10 h). After the assembly was cooled to room temperature, the resulting precipitates were washed by repeated cycles of agitation with methanol, centrifuging and decantation, and then air-dried.

Powder X-ray diffraction (XRD) was measured on a Shimadzu XD-D1 diffratormeter using CuKα radiation and a carbon monochromator. Crystallite size was calculated from the peak at 2θ = 64° by the Scherrer equation. Simultaneous thermogravimetric (TG) and differential thermal analyses (DTA) were performed on a Shimadzu DTG-50 analyzer: A weighed amount (ca. 20 mg) of the sample was placed in the analyzer, dried in a 40 ml/min flow of dry air until no further weight decrease was observed, and then heated at a rate of 10 °C/min in the same gas flow. Morphologies of the products were observed with a scanning electron microscope (SEM), Hitachi S-2500X. The nitrogen adsorption isotherms were measured at liquid-nitrogen temperature by the usual constant volume method with a Quantachrome Autosorb-1 analyzer. The products obtained by the solvothermal method were previously outgassed at 300 °C for 30 min. Surface areas were calculated by the BET single point method, on the basis of the nitrogen uptake measured at 77 K using a Micromeritics Flowsorb II 2300 analyzer. The average area occupied by a nitrogen molecule was assumed to be 0.162 nm^2.

5-3. Results and discussion

5-3-1. Reaction of gallium metal in various solvents

The reaction of gallium metal in 1-butanol or 2-methoxyethanol at 300 °C for 2 h did not proceed and unreacted gallium metal was recovered even with prolonged reaction time. Whereas the reaction of aluminum metal in primary alcohols yielded alkyl derivatives of boehmite [30]; gallium metal did not react in these solvents. This difference can be explained by the fact that aluminum metal is easier to be oxidized than
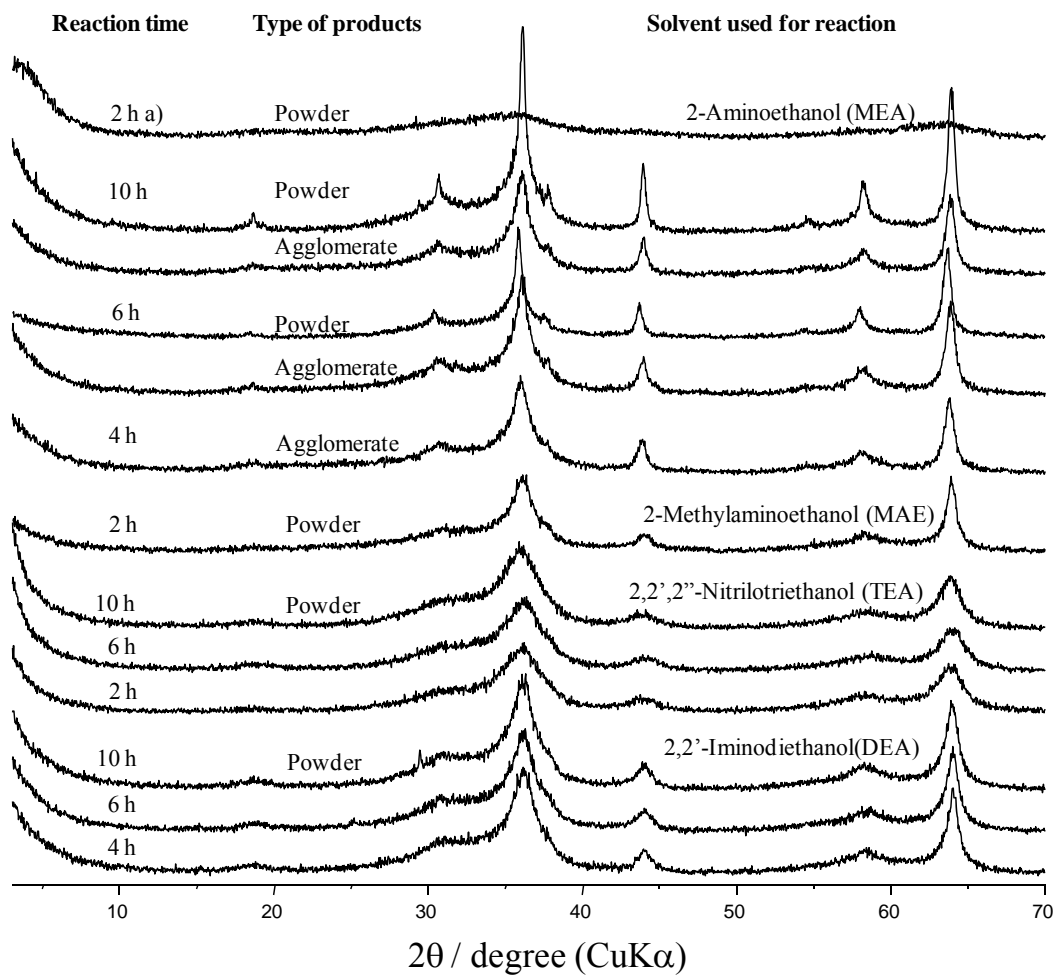
Fig. 5-1. X-ray diffraction patterns of the products obtained by the solvothermal oxidation of gallium metal in aminoalcohols shown in the figure: a) Solid product precipitated from the solution after the colloidal solution was kept standing for one month.

Table 5-1. Preparation of gallium oxide by the solvethermal oxidation of gallium metal at 300 $^{\circ}$C

Medium [a]	Type of products	Reaction time(h)	Conversion of gallium metal (wt%)	Surface area [b] (m²/g)	Crystallite size (nm)	Crystall phase of products [c]
MEA	Solution	2	60.6	no solid product		
	Aggromerate	4	53	8	17.6	γ
	Aggromerate	6	52	34	19.1	γ
	Powder			9	25.9	γ
	Aggromerate	10	66.7	17	28.3	γ
	Powder			7	30.2	γ
DEA	Solution	2	100	no solid product		
	Powder	4	100	6	14	γ
	Powder	6	100	4	12.5	γ
	Powder	10	100	7	11.6	γ
TEA	Powder	2	97.5	71	4.5	γ
	Powder	6	96.4	83	4.7	γ
	Powder	10	96.8	76	5.9	γ
MAE	Powder	2	57.5	10	17.3	γ
DMAE	Solution	2	4.2	no solid product		

a): MEA, 2-aminoethanol; DEA, 2,2'-iminodiethanol; TEA, 2,2',2''-nitrilotriethanol; MAE, 2-methylaminoethanol; DMAE, 2-(*N*,*N*-dimethylamino)ethanol

b): Pre-treatmented at 300 $^{\circ}$C for 30 min

c): γ, γ-Ga_2O_3

gallium metal: Standard reduction potential of aluminum ion (-1.676 V) is lower than that of the gallium ion (-0.53 V). However, when aminoalcohols such as 2-aminoethanol (ethanolamine; MEA) and 2,2'-iminodiethanol (diethanolamine; DEA) were used as reaction media, the reaction proceeded; this fact indicates that the reaction requires alcohols with functional groups (other than the hydroxyl group) having strong ability to donate lone pair electrons.

5-3-2. Crystal structure of the products obtained by the solvothermal reaction

The XRD patterns of the products are shown in Fig. 5-1, which shows that γ-Ga$_2$O$_3$ was formed by the reaction of gallium metal in these organic solvents. By the reaction in MEA for 4 h (Fig. 5-1), only agglomerated particles were obtained but increased reaction time afforded mixtures of agglomerates and powders: Agglomerated particles were settled down in the bottom of the test tube, while powder particles were floated in the solution. They were collected by centrifugation. Crystallite size of the powders was bigger than that of agglomerates and both increased with the reaction time (Table 5-1). The latter result shows a clear contrast against those for the reaction in DEA and 2,2',2"-nitrilotriethanol (triethanolamine; TEA), where crystallite size of the products was not changed by increasing the reaction time. These results indicate that dissolution and recrystallization of γ-Ga$_2$O$_3$ took place in highly polar MEA ($\varepsilon = 37.72$ at 25 $^{\circ}$C [25]), while this process did not occur in less polar solvents (DEA, $\varepsilon = 24.69$; TEA, $\varepsilon = 28.11$ [26]). It is rather surprising to know that γ-Ga$_2$O$_3$ was fairly well-crystallized, since this phase is usually only poorly crystallized having the crystallite size less than 5 nm.

Table 5-1 summarized the results for the reaction of gallium metal in various

Table 5-2. Effect of the pre-treatment of gallium metal on the solvothermal oxidation of gallium metal in 2-aminoethanol

Pre-treatment condition of gallium metal	Precursor gallium metal(g)	Recovered gallium metal(g)	Reacted gallium metal(g)	Conversion of gallium metal(wt%)
Without pre-treatment	0.249	0.098	0.151	60.6
Supersonic treatment	0.286	0.089	0.196	68.5
Supersonic treatment +stirring	0.181	0.0215	0.16	88.4

Reaction condition : Temperature; 300 ^{o}C, time; 2 h
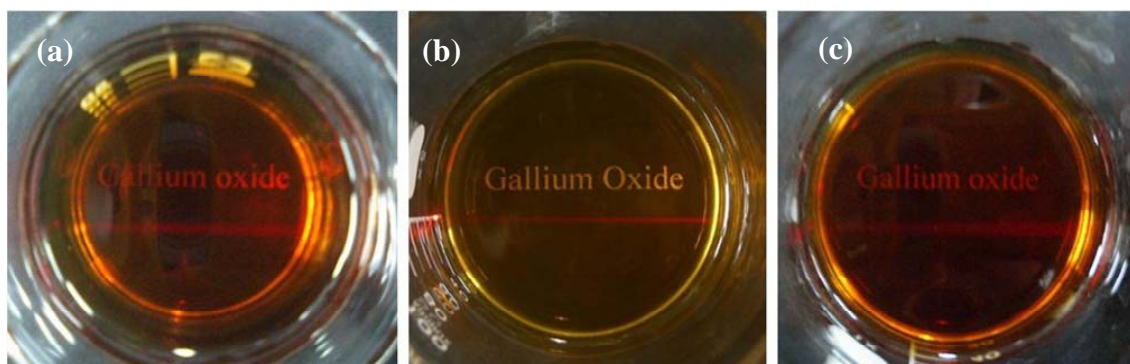
Fig. 5-2. Photographs showing the Tyndall phenomena for the solutions obtained by the reaction of gallium metal in 2-aminoethanol: a), solution obtained by the reaction for 2 h; b), Solution diluted 5 times with water; c), Solution obtained by adding the precipitates to methanol: The precipitate was obtained by keeping the colloidal solution for one month.

media.

When the reaction in *N*-methylaminoethanols are compared, the conversion of gallium metal decreased with the increase in the number of the methyl substituent of the amino group, indicating that methyl substitution of hydrogen atom of the amino group reduces the reactivity of the solvent because of the increase in the steric hindrance.

When the reaction in MEA was quenched at the reaction time of 2 h, 60.6 % of gallium metal was converted, but no solid product was obtained. When the reaction system (gallium metal tip–MEA) was slightly warmed to melt gallium metal (mp = 29.75 $^{\circ}$C) followed by ultrasonic irradiation to disperse metal particles prior to the reaction, the conversion of gallium metal slightly increased (69 %) (Table 5-2). When the reaction was carried out with stirring after the dispersion of gallium metal as mentioned above, the conversion of gallium metal further increased (88 %). However, gray solid particles remained at the bottom of the vessel after the reaction.

When the solution obtained by the reaction in MEA for 2 h was diluted fivefold with water and irradiated by a laser beam, Tyndall phenomenon was observed (Figs. 5-2a and 5-2b); therefore, colloidal particles seem to be present in the solution. To obtain solid products, ammonia or saturated NaCl solution was added; however, precipitate was not formed. Since the solution was highly basic because of the presence of aminoethanol used as the reaction medium, it was neutralized by an addition of HNO$_3$ and then NaCl or Al(NO$_3$)$_3$ solution was added. However, precipitation did no occur. At this stage, therefore, no evidence other than Tyndall phenomenon was obtained for the presence of colloidal particles, so further work is in progress using a small-angle X-ray scattering technique. Note that when this solution was kept standing for one month, a solid product was precipitated out from the solution. The XRD patterns
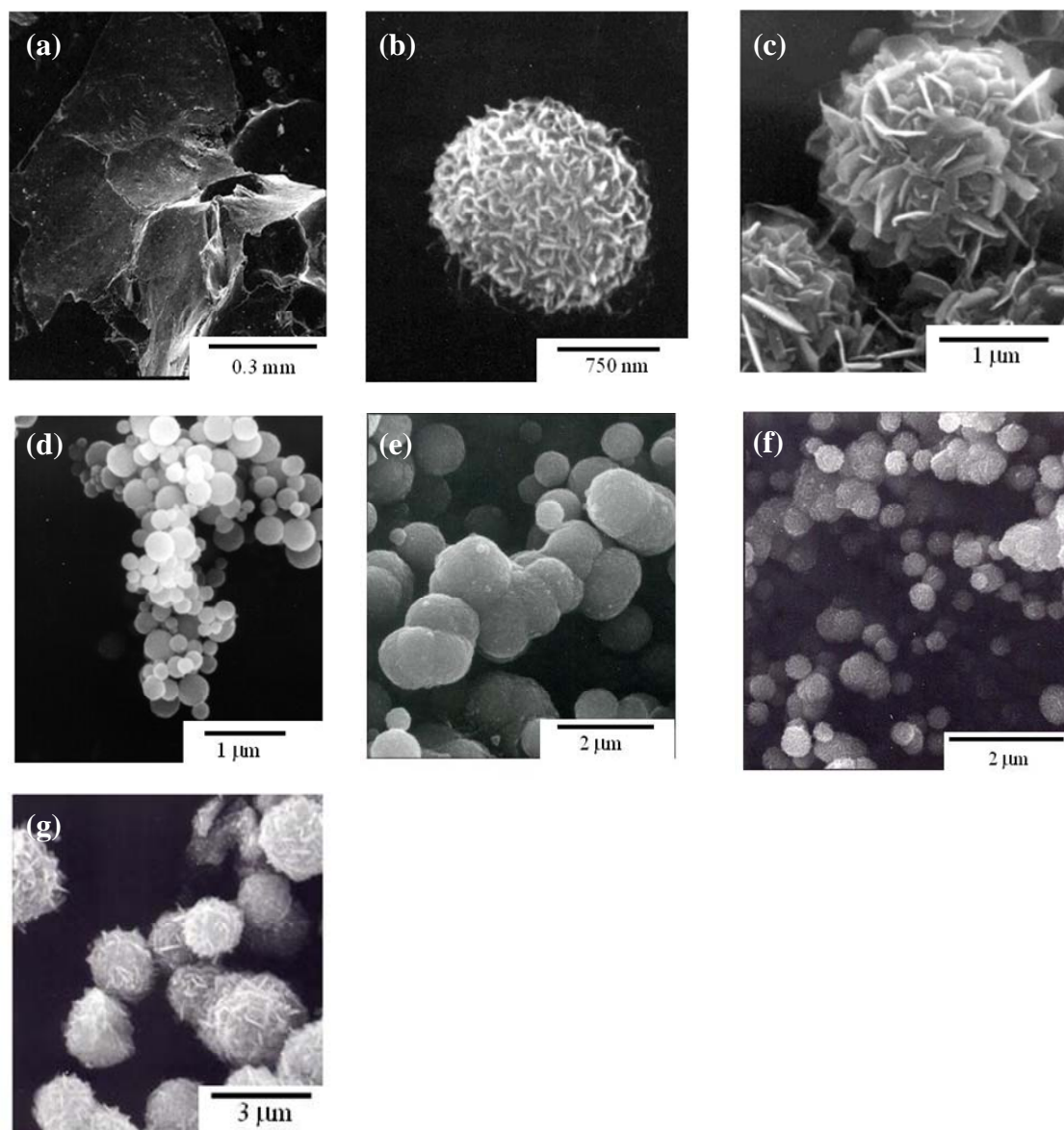
Fig. 5-3. Scanning electron micrographs of the products obtained by the solvothermal reaction of Ga metal.

Reaction conditions (solvent, reaction time) and the morphology of the obtained products are   a) 2-aminoethanol, 4 h, agglomerate;   b) 2-aminoethanol, 6 h, powder;   c) 2-aminoethanol, 10 h, powder;   d) 2',2',2''-nitrilotriethanol, 2 h; e) 2,2'-iminodiethanol, 4 h;   f) 2-methylaminoethanol, 2 h;   g) the product obtained by calcination of   c)   in air at 1000 $^{\circ}$C   for 30 min.

126

of the product indicated that the product was poorly crystallized γ-Ga$_2$O$_3$ (Fig. 5-1, top). A transparent solution was obtained by adding the precipitate to methanol. When NaCl solution was added to this transparent solution, precipitate was not formed but Tyndall phenomenon was observed by a irradiation of laser beam to this transparent solution (Fig. 5-2c).

5-3-3. Morphologies of the products

Scanning electron micrographs (SEM) of the products are shown in Fig. 5-3. The agglomerated product obtained by the reaction in MEA was composed of irregularly-shaped plate-like particles having numerous voids with various sizes (Fig. 5-3a). On the other hand, the powder product was composed of spherical particles formed by aggregation of thin plate particles (Fig. 5-3b) and the plate particles were developed by prolonged reaction time (Fig. 5-3c). Similar morphology was also observed for the products obtained in MAE, although spherical secondary particles were much smaller than those observed in the products obtained in MEA (Fig. 5-3f).

These morphologies are rather unexpected because γ-Ga$_2$O$_3$ has a defect spinel structure having no anisotropy in the crystal structure. Presumably, thin plates were formed through an intermediate having anisotropic crystal structure. However, quenching the reaction with a short reaction time resulted in the formation of a colloidal solution, as mentioned above. On the other hand, the products obtained in TEA and DEA were composed of spherical particles with a smooth surface (Figs. 5-3d and 5-3e).

5-3-4. Pore structure of the products

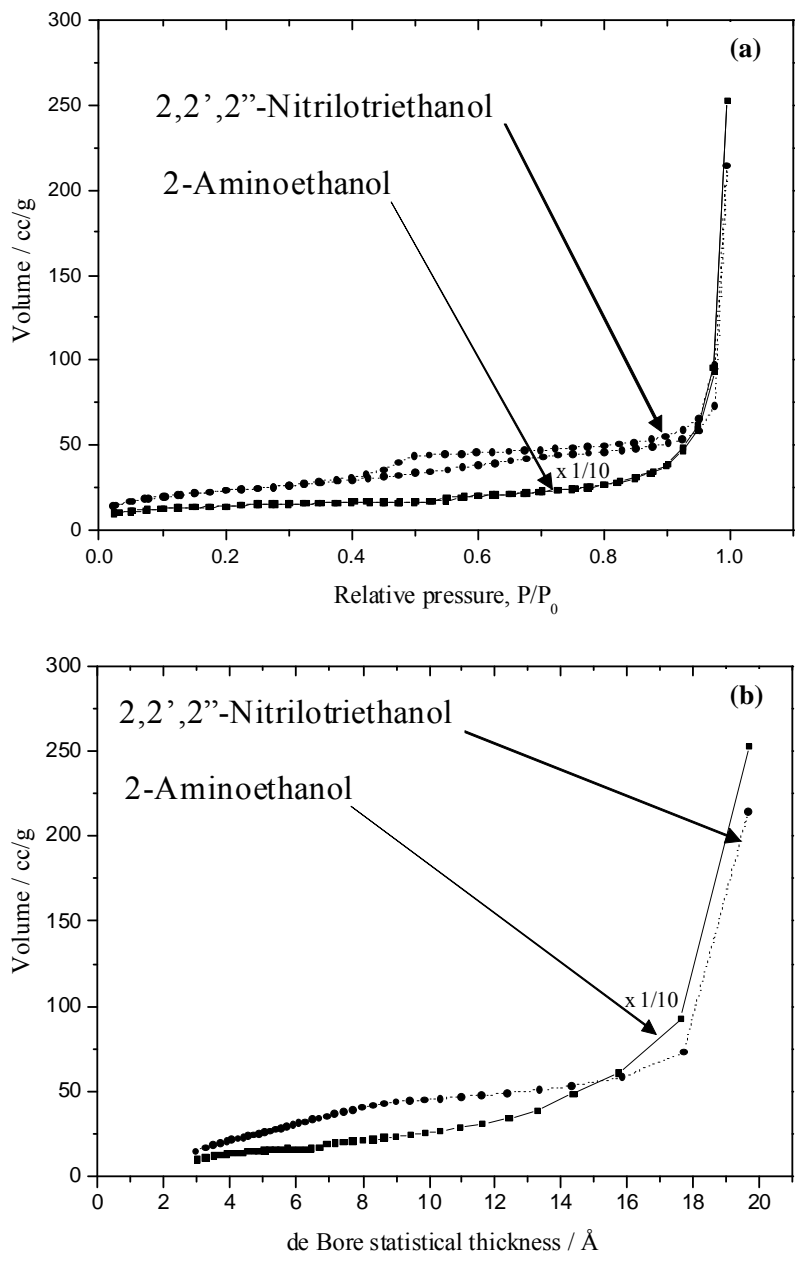Nitrogen adsorption isotherms of the products obtained in MEA and TEA are shown in

Fig. 5-4. Nitrogen adsorption isotherms (a) and *t*-plot (b) of the powder obtained by the solvothermal oxidation of gallium metal.

Fig. 5-4. The product obtained by the reaction in MEA for 10 h exhibited a very low nitrogen uptake and no hysteresis loop was seen, indicating that the products has no meso-pores; however, an increase in nitrogen uptake at the high relative pressure region (Fig. 5-4a) indicates the presence of macro-pores formed between plate-like particles shown in the SEM image (Fig. 5-3c). In the t-plot (Fig. 5-4b) derived from the isotherm, the plot exhibits a straight line going through the origin at region lower than 12 Å, indicating the absence of micro or meso-pore in the sample. The larger increase in the slope of the t-plot indicates the presence of macro-pores in the sample.

On the other hand, the product obtained in TEA suggests that the product had micro-pores, which is shown by the abrupt decrease in the slope of the t-plot at $t = 8$ Å. The presence of micro-pores suggests that each spherical particle (Fig. 5-3d) is composed of much smaller primary particles between which the pore-system is formed. Relatively small crystallite size of this product also supports this argument. The hysteresis loop suggests that slit-shaped pores were formed. The micro-pores may have been formed between the plate-like crystals. This product also has macro-pores formed between small spherical particles (Fig. 5-3d) because an abrupt increase in nitrogen uptake at high relative pressure region, which is also shown by the t-plot of this product (increase of the slope at high t region).

5-3-5. Thermal analysis

The results for the thermal analysis of the products are shown in Fig. 5-5. The TG–DTA profile showed a weight decrease process at 300–400 ^{o}C, which was associated with an exothermic response in DTA, suggesting that the weight decrease is due to combustion of the organic moieties remaining on the surface of the product
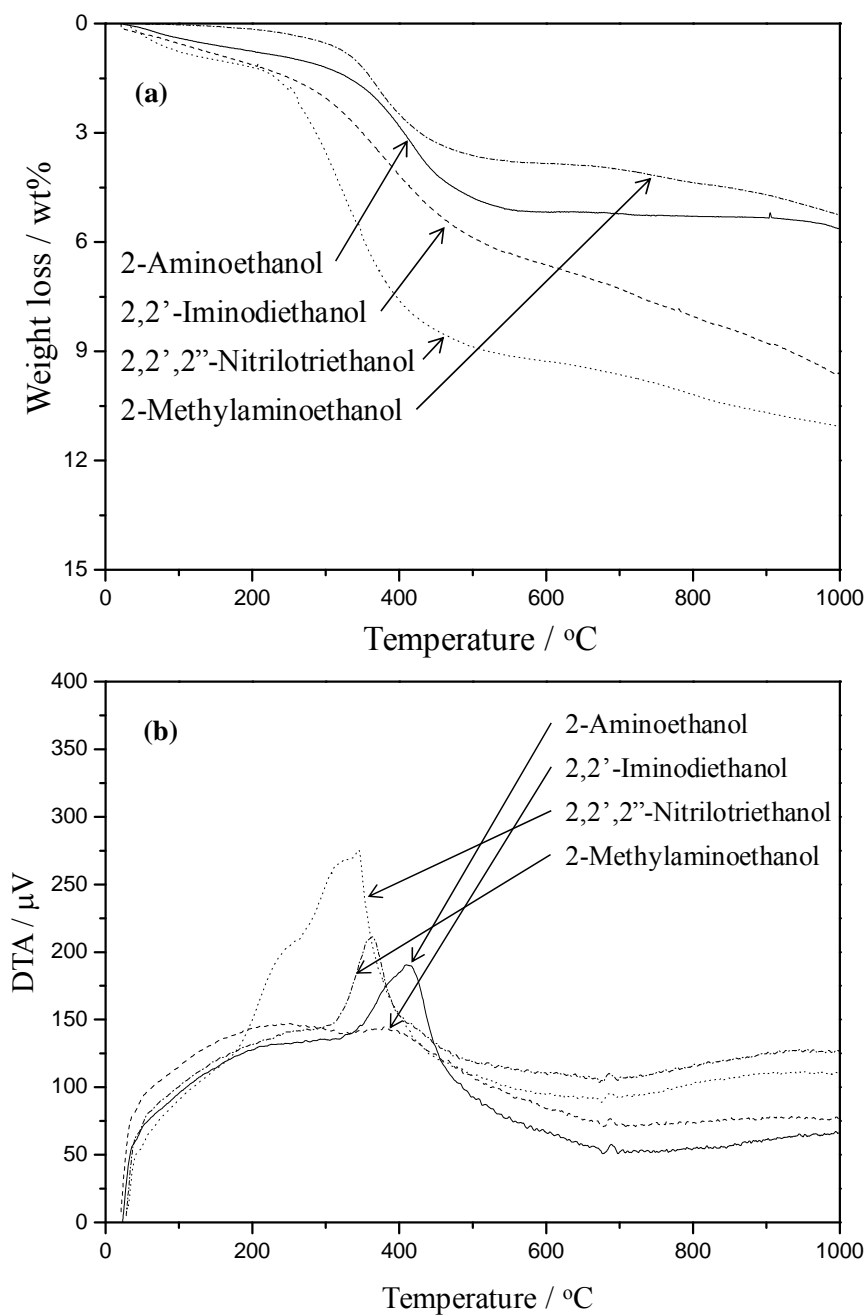
129

Fig. 5-5. Thermal analysis of the products obtained by the reaction of gallium metal in various solvents in a 40 ml/min flow of dried air at the heating rate of 10 $^{\circ}$C/min, a) TG, b) DTA.
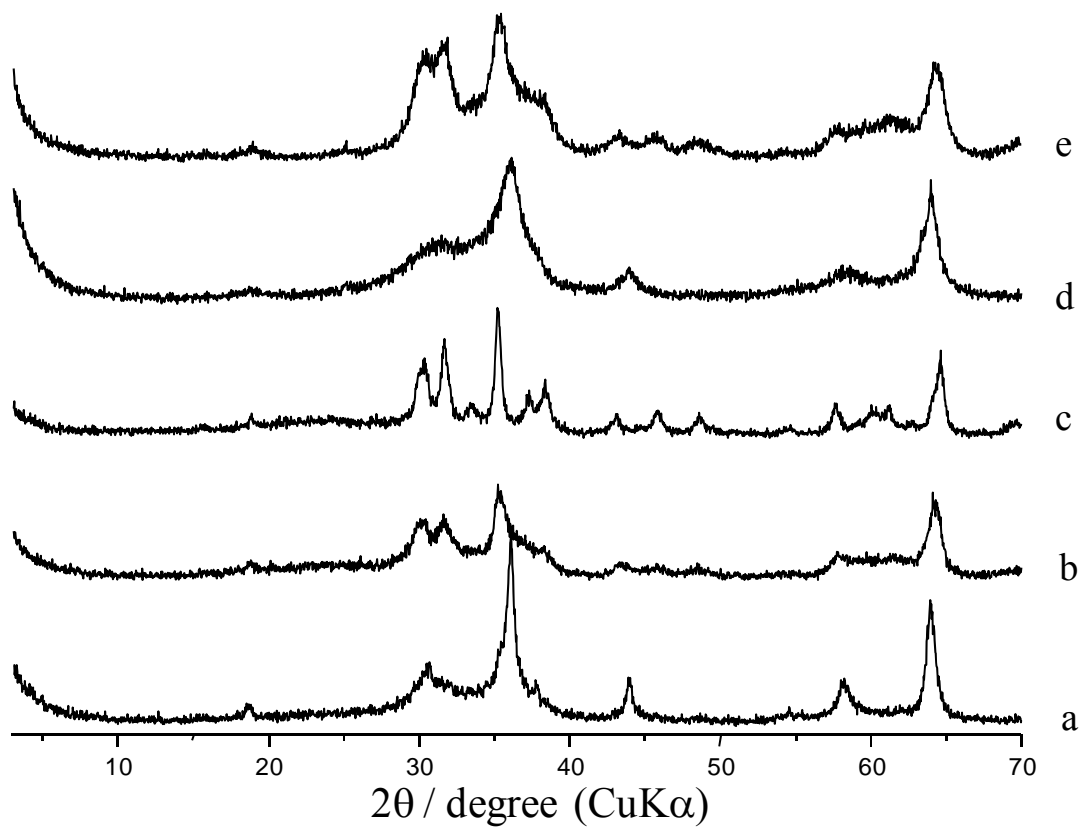
Fig. 5-6. X-ray diffraction patterns of the samples obtained by calcination of the products at: a), 600 ^{o}C; b), 800 ^{o}C; c), 1000 ^{o}C; d), 750 ^{o}C; e), 900 ^{o}C in air for 30 min. The products were obtained by the solvothermal oxidation of gallium metal: a)–c), in 2-aminoethanol at 300 ^{o}C for 10 h; d), e), in 2,2'-iminodiethanol at 300 ^{o}C for 6 h.

Table 5-3. Surface areas and phases of the calcined products

Medium [a]	Reaction time (h)	Product [b]	calcination temperature (°C)	Surface area (m²/g)	Crystal phase [c]
MEA	10	A	as syn	17	γ
			600	21	γ
			800	4	γ, β
			1000	5	β
		P	as syn	7	γ
			600	25	γ
			800	20	γ, β
			1000	5	β
TEA	6	p	as syn	83	γ
			600	75	γ
			800	56	γ, β
			1000	19	β
	10	p	as syn	76	γ
			600	71	γ
			800	61	γ, β
			1000	28	β

a): MEA, 2-aminoethanol; TEA, 2,2',2"-nitrilotriethanol

b): A, Aggromerate; P, Powder

c): γ, γ-Ga_2O_3; β, β-Ga_2O_3

particles. The peak temperature for the exothermic response depended on the solvent used in the reaction and had a tendency to increase with the increase in basicity of the solvent (pKa values of MEA, DEA, and TEA are 9.50, 8.88, and 7.76, respectively). This result suggests the nitrogen atom of the solvent molecule firmly coordinates to the surface acid site of the products particles.

5-3-6. Calcined products

The XRD patterns of the calcined samples are shown in Fig 5-6. The γ-phase transformed into β-phase after calcination at 600–800 ^{o}C. Although it is generally accepted that γ→β transformation temperature is 650 ^{o}C, the present products required a slightly higher temperature for this transformation (see Fig 5-6d), which may be due to higher crystallinity of the present products. It is interesting to note that the γ→β transformation was not accompanied by enlargement of the crystallite size. This result shows a sharp contrast against those for the ordinary γ-Ga_2O_3 samples, where β-Ga_2O_3 with quite a large crystallite size is formed from poorly crystallized γ-Ga_2O_3 phase.

A SEM photograph of the calcined sample is shown Fig. 5-3g. Formation of β-Ga_2O_3 did not alter the essential the feature of the morphology of the products. This result also shows a clear contrast against the alumina chemistry where formation of thermodynamically stable α-alumina from transition aluminas completely alters the morphology. This seems to be due to the fact that stacking of oxygen sublattice for γ- and β-Ga_2O_3 are essentially identical, while γ- to α-alumina transformation requires rearrangement of oxygen stacking from cubic closest packing to hexagonal one.

Change of surface area by calcination in air was investigated and the results are shown in Table 5-3. In the case of the product obtained in TEA, surface area decreased

133

with the increase in calcination temperature, while surface area of the product obtained in MEA increased by calcination at 600 $^{\circ}$C. However, the surface area of the latter product is much smaller than that expected from the SEM image, and voids between the plate-like particles in the core of the spherical aggregate seems to be filled with MEA. Since the desorption temperature of MEA is quite high (Fig. 5-3), MEA is not desorbed from the product particles by the pretreatment prior to the nitrogen adsorption.

5-4. Conclusion

Phase-pure γ-Ga$_2$O$_3$ was formed by solvothermal oxidation of gallium metal in aminoalcohols such as MEA, MAE and TEA. For the reaction in 2-aminoethaol, crystallite size of the product increased with prolonged reaction time. The products had unique morphologies.

References

[1] R. Roy, V. G. Hill, E. F. Osborn, *J. Am. Chem. Soc*., 74 (1952) 719.

[2] K. Shimizu, A. Satsuma, T. Hattori, *Appl. Catal. B*, 16 (1998) 319.

[3] M. D. Fokema, J. Y. Ying, *Cat. Rev. - Sci. Eng*., 43 (2001) 1.

[4] G. L. Price, V. Kanazirev, *J. Catal*., 126 (1990) 267.

[5] Y. Ono, K. Kanae, *J. Chem. Soc., Faraday Trans*., 87 (1991) 669.

[6] C. R. Bayense, A. J. M. van der Par, J. H. C. van Hooff, *Appl. Catal*., 72 (1991) 81.

[7] M. Haneda, Y. Kintaichi, H. Hamada, *Appl. Catal. B*, 20 (1999) 289.

[8] M. Haneda, H. E. Jonbert, J. C. Menezo, D. Duprez, J. Barbier, N. Bion, M. Daturi, J. Saussey, J. C. Lavalley, H. Hamada, *Phys. Chem. Chem. Phys*., 3 (2001) 1366.

[9] Y. N. Pushkar, A. Sinitsky, O. O. Parenago, A. N. Kharlanov, E. V. Lunina, *Appl. Surf. Sci*., 167 (2000) 69.

[10] M. Takahashi, T. Nakatani, S. Iwamoto, T. Watanabe, M. Inoue, *Appl. Catal*. B, 70 (2007) 73.

[11] C. Otero Areán, A. López Bellan, M. Peñarroya Mentruit, M. Rodríguez Delgado, G. Turnes Palomino, *Microporous Mesoporous Mater*., 40 (2000) 35.

[12] M. Zinkevich, F. M. Morales, H. Nitsche, M. Ahrens, M. Rühle, F. Aldinger, *Z. MetaIlkd*., 95 (2004) 756.

[13] S. E. Collins, M. A. Baltanás, A. L. Bonivardi, *J. Phys. Chem. B*, 110 (2006) 5498.

[14] M. Rodríguez Delgado, C. Otero Areán, Zeitschrift, *Z. Anorg. Allg. Chem*., 631 (2005) 2115.

[15] B. Zheng, W. Hua, Y. Yue, Z. Gao, *J. Catal*., 232 (2005) 143.

[16] Y. Hou, L. Wu, X. Wang, Z. Ding, Z. Li, X. Fu, *J. Catal*., 250 (2007) 12.

[17] K. Pohl, *Naturwiss*., 55 (1968) 82.

[18] H. Bremer, B. Bogatzki, *Z. Chem.*, 8 (1968) 309.

[19] M. Inoue, T. Nishikawa, H. Otsu, H. Kominami, T. Inui, *J. Am. Ceram. Soc.*, 81 (1998) 1173.

[20] T. Chen, K. Tang, *Appl. Phys. Lett*., 90 (2007) 051304.

[21] M. Inoue, M. Kimura, T. Inui, *Chem. Mater.*, 12 (2000) 55.

[22] M. Inoue, M. Kimura, T. Inui, *Adv. Sci. Techno*l., 16 (1999) 593.

[23] M. Inoue, M. Kimura, T. Inui, *Chem. Comm.*, 11 (1999) 957.

[24] M. Inoue, H. Tanino, Y. Kondo, T. Inui, *J. Am. Ceram. Soc.*,72 (1989) 352.

[25] J. A. Riddick, W. B. Bunger, T. K. Sakano, "Organic Solvents-Physical Properties and Methods of Purification," (4th Ed. in: Techniques of Chemistry, Vol. II, John Wiley & Sons, New York, 1970).

[26] C.-J. Hsieh, J.-M. Chen, M.-H. Li, *J. Chem. Eng. Data*., 52, (2007) 619.

General Conclusion

This thesis deals with the synthesis of Al_2O_3 and Ga_2O_3 by the solvothermal reaction in various organic solvents. The change of the surface structure of Al_2O_3 derived from the products obtained by the reaction (alkyl derivatives of boehmite) is discussed to elucidate the characteristic of the solvothermal reaction. The synthesis of Ga_2O_3 by the solvothermal reaction of Ga metal with various organic solvents and is also explained. The outline of each chapter is as follow.

In Chapter 1, the characteristics of the pore structures of aluminas derived from the alkyl derivatives of boehmite are described. These products belong to a class of intercalation compounds where the guest moieties are covalently bonded to the host inorganic (boehmite) layers. The alumina derived from the ethyl derivative of boehmite had a broad pore-size distribution, while the pore-size of the aluminas obtained from the alkyl derivatives of boehmite with long alkyl chains distributed in a narrow range in the mesopore region. The mode pore diameter of the latter aluminas increased with an increase in calcination temperature (as-syn., 39 Å; 600 $^{\circ}$C, 54 Å; 800 $^{\circ}$C, 58 Å; 1000 $^{\circ}$C, 68 Å; for ADDOH), and narrow pore-size distribution was maintained even after calcination at high temperatures. These results indicate that stronger van der Waals interaction between the alkyl chains facilitated the formation of the boehmite layers having a smaller number of defects, and that the collapse of the well-developed boehmite layers gave aluminas with narrow pore-size distributions.

Chapter 2 deals with the preparation of aerogel or xerogel of alkyl derivatives of boehmite by a simple procedure, that is solvothermal reaction in an autoclave followed by removing the solvent at the end of the reaction. By this method, aerogel or xerogel can be obtained directly in a reaction vessel. The thus-obtained products, alkyl

derivatives of boehmite, had higher crystallinity than the products recovered by the conventional drying method. Alumina derived from these products had large pore volumes (AEtOH(800), 2.56 cm^3/g; ABuOH(800), 1.1 cm^3/g; AHeOH(800), 1.73 cm^3/g; AOcOH(800), 1.35 cm^3/g; ADDOH(500), 1.35 cm^3/g). For AEtOH which was recovered as an aerogel, transformation into α-Al$_2$O$_3$ was retarded even after calcination at 1200 ^{o}C and θ-Al$_2$O$_3$ was main species in AEtOH(1200). Considering the above results, the expanded volume of solvents at reaction temperature (300 ^{o}C) makes large voids in the products on removing solvents at reaction temperature and these voids contribute to the increased pore volume in the final product.

In Chapter 3, the method to obtain alumina with large pore volume is discussed. In order to obtain alumina with large pore volume by expanding the reactant volume in the autoclave, the various feed ratios of AIP/alcohol in a 300 ml autoclave were employed. Ethanol and 1-hexanol were used as the solvents. The feed ratio of reactant affected to the crystallinity of alkyl derivatives of boehmite. At large feed ratios (AIP/alcohol), the crystallite size of alkyl derivatives of boehmite decreased due to the incorporation of 2-propanol liberated from AIP into the layer of the alkyl (EtOH, HeOH) derivatives of boehmite by an exchange reaction. The partial incorporation of 2-propyl groups in the *n*-alkyl layers weakens the van der Waals interaction between the alkyl groups. In the product obtained by the solvothermal reaction in ethanol, χ-Al$_2$O$_3$ was obtained by the thermal decomposition of AIP in a large AIP/EtOH region (0.25). The morphologies of the products were also affected by feed ratio change. The change in the crystallinity and morphologies of alky derivatives of boehmite affects the transformation sequence of Al$_2$O$_3$; the transformation to α-Al$_2$O$_3$ on calcination of the products having a well developed sheet-like structure was retarded. Alumina derived

from these products had a large pore volume (AAEt(12.5-130), 1.16–2.56 cm^3/g; AXHe(12.5-50), 1.16–3.24 cm^3/g) compared with aluminas derived from products recovered by washing process with methanol (AMHe(12.5-130), 0.45–1.24 cm^3/g). The pore structure of the products recovered as aero/xerogel is robust against thermal treatment.

Molecular mechanics calculation suggests that the layered structure of the alkyl derivatives of boehmite is maintained even when the alkyl chains are partially removed; partial removal of the alkyl chains creates the voids in the alkyl layers because the alkyl chains are attached to the boehmite layers. In this respect, Chapter 4 discusses whether the voids surrounded by the alkyl chains are actually generated by heat treatment of the alkyl derivative of boehmite. The solvothermal reaction of AIP in 1-decanol yielded the decyl derivative of boehmite [AlO(OH)$_{(1-X)}$(OC$_{10}$H$_{21}$)$_X$]. The alkyl chains in the boehmite layers were partially removed by heat treatment in a He flow. The XRD, TG, and N$_2$ adsorption measurements showed that the voids surrounded by alkyl chains were generated by the heat treatment. When the decyl derivative of boehmite was heated at 310 ºC for 3 h in He flow, the voids had the largest volume, but prolonged heat treatment resulted in the partial collapse of the boehmite layers causing a smaller void volume.

In Chapter 5, solvothermal oxidation of gallium metal with various aminoalcohols at 300 ºC is discussed. This reaction was carried out with an aim to develop a novel synthetic procedure of Ga$_2$O$_3$. The structure and property of the products obtained was examined. The reactions proceeded only in aminoalcohols such as 2-aminoethanol (ethanolamine; MEA) and 2,2'-iminodiethanol (diethanolamine; DEA), indicating that the reaction requires alcohols with functional groups (other than

the hydroxyl group) having a strong ability to donate its lone pair electrons. When *N*-methylaminoethanols were used, conversion of gallium metal decreased with an increase in the number of methyl group, indicating that methyl substitution of hydrogen atom of the amino group reduces the reactivity of the solvent because of the increased steric hindrance. The γ-Ga_2O_3 obtained in the reaction was well-crystallized. The powder Ga_2O_3 product was composed of spherical particles (second particle) formed by aggregation of thin platelike particles. The size of the platelet particles itself developed by prolonged reaction time. Similar morphology was also observed for the products obtained in MAE. Although it is generally accepted that $\gamma \rightarrow \beta$ transformation takes place at 650 ^{o}C, the above products required a slightly high temperature for this transformation.

In summary, it is clearly shown that solvothermal reaction is a very efficient synthetic method to prepare Al_2O_3 and Ga_2O_3 having unique properties compared to conventional method. Metal oxides useful in catalytic application as supports are prepared by this method. The solvothermal reaction will attract more attention in the future to prepare catalysts having enhanced catalytic activities. I believe that the solvothermal method presented in this thesis will offer a good solution to develop catalysts with high performance for various catalytic processes.

List of Publications

Chapter 1

"Pore structure of alumina derived from the alkyl derivatives of boehmite"

S.-W. Kim, S. Iwamoto, M. Inoue,

Advances in Science and Technology, 45 (2006) 2153.

"Pore structure of aluminas derived from the alkyl derivatives of boehmite"

S.-W. Kim, S. Iwamoto, M. Inoue,

Journal of Porous Materials,16 (2009) 605.

Chapter 2

"Surface and pore structure of alumina derived from xerogel/aerogel"

S.-W. Kim, S. Iwamoto, M. Inoue,

Journal of Porous Materials, in press.

Chapter 3

"Novel synthesis method of alumina having a large pore volume"

S.-W. Kim, S. Iwamoto, M. Inoue,

Topics in Catalysis, in press.

Chapter 4

"Generation of voids in the alkyl layers of an alkyl derivative of boehmite by heat treatment and adsorption behavior of the voids"

M. Kobayashi, S.-W. Kim, S. Iwamoto, M. Inoue,

Journal of Physics and Chemistry of Solids, 69 (2008) 1367.

Chapter 5

"Solvothermal oxidation of gallium metal"

S.-W. Kim, S. Iwamoto, M. Inoue,

Ceramics International, 35 (2009) 1603.

Papers not included in this thesis.

1.　　"**Photocatalytic decomposition of gaseous formaldehyde using TiO$_2$, SiO$_2$-TiO$_2$ and Pt-TiO$_2$**"

B.-Y. Lee, S.-W. Kim, S.-C. Lee, H.–H. Lee, S.–J. Choung,

Int. J. Photoenergy, 5 (2003) 21.

2.　　"**Preparation of a TiO$_2$ film using TEOS binder and its application to the photodegradation of benzene**"

S,-W. Kim, M. S. Kang, S.-J. Choung,

J. Ind. Eng. Chem., 11 (2005) 416.

Acknowledgments